UNIVERSITY OF GAZIANTEP

GRADUATE SCHOOL OF

NATURAL & APPLIED SCIENCES

INVESTIGATION OF REPLACEMENT OF STIRRUPS WITH STEEL FIBERS IN SELF-COMPACTING REINFORECED CONCRETE HAUNCHED BEAMS

M.Sc. THESIS

IN

CIVIL ENGINEERING

By

SAFAA YASEEN AL-DARRAJI

APRIL 2018

Investigation Of Replacement Of Stirrups With Steel Fibers In Self-Compacting Reinforced Concrete Haunched Beams

M.Sc. Thesis

In

Civil Engineering

University of Gaziantep

Supervisor

Assist. Prof. Dr. Mehmet Eren GÜLŞAN

By

Safaa Yaseen AL-DARRAJI

April 2018

REPUBLIC OF TURKEY
UNIVERSITY OF GAZİANTEP
GRADUATE SCHOOL OF NATURAL & APPLIED SCIENCES
CIVIL ENGINEERING DEPARTMENT

Name of the thesis: Investigation of Replacement of Stirrups with Steel Fibers in
Self-Compacting Reinforced Concrete Haunched Beams

Name of the student: Safaa Yaseen AL-DARRAJI

Exam date: 16.04.2018

Approval of the Graduate School of Natural and Applied Sciences

Prof. Dr. A. Necmeddin YAZICI
Director

I certify that this thesis satisfies all requirements as a thesis for the degree of Master
of Science.

Prof. Dr. Hanifi CANAKCI
Head of Department

This is to certify that we have read this thesis and that in our opinion, it is fully
adequate, in scope and quality, as a thesis for the degree of Master of Science.

Assist. Prof. Dr. Mehmet Eren GÜLŞAN
Supervisor

Examining Committee Members: Signature

Prof. Dr. Abdulkadir ÇEVİK   ....

Assist. Prof. Dr. Derya BAKBAK   ....

Assist.Prof. Dr. Mehmet Eren GÜLŞAN   ....

I hereby declare that all information in this document has been obtained and presented in accordance with academic rules and ethical conduct. I also declare that, as required by these rules and conduct, I have fully cited and referenced all material and results that are not original to this work.

Safaa Yaseen AL-DARRAJI

ABSTRACT

INVESTIGATION OF REPLACEMENT OF STIRRUPS WITH STEEL FIBERS IN SELF-COMPACTING REINFORECED CONCRETE HAUNCHED BEAMS

AL-DARRAJI, Yaseen Safaa
M.Sc. in Civil Engineering
Supervisor: Assist. Prof. Dr. Mehmet Eren GÜLŞAN
April 2018
93 pages

Reinforced Concrete Haunched Beams (RCHBs) are important structural members in the construction sector. Usage of steel fiber reinforced concrete (SFRC) can be considered as a possible replacement to use of traditional shear in RCHBs. Usually one of the disadvantages related to the use steel fiber is that adding fiber to a regular concrete mixture can occur large problems in workability of concrete. Therefore, the use of self-compacting concrete (SCC) is a suitable solution to such a problem and can enhance workability of fresh concrete.

This thesis presents the experimental study for one type of RCHBs. The experimental work consists of 9 self-compacting fiber reinforced concrete (SCSFRC) beams, which is classified into 6 RCHBs and 3 prismatic beams which examined under four-point loading. One type of steel fiber that has a hooked end was used in this study. The studied variables included inclination angle, beam type, and steel fiber percentage. These variables have been significantly influential on the shear behavior of RCHBs. The results show that the higher inclination angle of SCSFRC haunched beams has a negative influence on shear load capacity due to increase in shear stress. Also, the results indicated that the combination of the use SCC and steel fibers in RC beams can significantly improve shear strength, post-cracking behavior, and ductility. Steel fibers both reduced the crack width and converted the failure mode from brittle and sudden to ductile. Furthermore, the results showed that the use of 1% volumetric ratio can be a substitute of minimum shear reinforcement in RCHBs.

Keywords: Reinforced Concrete Haunched Beam, Steel Fibers, Self-compacting Concrete, Shear Capacity, and Failure Mode.

ÖZET

KENDİLİĞİNDEN YERLEŞEN BETONLA ÜRETİLMİŞDEĞİŞKEN KESİTLİ KİRİŞLERDE ETRİYENİN YERİNE ÇELİK LİFLERİN KULLANILABİLİRLİĞİNİN ARAŞTIRILMASI
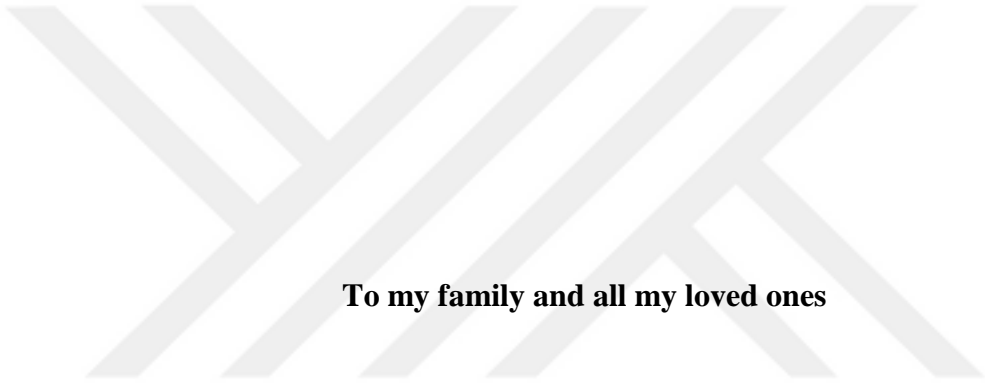
AL-DARRAJI, Yaseen Safaa
Yüksek Lisans Tezi, İnşaat Mühendisliği
Tez Danışmanı: Dr. Öğr. Üyesi Mehmet Eren GÜLŞAN
Nisan 2018
93 sayfa

Betonarme değişken kesitli kirişler yapı sektöründe tercih edilen önemli yapı elemanlarındandır. Çelik lif katkılı betonun kullanımı ise betonarme değişken kesitli kirişlerde kesme kuvvetine karşı etriye yerine olası bir alternatif olarak düşünülebilir. Çelik lif kullanımı ile ilgili dezavantajlardan biri, lifin normal bir betona eklendiği zaman betonun işlenebilirliğinde oluşturduğu büyük problemlerdir. Bundan dolayı, kendiliğinden yerleşen betonun kullanımı böyle bir problem için uygun bir çözümdür ve taze betonun işlenebilirliğini iyileştirmektedir.

Bu tez bir türdeki değişken kesitli betonarme kirişler üzerine deneysel bir çalışmayı sunmaktadır. Deneysel çalışma 6'sı değişken kesitli, 3'ü prizmatik olmak üzere 9 adet çelik lif katkılı betonarme kirişten oluşmaktadır ve bütün kirişler dört nokta yükleme testiyle yüklenmiştir. Çalışmada kanca uçlu çelik lifler kullanılmıştır. Çalışmada dikkate alınan değişkenler kiriş eğim açısı, kiriş türü ve çelik lif oranıdır. Bu değişkenler, değişken kesitli kirişlerin kesme kuvvetine karşı davranışında önemli bir etkiye sahiptirler. Sonuçlar eğim açısının kirişlerin kesme kuvveti kapasitesi üzerinde negatif bir etkiye sahip olduğunu göstermiştir. Ayrıca, deney sonuçları, kirişlerde kendiliğinden yerleşen betonun ve çelif lifin birlikte kullanımının kirişlerin kesme mukavemetini, çatlama sonrası davranışını ve sünekliğini iyileştirdiğini göstermiştir. Çelik tel katkısı hem çatlak genişliğini azaltmış hem de göçme türünü ani ve kırılgandan süneğe dönüştürmüştür. Daha da ilerisi, deney sonuçları yüzde 1 oranında çelik lif oranının değişken kesitli betonarme kirişlerde gerekli minimum kesme donatısı yerine kullanılabileceğini göstermiştir.

Anahtar Kelimeler: Değişken kesitli betonarme kiriş, Çelik tel, Kendiliğinden yerleşen beton, Kesme kuvveti kapasitesi, Göçme türü.

To my family and all my loved ones

ACKNOWLEDGEMENTS

CONTENTS

LIST OF FIGURES

xv

LIST OF TABLES

LIST OF SYMBOLS

a	Shear span of beam
a/d	Shear span-to-depth proportion
Af	Cross-sectional area of fiber
As	Cross sectional area of main reinforcement
b	Width of beam
d	Effective depth for beam
d_{cr}	The effective depth at the critical section
Df	Diameter of fiber
F	Fiber factor
f'_c	The cubic compressive strength of concrete
$f_{Rk}{}^{f}$	Function of residual post-cracking strength
F_{Ftuk}	Function of residual post-cracking strength
$F_{ftd,res}$	Residual strength as defined in the Norwegian code
F_{Rk}	Function of a fraction of the residual post-cracking strength
f_{ct}	Splitting tensile strength of concrete
fr	Modulus of rapture of concrete
fu	Ultimate stress of longitudinal steel reinforcement
fy	Yield strength of main reinforcement
h	Height of beams
hf	Depth at middle of haunched beam
hs	Depth at the supports of haunched beam

Lf	Length of fiber
Lf / Df	Fiber aspect ratio
M_{Ed}	The bending moment at the effective depth (at the critical section)
V	Shear stresses capacity of RC member
Vc	Shear force capacity of RC beam
V_f	Steel fiber percentage amount
V_{Ed0}	Shear force caused by live and dead loads
V_{ccd}	Design shear caused by inclination of compression chord of beam.
V_{td}	Design shear strength component of inclined longitudinal tension bars.
V_{pd}	Design shear strength component of prestressed force.
V^{α}_{Rd}	Design magnitude of shear bearing capacity of haunched beams at design section
V_{pc}	Concrete shear strength of parallel-side beam
Vu	The maximum shear stress
α	Inclination angle of haunched beam
α	Fiber orientation factor
γ_c	Unit weight of normal concrete
ρ	Longitudinal steel reinforcement proportion
λ	Factor that accounts for concrete type
η_0	The steel fiber orientation factor
τ_{fd}	Fraction of the residual strength as defined in the Norwegian code

CHAPTER 1

INTRODUCTION

1.1 General

Usage of reinforced concrete haunched beams (RCHBs) become more common during the last decades in structural elements such as retaining wall, continuous bridges in mid-rise framed buildings, and structural portal frames because designers consider that these elements can add a number of advantages compared to the prismatic beams such as economic member, easy installation of infrastructure in the building (electrical, plumbing, sewage, etc.), and aesthetic reasons, as seen in Fig. 1.1. Therefore, this thesis focuses on the mechanical shear performance of reinforced concrete haunched beams without shear reinforcement or stirrups. In general, the accepted shear design model is still not obtainable, especially for reinforced concrete members without stirrups, which can often be obtained in a several of structural elements such as retaining walls, bridge slabs, and tunnels.

Figure 1.1 Reinforced Concrete Haunched Beams (RCHBs)

Source https://theconstructor.org/   Source http://www.hpcbridgeviews.com/

The available experimental studies summarized that the mechanical behavior of the RCHBs have shown various behaviors compared to prismatic beams, the results of the experimental works declared that the different depth along the RCHB affects the mechanism of the shear failure (Debaiky and El-Niema 1982, Stefanou 1983, Tena et

al. 2008, Nghiep 2010). It is strange and surprising to know that there is no practical code except the German code DIN 1045-1 to provide details of guidance for the design of these structures. In addition, other design codes did not mention the shear design of the RCHBs.

Through previous studies, it has been shown that the shear strength capacity of haunched beams is greater than the prismatic beam, though haunched elements clearly have less amount of concrete and steel reinforcement. This truth encourages further study of this type of beams. It is also unexpected that there was very limited research which has been performed on this subject. In addition, this thesis will focus on the usage of steel fiber with self-compacting concrete to study the mechanical behavior of shear strength for haunched beams which have not been studied by previous researchers.

1.2 Steel Fiber Reinforced Concrete (SFRC)

Steel fiber reinforced concrete (SFRC) can be defined as a composite material made of hydraulic cement, fine aggregate, coarse aggregate, and incorporating separated disconnected fibers. Fibers have different geometrical characteristics (diameter, length, cross-sectional shape, longitudinal shape, and surface roughness). Fibers are made of various materials and in different forms, these fibers are the most common in the concrete industry. Steel fibers are short (typically from 1.25cm to 6.25cm) and generally deformed to enhance the bond with the concrete, as shown in Fig. 1.2. Steel fibers are known as separated lengths of steel that have an aspect ratio (the ratio of length to the diameter equal to range 20 to 100), and which are small to be randomly oriented dispersed in the concrete mix using normal mixing procedures (ACI 544.1R-96 Report, 2002). SFRC is the general term used to identify a composite material that components include the traditional concrete and steel fibers.
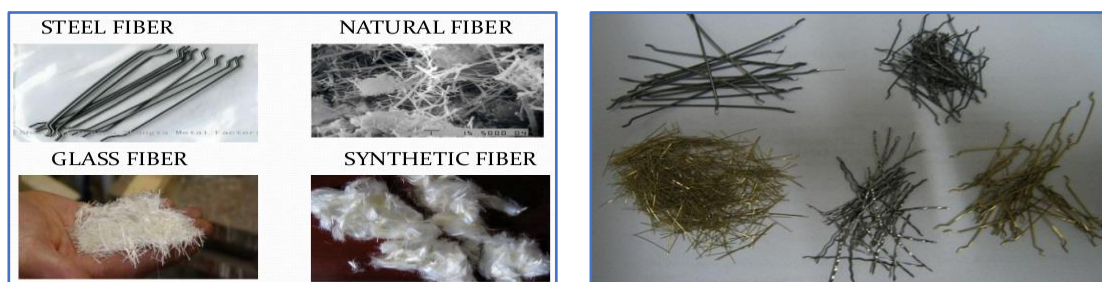
Figure 1.2 Different Types of Fibers

Source https://www.slideshare.net/   Source http://zhuokainet.com/

A reinforced concrete beam that without shear reinforcement can fail in shear prior approaching its maximum flexural strength. Generally, shear failure of a reinforced concrete beam happens when the principal tensile stress inside the shear span overtakes the tensile strength capacity of concrete, and immediately followed by the spread a diagonal shear crack inside the shear span. This type of failure is sudden and without any warning before the collapse failure. The beams are reinforced with conventional shear to prevent shear failure. However, the usage of shear reinforcement or stirrups is not always cost-effective in terms of increases the cost of construction work, and can make the concrete process difficult in cases where closely-spaced shear reinforcement is desired. For these reasons, it is necessary to use steel fibers in concrete.

Steel fiber reinforced concrete was developed in the early 1960s. The much experimental research was conducted on steel fiber reinforced concrete. When steel fibers are added to the concrete, significant improvements are achieved in the post-cracking tensile strength and toughness (Hannant, 1978), hence the shear capacity of reinforced concrete beams is significantly enhanced, also improves the energy absorption capacity of concrete. Whereas in the case compression, many researchers have observed that a maximum compression strength has a gain of 15% (Fanella and Naaman, 1985; ACI 544.1R-96 Report, 2002; Thomas and Ramaswamy, 2007). Therefore, the addition of fiber does not have a significant influence on the compression strength.

The widespread use of fibers is mostly in nonstructural applications such as industrial floors, bridge deck overlays, tunnel linings, highway pavements, and concrete containers. Recent examples include the Barr Lake Dam (Mass, 1997) and the Gotthard Base Tunnel (Kronenberg, 2006). However, the usage of SFRC in buildings was very limited, although steel fibers have been proven to enhance the flexural (Hannant, 1978), and shear (for example, Batson and Jenkins, 1972) behavior of concrete members. The limited usage of SFRC in building structures is primarily because of the shortage of design provisions in building codes.

The potential reason for the shortage of shear design provisions is that the shear strength mechanisms in RC beams are not fully understood. When steel fibers are added to RC beams, these mechanisms become more complex. Generally, fibers are used as a substitution to control cracking for the steel bars and wire mesh. In addition

to the usage of fiber in non-structural applications, there is a benefit in using fibers in some structural applications. Hence, recently it has been used in structural applications as a substitution engineering materials completely or partially to replace transverse stirrups and have the same effect in terms of shear strength. Where the usage of hooked end steel fibers instead of a minimum shear stirrup is currently allowed in ACI Code Section 11.4.6 (ACI Committee 318, 2008).

In the failure modes, the use of steel fiber in a suitable amount results in considerable increase in shear strength capacity, and in certain cases these fibers can convert the failure mode from shear to flexural. Adding steel fibers has a much more influence on the tensile behavior of the shear strength. In addition, the fibers bind the crack in the concrete and help to transfer forces through cracks, therefore crack widths are less than of plain concrete.

The form of hooked end steel fiber will be used in this work because it is one of the most widely used types by researchers and in the construction industry. Where extensive experimental data on the usage of this type of fiber is available in the literature. This type of fiber provides great performance compared to straight fiber due to the influence of the hooks on pullout strength. Generally, fibers are added to the concrete during mixing as glued packs and disperse homogeneously during the mixing process.

1.3 Combining the Usage of Self-Compacting Concrete (SCC) and Steel Fiber (SFR)

Self-compacting concrete (SCC) was proposed by researchers at the University of Tokyo for more than three decades. SCC is defined as high-flow concrete with the ability to consolidate under its self-weight. ACI Committee 237 defines SCC as a cementitious material with high flowability and non-segregation characteristics which allow the concrete to be distributed in place and fill the mold as well as flow around the reinforcement without exhibiting any blocking (Liao et al. 2006). Furthermore, the usage of SCC in pre-cast and cast-in-place applications can result in reduced construction times and labor costs (Liao et al. 2006).

SCC has numerous properties that make it desirable and alternative to conventional concrete, these properties include:

- Filling ability: SCC can flow and fill formwork without vibration or compaction process. Common tests to calculate the filling ability of SCC in a fresh status are slump flow, U-Box, L-Box, and V-funnel tests.

- Segregation strength: Although they are high-flow, SCC has the ability to stay in a consistent matrix during mixing and filling. Some tests that can be used to determine segregation strength are the V-funnel test and visual observation during the slump flow test.

- Passing ability: SCC can flow through the narrow parts without blocking, or loss inhomogeneity. The tests that can be utilized to determine the passing capability of SCC are the V-funnel test, J-ring in combining with the slump flow test, L-Box, and U-Box tests.

Despite fibers can improve many conventional concrete properties, adding fibers in volumes more than 1.0% can produce problems in placement in the fresh- status. Therefore, one solution to this problem is to combine the use of SCC and steel fibers. Due to the high flowability of SCC, higher fiber ratios can be used without significant influence on workability.

There are several factors that affect the properties of SCSFRC, in the status of SCC the addition of fiber improves performance only within a limited range of fiber properties (L_f / D_f) and volume fractions (V_f), where researchers have shown that higher aspect ratios and volume fractions can lead to reduced flow-ability and the conclusive loss of SCC properties (Liao et al. 2006). Despite flowing and filling ability of SCC usually decrease whenever fibers are added to the SCC, researchers found that the flow-ability can be maintained at medium fiber contents. Whereas, higher fiber contents (usually $V_f > 2\%$) produce a loss in properties of SCC (Grunewald,2004).

Other factors that can affect flow-ability of the SCC are the maximum aggregate size, the percentage of the coarse and fine aggregate in the concrete. The use of larger aggregate size can produce fiber "balling" and lastly lead to loss of SCC properties (Swamy & Mangat, 1974; Johnston, 1996; Grunewald, 2004). In addition, increasing the coarse aggregate content also results in reduced workability. Therefore, in order to maintain the acceptable performance of SCSFRC in the fresh-status, it requires reducing quantities of certain materials such as the fiber amount,

the maximum aggregate size, and the coarse aggregate amount (by increasing the fines-to-aggregate proportion).

1.4 Research Significance

Previous experimental investigations have indicated that adding a sufficient amount of steel fiber in concrete significantly improves the shear capacity and ductility capacity of the SFRC prismatic beam. In addition, the result Parra-Montesinos (2006) recommended that a minimum steel fiber amount by 0.75% in order to substitute for minimum shear reinforcement which was implemented in the 2008 edition of the ACI-318 code, and permits the usage of SFRC to replace a minimum shear reinforcement in a prismatic beam. Whereas for a haunched beam, there is no study involving the usage of steel fiber, thus one of the objectives of this study is the possibility of replacing a minimum shear reinforcement using the amount of steel fibers. The use of steel fiber is able to facilitate the casting of the haunched beam because of its ease of placement as compared to the placement of stirrups. Moreover, it is more economical as compared to conventional haunched beam fabrication, where the workmanship and material costs of reinforcement processes were significantly reduced. Steel fiber reinforced concrete haunched beams require a detailed information and research, where there is no information about design rule and mechanical behavior of SCSFRC haunched beams. Moreover, the orientation of steel fiber affects the mechanical characteristics of concrete significantly, and this leads to uncertainty in various the mechanical properties of SCSFRC. Therefore, detailed research is required about steel fiber reinforced concrete haunched beam to find out what is new in this field.

1.5 Aims of Research

The objectives of this thesis introduce an extensive study about the RCHBs, the main aims can be summarized in following:

1-To study the mechanism of the shear strength behavior of self-compacting steel fiber reinforced concrete (SCSFRC) without shear reinforcement for the prismatic and haunched beam.

2- To examine whether the use of 1 percentage volumetric ratio of steel fibers as a substitution to shear reinforcement in haunched beams will provide sufficient strength compare to the reinforcement bars used as a minimum shear reinforcement.

3- To study variations in shear behavior between the prismatic and haunched beams using self-compacting fiber reinforced concrete (SCSFRC) without stirrups.

4- To study the influence of some variables on the shear strength capacity like a change in the inclination angle and the steel fiber ratio.

5- To investigate crack modes and crack width of each beam.

1.6 Thesis Organization

Chapter one, presents information about the topic and gives summary information about the RCHBs and steel fiber reinforced concrete (SFRC) as well as self-compacting concrete with fibers. The objectives of the thesis and research significance are also of the research objectives.

Chapter two, provides a comprehensive review of the literature on this topic.

Chapter three, summarizes the specifics of the experimental study, which includes material properties, a design of specimens, test setup, and the test procedures for all beams, as well as summarizes the specifics of the experimental program, which includes material properties, beam properties, and test preparation.

Chapter four, summarizes the experimental results of all the prismatic and haunched beams tested in the experimental study and discusses the experimental results, and compares them to check the effect of some variables on the mechanical behavior of shear strength of SCSFRC haunched beams.

Chapter five, presents the summary, conclusions, and recommendations for research in the near future.

CHAPTER 2

LITERATURE REVIEW

2.1 Overview

This chapter submits a background of shear behavior for the reinforced concrete haunched beams without shear stirrups. Initially, the review starts with the experimental study available around the RCHB. Although there are a few previous articles on the subject, they give clear indications that recognize their behavior compared to prismatic beam. It also highlights the effect of some parameters on haunched beams. The experimental study available on the haunched beams took into consideration the effect of most parameters and showed their effect on mechanical behavior. However, these studies did not examine the usage of steel fibers instead of the minimum shear reinforced on this type of beams. Since the structural behavior of SFRC members is dependent on the mechanical properties of the fiber, these fibers can be considered as an enhancement material because they are randomly distributed in all parts of the concrete. Adding fibers to concrete significantly promote shear strength. The effective range of fiber reinforcement to increase shear strength depends on many factors that include the matrix properties, fiber properties (material properties, aspect ratio, and type), and fiber ratio.

In literature, it appears that fiber can partially replace the shear reinforcement for the prismatic beam. Therefore, some researchers confirm the advantage of fibers in industrial applications. It was expected that the minimum shear reinforcement requirement can be replaced with fibers in sufficient quantity. Indeed, fibers have been able to replace the minimum transverse reinforcement for a prismatic beam that achieves the minimum standards of shear strength in design codes (Parra, 2008).

2.2 Previous Studies about Reinforced Concrete Haunched Beams (RCHBs)

The first researchers who have studied the shear behavior of RCHBs were Debaiky and Elniema. The study consisted of more than 30 reinforced concrete beams to

examine the behavior of RCHBs, a number of these beams were prismatic and the rest were haunched beams. The studied parameters were various such as, concrete strength, shear span, the inclination of haunch, beam geometry, and proportion both of flexure and shear reinforcement. The researchers concluded that beams that have increased the depth at the support did not improve the shear strength capacity. The nominal shear contribution of the concrete and the longitudinal bars were affected by the haunch's inclination, whereas the nominal contribution of the stirrups was not (Debaiky and Elniema 1982).

In (1983), Stefano produced an experimental investigation of shear strength of RC haunched beams. Experimental work consisted of beams that were without and with the stirrups for two types of inclination cases, as shown in Fig 2.1. All beams were simply supported, and tested at three load point. The work discussed the performance of international building codes. The results were contradictory and unsatisfactory (Stefanou 1983).

Macleod and Houmsi, in 1994 published another paper, where they investigated regarding the shear strength of RCHBs. The work described six full-scale RCHBs where the angle of inclination was varying degrees. The researchers summarized that decreasing the volume of concrete in a shear span due to increasing inclination angle lead to improved shear strength capacity and produced ductile failure (Macleod and Houmsi 1994).

Nghiep (2010) examined the shear design of RCHBs without stirrups, all of the RCHBs had one mode which was inclined upper surface and tested under focused load at mid-span, as shown in Fig. 2.2. The main result was that the inclination angle had a significant effect on the shear strength capacity (Nghiep 2011). Another researcher (Carlos Zanuy et al. 2015) submitted results of RCHBs without stirrups, which were tested using load fatigue. Two types of failure modes have been obtained, either due to fatigue of reinforcement or due to shear fatigue. The study concluded that the RCHBs without shear reinforcement is able to afford fatigue.

The recent experimental work studied the mechanical behavior of different types of RCHBs that were published by (Albegmprli et al. 2017). The experimental program included 24 beams divided into 3 prismatic and 21 haunched beams. The parameters studied in this study were varied such as the inclination angle, the proportion of

inclined reinforcement, shear reinforcement and the shape of the beam, as shown in Fig. 2.3. The study examined the influence of the design variables on the shear strength like inclination angle, inclined reinforcement, material properties, and shape mode. In addition, the researcher concluded that the inclination angle and the inclined reinforcement were the most influential parameters on the behavior of RCHBs.
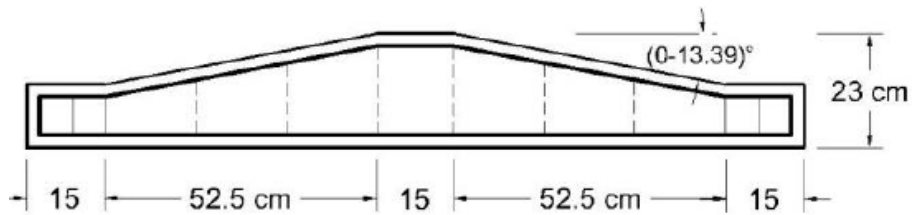
Figure 2.1 Experimental Tested Beams by [Stefanou (1983)]
[Adapted from Albegmprli (2017)]
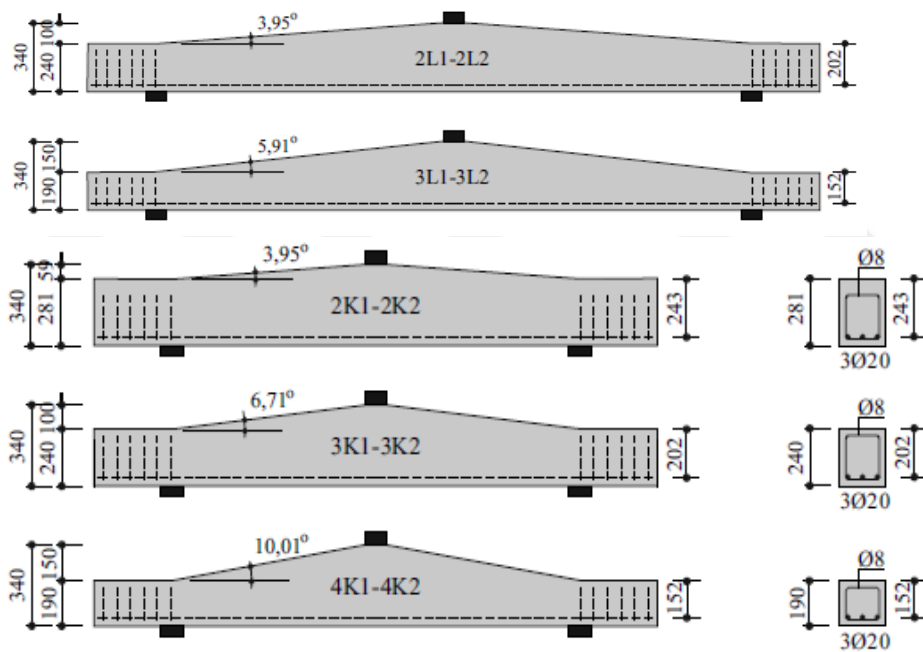
Figure 2.2 Experimental Tested Beams by [Nghiep (2011)]
[Adapted from Nghiep (2011)]
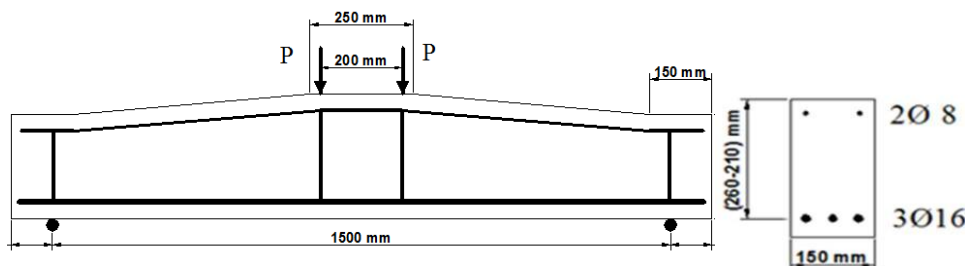
Figure 2.3 Experimental Tested Beams by [Albegmprli (2017)]
[Adapted from Albegmprli (2017)]

10

2.3 Shear Behavior of RC Beams

2.3.1 Introduction

Generally, beams without shear reinforcement fail in shear shortly after the formation of diagonal shear cracks. Therefore, it is necessary to determine the strength of shear concrete accurately. This concrete contribution to resistance is a function of several parameters such as cross-sectional geometry, beam dimensions, loading, and material properties. The concrete contribution to resisting the shear is considered insufficient, therefore modern codes must require additional shear strength in the form of transverse steel reinforcement.

2.3.2 Classification of RC Beam Behavior

The failure of a prismatic reinforced concrete beam without shear reinforcement is strongly affected by the beam's length-to-depth proportion (*a/d*). The behavior can be grouped into three groups as a function of the (*a/d*) proportion:

- Deep Beams: Beams with a short length $(1 < (a/d) < 2.5)$ called a deep beam. In these beams, the load is resisted by a combination of redistribution of internal forces and arch.

- Slender Beams: Beams that have a length-to-depth proportion within a range of 2.50 to 6 are called slender. In slender beams without stirrups, the development of the inclined cracks affects the equilibrium between internal strength and applied load, and the beam will fail quickly after forming the flexure-shear cracks.

- Very Slender Beam: Beams that have a length-to-depth proportion not more than 6. In these beams, failure may occur in flexural before the forming of inclined shear cracks.

It is common that researchers have described failure mechanisms based on the primary failure crack modes, as shown below and in Fig. 2.4 :

- Flexural failure.

- Shear-Tension failure.

- Diagonal-Tension failure.

- Shear-Compression failure.
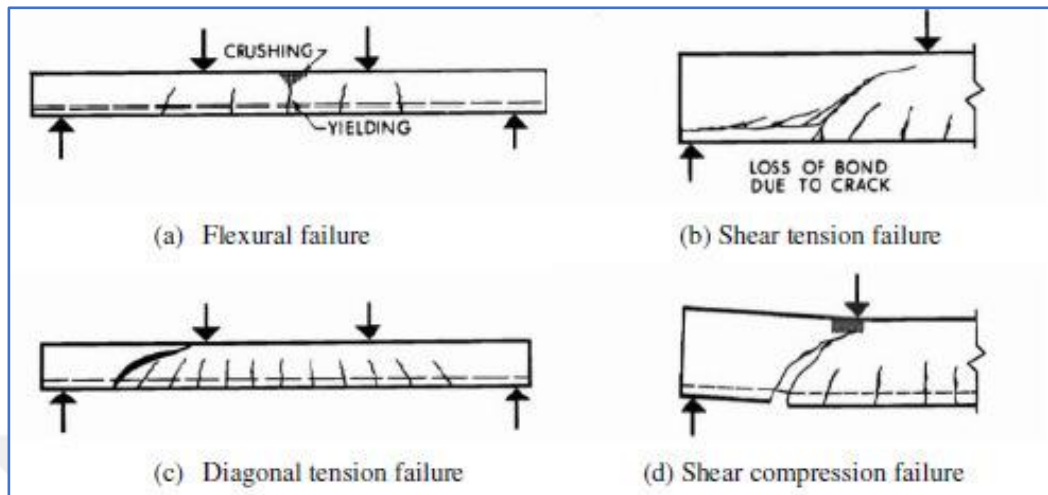
Figure 2.4 Beam failure modes [Adapted from Dinh (2009)]

2.3.3 Factors that Affect Shear Strength Mechanisms in Beams Without Stirrups or Shear Reinforcement

In slender beams without stirrups, the failure occurs directly when the shear cracks appear. Therefore, the shear capacity of these beams is controlled by the inclined shear cracking load. In addition, this capacity is affected by several factors, like the compressive strength of the concrete, shear length-to-depth proportion, the amount of longitudinal reinforcement, axial load, beam size, etc.

2.3.3.1 Compressive Strength of Concrete

Compressive strength is one of the important factors affecting the shear strength capacity of reinforced concrete beams. The concrete contribution of shear strength is directly affected by the diagonal tension capacity of the concrete. When the diagonal shear tension exceeds the tension capacity of concrete the diagonal shear cracks will be formed. It is noticeable that in the case of normal-strength concrete, the concrete strength is less than the aggregate crushing strength, the crack path generally will go around the aggregates; therefore the shear strength is improved due to the rough and uneven surface of the crack. Whereas, in the case of high-strength concrete, the

12

cracks may go through the coarse aggregates instead of passing around them; this will make the fracture surface smoother, and reduce aggregate interlock so it may lead to reduced shear capacity (Sherwood, 2008).

2.3.3.2 Longitudinal Reinforcement

The proportion of longitudinal reinforcement bars (ρ) is another factor which has an effect on the shear strength capacity of beams without stirrups. Research has found that increasing the longitudinal reinforcement proportion (ρ) produces an improvement in the shear strength capacity of reinforced concrete beams. Comparing two equivalent beams, but with a different longitudinal reinforcement ratio (ρ), with respect to the beam with a low reinforcement ratio the results of tensile strains were greater, crack widths were wider and shear strength was lower compared to the beam with a high reinforcement ratio. This decrease in shear capacity is likely to be due to a decrease in aggregate interlock as (ρ) reduces (Sherwood, 2008). In addition, as the proportion of the longitudinal reinforcement increase, it may lead to an increase in dowel action, leading to the high capacity of shear strength (Dinh, 2009).

2.3.3.3 Shear Span-to-Depth Proportion

The shear span-to-depth proportion (*a/d*) has an important effect on the mechanisms governing the failure of reinforced concrete beams. In deep beams (*a/d* < 2.5), the redistribution of stresses occurs and produces a development in arch action, and the larger shear stresses are transferred to the supports by the compression struts (Wight and MacGregor, 2009). Because of the complex nature of this type of failure mechanism, these beams are the best model using struts and tie models or other analysis techniques. Whereas, beams that have a small (*a/d*) proportion can withstand higher shear stresses compared to slender beams (*a/d* > 2.50). Moreover, the proportion value of shear span-to-depth has less effect on shear strength capacity in beams that have (*a/d*) larger than 2.50.

2.3.3.4 Beam Size

For a beam without shear reinforcement, increased the depth lead to reduce the shear stress at failure if all other properties are kept constant. Further increasing the beam depth leads to an increase in crack widths which reduces the maximum concrete shear stress that is moved through the crack by aggregate interlock which in turn

reduces the shear capacity (Wight and Macgregor, 2009). Studies have shown that the effect of size has less effect on shear strength in beams with shear reinforcement or containing longitudinal reinforcement distributed well along the depth.

2.3.3.5 Axial Force

In the absence of shear reinforcement in a beam, studies have exhibited that the shear strength capacity is influenced by the application of axial load. The application of external compressive axial load contributes to the reduction of longitudinal strains, thus reducing the width of the crack, leading to an increase in shear capacity. On the other hand, the application of axial tension forces on the beam directly increases the stress and longitudinal strain, which can increase crack widths and reduce shear capacity.

2.3.3.6 Other Parameters

Other parameters that may influence the shear strength capacity of reinforced concrete beams include:

- Load status such as focused load, uniformly distributed load or non-uniform

- Cross section shape.

- Distribution of longitudinal reinforcement bars along the beam depth.

- Use a reduced size of aggregate.

- Use lightweight concrete.

2.4 ACI 318 Shear Design Provisions

In North America, Mörsch proposed the formation of a 45° truss model which became the basis for the shear design guidelines. The model assumes that the shear cracks formed at an angle of 45°, which allows engineers to assess the shear strength capacity of a reinforced concrete element with stirrups. This simplified model still forms the basis for the shear strength expressions provided by stirrups in several design codes, including the current ACI code (Sherwood, 2008). However, this model supposed that shear strength should be provided only by reinforcing the shear

and ignored the contribution of the concrete to shear strength. Therefore, research has begun to measure this concrete contribution. Based on these research efforts, the value of experimental shear stress 0.03 f'_c (psi) was proposed to calculate the "safely" shear contribution provided by the concrete, V (Sherwood, 2008). Along with the simplified truss model of Mörsch, this concrete contribution derived that empirically formed the basis of the ACI shear design provisions in the 1950s. Large beams are designed without shear reinforcement based on the supposition that they can resist the "safe" working shear stress of 0.03 f'_c (Sherwood, 2008). Significant research has begun to develop a reliable and safe model for calculating the shear strength provided by concrete. Based on a considerable database of empirical information, a simplified expression was suggested for predicting the shear strength capacity of concrete used in 1963 ACI code Eq. (2.1). This equation with 194 points for experimental data used in the suitable curve that was drawn in Fig. 2.5 (Sherwood, 2008).

$$\frac{V_C}{b_w\,d} = 0.142\sqrt{f'_c} + 17\frac{\rho_w V_d}{M} \leq 0.29\sqrt{f'_c} \qquad \text{(MPa)} \qquad (2.1)$$
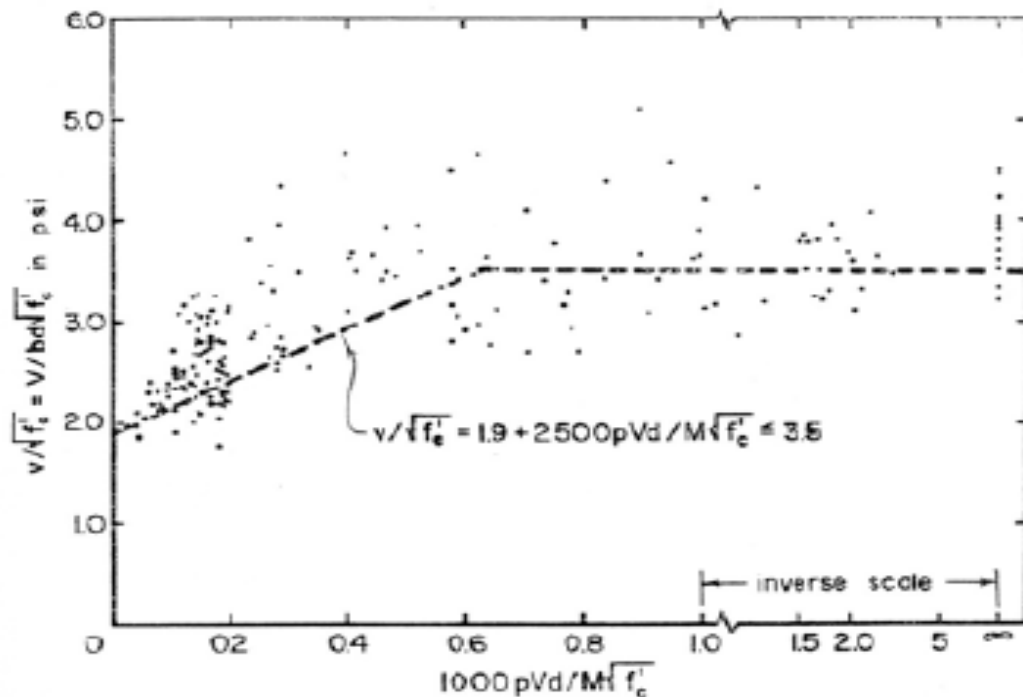
Figure 2.5 Plot showing derivation of ACI 318 shear equation [Reproduced from ACI Committee 326 (1962)] [Adapted from Dinh (2009)]

15

For most practical beam configurations values ($1000\ \rho\ Vd\ /M\ \sqrt{f_c'}$) are located to the left of Fig. 2.5, and therefore, Eq. 2.1 can be simplified to the following formula, a simplified formula used in the current shear provisions of the ACI 318 code (ACI Committee 318, 2008).

$$V_c = 0.167\sqrt{f_c'}\,b\,d \qquad\qquad (MPa) \qquad\qquad (2.2)$$

2.5 Shear Strength of Haunched Beams

Despite the widespread use of these members in the concrete structures, there were little investigations into their behaviors under the shear. Absolutely most codes do not provide any guidance for the design of such structures except the ACI code and the German DIN code.

In part 11.1.1.2 of ACI code 318−05, the expression "effects of inclined flexural compression" was used to illustrate the various stress distribution of RC haunched beams compared to the prismatic beams. The stress distribution leads to a shear force as a perpendicular component of inclined flexure stresses.

The German code DIN 1045-01 shows the shear mechanism of RC haunched beams and gives detailed design guides in the part 10.3.2 (4). The formula of the shear design for RC haunched beams is shown as follows;

Where:

$$V_{ED} = V_{Ed0} - V_{ccd} - V_{td}\ - V_{pd} \le V_{Rd}^\alpha \qquad\qquad (2.3)$$

V_{Ed0} : Shear force caused by live and dead loads,

V_{ccd} : Shear strength is caused by an inclination of the compression chord of a beam,

V_{td} : Shear strength component for longitudinal inclined bars,

V_{pd} : Shear strength component of pre-stressed force,

V_{Rd}^α: The value of shear carrying capacity of RC haunched beams at design section.

For elements without prestressing and horizontal longitudinal tension bars, where the values of V_{pd} and $V_{td} = 0$, thus the formulation of the design shear strength becomes as follows;

$$V_{ED} = V_{Edo} - V_{ccd} \leq V_{Rd}^{\alpha}$$

or in another form:

$V_{EdO} \leq V_{Rd}^{a} + V_{ccd}$ The value of V_{ccd} is defined as follows;

$$V_{ccd} = \frac{M_{Ed}}{0.9d} . \tan\alpha$$
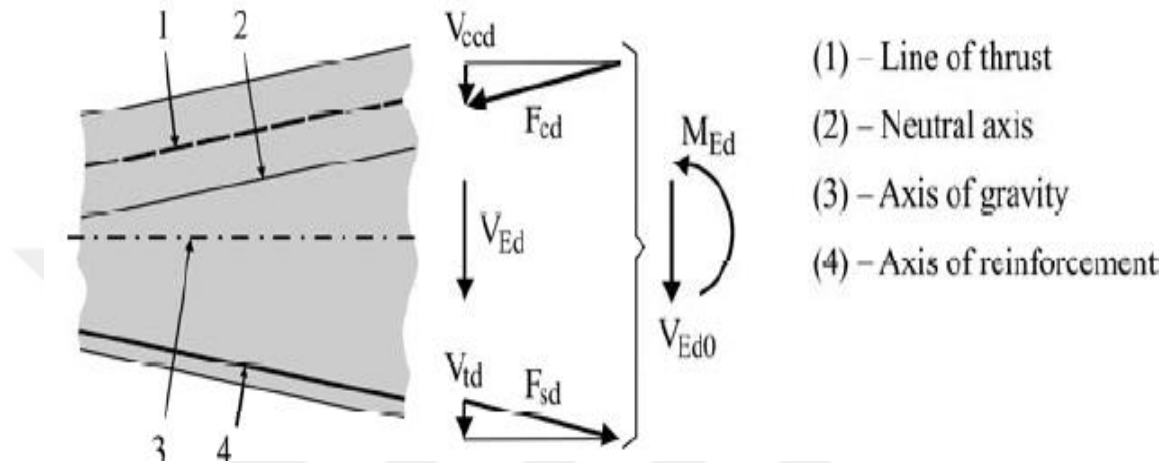
Figure 2.6 Components of Shear Strength for the Haunched Concrete Elements
[DIN 1045-01(2001)] [Adapted from Nghiep (2011)]

With respect to other codes which did not mention the shear design of haunched beams concrete elements, these elements are generally divided into many periods with average depths to maintain the same stiffness of the main structures. Therefore, this technique might acceptable for flexural design, however it has been found to be inaccurate for shear design due to shear failure is usually a result of a diagonal crack that has been shown to be affected by structures geometry properties.

Mörsch in 1922 was the first author who carried out test specimens for haunched concrete beams. Fig. 2.7 shows the design of test specimens.

The test results showed that the load capacity of the haunched specimen number 1034 ($\alpha \approx 18.5°$) without shear reinforcement was 20 % less than the prismatic specimen number 1027. The results show that the specimen number 1037, with shear reinforcement in the support area has a much larger load capacity than the specimen number 1034 without the shear reinforcement as shown in Fig. 2.7.
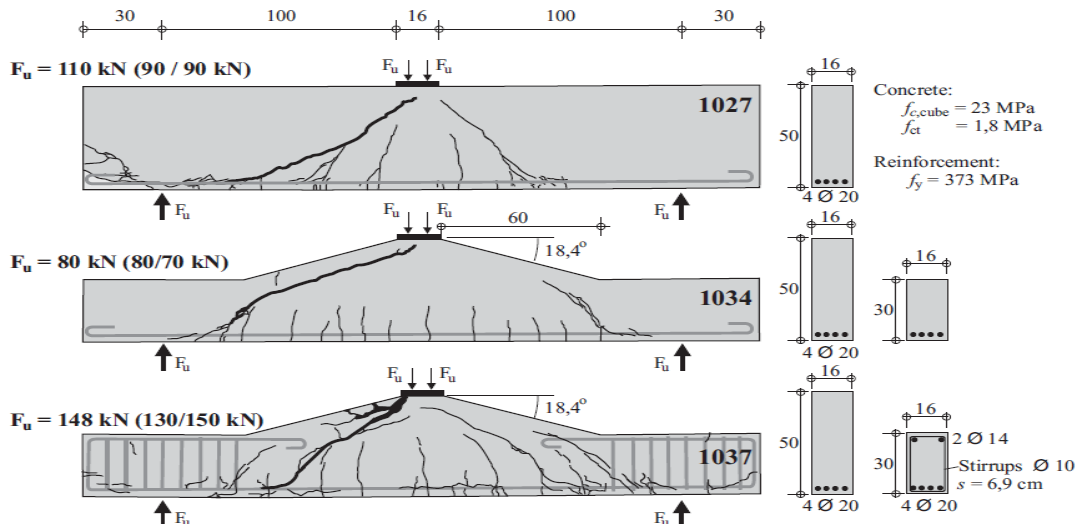
Figure 2.7 Tests Beams Examined by Mörsch (1922) [Adapted from Nghiep (2011)]

Debaiky et al. (1982) continued to study and investigate the shear strength behavior of reinforced concrete haunched beams. After performing 33 exams of RC beams with various inclinations as shown in Fig. 2.8. The researchers found that there was no significant change in the magnitude of the load that caused the first crack. They Also found that the critical shear crack began in many locations for beams that have different inclinations. In addition, the researchers proposed that the shear contribution in concrete was affected by the inclination of the haunched beam, which can be determined by the following equation;

$$V_{Rm}^a = 0.1661\sqrt{f_c'}\,(1 + 1.7\tan\alpha)b\,d \qquad\qquad (2.5)$$
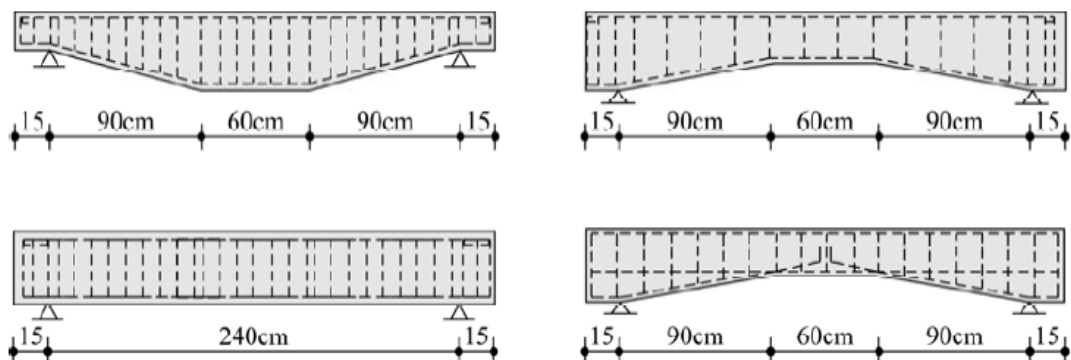
Figure 2.8 Test Beams Examined by Debaiky et al. (1982) [Adapted from Nghiep (2011)]

18

Since the mentioned equation is formulated in the same form as in ACI's equation, therefore it can understand that the inclination of the haunch beam increases the shear strength capacity by the expression (1+1.7tanα). It can also be observed that a series of tested beams that were with shear reinforcement and designed so that the haunched part of the beam is down tension stress, whereas the straight part is down compression stress. This design was unusual because most of the haunched beams were practically designed in the manner that the haunched part is in the compressed region.

MacLeod et al. (1994) suggested a formula for determined the shear strength capacity of RC haunched beams without stirrups. Mainly, this method was based on the formula proposed in the German Code DIN (1045-01) with a new proposition on the section that should measure shear strength. As a result, factor (F') was taken to provide another formula for shear strength capacity of RC haunched beams without stirrups as following;

$$V_{Rm}^a = V_{pc} + \frac{M_{Ed}}{d_{cr}} F'. \tan\alpha \tag{2.6}$$

Where: V_{pc} : The concrete shear strength capacity of parallel beam specimen with effectual depth (d_0) based on section (3.4.5.3) of the BS (8110) as follows:

$$V_{pc} = V_c. b. d_{cr}$$

$$V_c = \left(\frac{0.79}{1.25}\right)\left(\frac{f_{c'}}{25}\right)^{0.33}\left(\frac{100A_s}{b.d_{cr}}\right)^{0.33}\left(\frac{400}{d_{cr}}\right)^{0.25}$$

$f_{c'}$: The concrete compressive strength of cubic sample

M_{ED} : Bending moment in the critical section of the depth beam (d_{cr})

(d_o, C_h, S & α) are shown in fig. 2.9.

$$M_{ED} = V_C. b. d_{cr} C_h$$

$$F' = 0.27(1 + \tan\alpha)^{10}$$

The critical section is shown as in the Fig. 2.9

The effectual depth (d_{cr}) at the critical section as fallows $d_{cr} = d_o + (C_h - S).\tan\alpha$

$$C_h = d_o + \frac{d_o(1 + \tan\alpha) - S.\tan\alpha}{0.68 - \tan\alpha} \approx 2.7d_o$$

The authors also conducted six tests of haunched beams with inclination angles in the range of 5° to 10° to examine the proposed formula as shown in Fig. 2.9. Although the proposed formula factually did not give a perfect agreement with the results obtained, it is known that the preparation of these exams showed the working conditions of RC haunched beams practically as the haunched part is down compression.
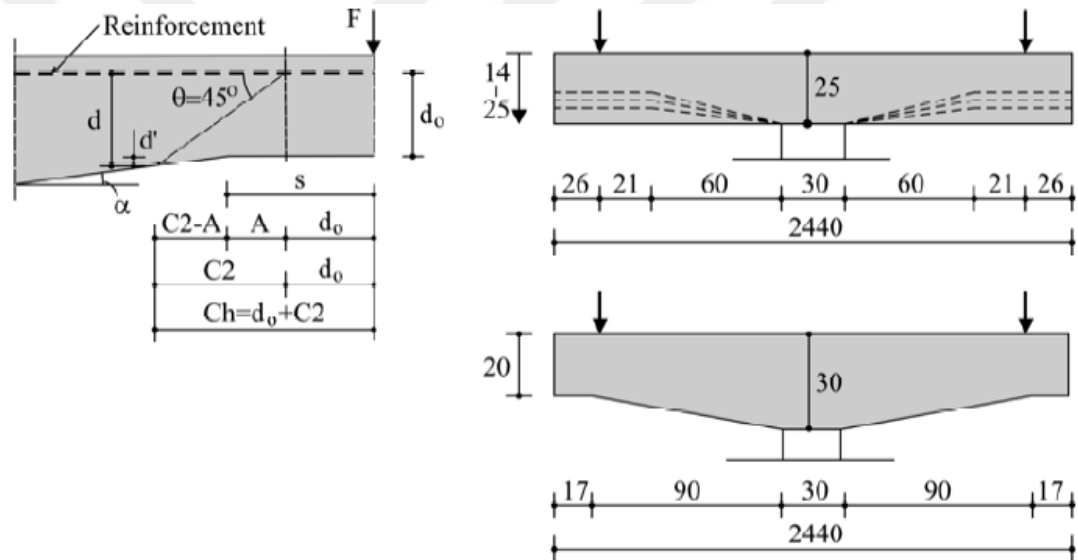
(a) Critical Shear Section   b) Examine Beams

Figure 2.9 Critical Shear Section and Examine Beams by MacLeod et al.(1994)

[Adapted from Nghiep (2011)]

The recent equation has been suggested to estimate the shear strength of RCHBs by (Nghiep, 2011). The proposed equation was derived and investigated using 14 RCHBs, and all beams are inclined at the compression part. The expression of the formula as follows:

$$V_{Rd}^a = 7\left(\frac{f_{ck}}{a}\right)^{1/4}.\rho_l^{1/3}.(1 + \tan\alpha)b.d$$

Where:

(c) Compressive strength of concrete,

(a) Shear-span length,

(ρ_t) Flexural longitudinal reinforcement proportion,

(α) Inclination angle of the haunched beam,

(d & b) Depth and width of the critical section, respectively.

2.6 Shear Behavior and Modeling of SFRC and SCSFRC Beams

2.6.1 Previous Research about Shear Behavior of SFRC Prismatic Beams

Shear strength is one of the possible applications of SFRC in the beams, as a result of the absence of previous studies on the usage of steel fibers in the haunched beams, it is necessary to refer to previous investigations about the usage of these fibers in the prismatic beams to compare these two types of beams. Research conducted over the past three decades has exhibited that the usage of steel fibers in reinforced concrete beams can be applied to enhance the shear strength. Adding fiber to a concrete beam without shear reinforcement improves shear behavior because of the ability of SFRC to support and redistribute diagonal tension stresses after cracking. In addition, the fiber can bind cracks and control their expansion. This can be explained by the fact that the fibers are very similar to traditional shear reinforcement. As a result, the use of fiber leads to an increase in the shear strength of the beam, and can enhance flexure failure and ductility. If fibers are added in appropriate quantities, it is probable to substitute traditional transverse reinforcement, and enhance flexural failure and ductility. In (2006), Parra-Montesinos presented a large database of test results that included results from 16 studies of SFRC beam. The results exhibited that all SFRC beams in the database contain $V_f \geq 0.5\%$ showed shear stress capacity at failure greater than ($0.17\sqrt{f_c'}$) equivalent to V which is known in the ACI-318 code (ACI, 2008), for beams containing $V_f \geq 0.75\%$ shear stresses capacity at failure was not less than $0.3\sqrt{f_c'}$. Based on the experimental evidence reported in the literature, the use of fibers in flexural elements has been permitted in some international design codes.

2.6.2 Models of Predictive Shear Strength for SFRC Prismatic Beams

Over the past three decades, some researchers have suggested formulas to estimate the shear strength of SFRC prismatic beams. These formulas include models proposed by Sharma (1986), Ashour et al. (1992), Narayanan and Darwish (1987), Mansur et al. (1986) and others. It should be noted that most models have calculated the contribution of SFRC to shear strength using the so-called fiber factor (F) as shown in Eq. 2.7 is a function of the steel fiber ratio (V_f) and fiber aspect-ratio (L_f/D_f). Other models have used material tests to measure the improvement in tensile strength and enhance shear capacity.

$$F = V_f \frac{L_f}{D_f} \tag{2.7}$$

Most of these models have been concluded from empirical formulae derived from a regression analysis of limited experimental data. Therefore, the results obtained from these models are uncertain in many cases to assess the shear strength capacity in SFRC beams (Minelli, 2005). In particular, the model suggested by Sharma (1986) and recommended by ACI Committee 544 has been shown to be inaccurate. The model proposed by Minelli and Plizzari (2006) modified the shear strength capacity formula given in Eurocode 2. In this formulation, a toughness parameter is used to modify the longitudinal reinforcement bars proportion. Studies show that the usage of fibers enhances shear capacity and ductility in the same way as using longitudinal reinforcement bars uniformly distributed along a beam depth, Which also improves shear capacity.

In addition to the empirical models discussed above, many researchers suggested more rational models for estimating and predicting the shear response of SFRC beams. The models of this group include the Variable Engagement Model (VEM) suggested by Voo and Foster (2003), and the strain-based shear strength model developed by Choi et al. (2007). Both models showed to result in more exact predictions of shear strength when compared to the empirically-based equations, although they generally require more computational effort.

2.6.3 Design Guidelines for Usage of SFRC in Prismatic Beams

The usage of steel fiber as a complete alternative for stirrups or shear reinforcement is still a matter of discussion due to the complexity and lack of a clear understanding of the shear contribution for the steel fiber in beams with and without stirrups. Another reason is the absence of confidence and accuracy of code-based equations to estimate the shear strength capacity of SFRC prismatic beams. However, some codes in North America and Europe permit guidelines for using SFRC in beams as shown in the Table (2.1).

Table 2.1 Abstract of some design guidelines for the shear strength of SFRC prismatic beams [Adapted from Cohen (2012)].

Design Guideline	Design Equation
RILEM TC-162 TDF σ-*w* method	$Vu = Vc + \sigma_{pd}(w_m).b_z$
RILEM TC-162-TDF σ-ε method	$V_u = V_{cd} + 0.7k_f k_1 \tau_{fd} b\, d$ where $\tau_{fd} = 0.12\, f_{Rk,4}$
DaftStb German Guidelines	$V_u = V_{cd} + 0.7k_f k_1 \tau_{fd} b\, d$ where $\tau_{fd} = 0.37\, f_{Rk}{}^f$
Swedish Betongrapport nr 4	$Vu = V_{cd} + V_{fd}$
Norwegian Recommendations	$Vu = V_{cd} + 0.8\, f_{ftd,res}\, b\, d$
Italia Recommendation	$V_u = \left[\dfrac{0.18}{\gamma_c} k \left(100\rho_1 \left(1 + 7.5\dfrac{f_{Ftuk}}{f_{ctk}}\right) f_{Ck}\right)^{1/3} + 0.15\sigma_{CP}\right] b\, d$
ACI 318 (2008	No Equation

2.6.3.1 ACI 318 Code

The 2008 publication of the ACI-318 code was the first code in North America that permitted the use of SFRC rather than shear reinforcement in beams. In particular, the code permits the limited usage of steel fiber as a replacement for the minimum shear reinforcement in certain conditions (ACI Committee 318, 2008).

In terms of the steel fibers, clause 3.5.8 specifies that the steel fibers should have a length-to-diameter proportion within a range of 50 to 100.

 At the material level, ACI code 318 clause 5.6.6.2 permits that SFRC will be suitable for shear strength if the coming conditions are met;

- The fiber weight per cubic meter should be ≥ 60 kg/m^3, which is equivalent to a volume fraction of 0.75%.

- According to the ASTM C1609 four-point bending test, the residual strength acquired at a mid-span displacement of (1/300) of the span must be more than or equal to 90% of the first maximum strength calculated from the flexural test, or 90% of the value (f_r) computed using Eq. (2.8), which one is bigger.

- In the same flexural test and at mid-span displacement of (1/150) of the length span, the calculated residual strength must be $\geq$ 75% of the first maximum strength obtained from the same test, or 75% of (f_r) computed using Eq. (2.8), which one is bigger.)

$$f_r = 7.5\lambda\sqrt{f_c'} \qquad\qquad (2\text{-}8)$$

In terms of the use SFRC as a replacement for the minimum transverse reinforcement, clause 11.4.6.1(f) permits the use of hooked fibers if the following conditions are met;

- The concrete strength (f'_c) must not overtake 41 MPa.

- The beam depth (h) must not overtake 610 mm.

- The maximum shear stress V_u must not overtake $\emptyset 2\sqrt{f_c'}\, b.d$

2.6.4 Previous Research on Shear Behavior of SCSFRC Prismatic Beams

There is much previous research that focused on the development of SCSFRC mix designs. In particular, there are some studies in the literature related to the use of SCSFRC in the prismatic beam. In (2008), Greenough and Nehdi conducted a study consisting of 13 slender SCSFRC beams with shear span-to-depth proportion (*a/d*) ≥ 3 and a ratio of steel fiber ranging from (0.5-1.0%). There were three different types of steel fiber used in this research and one of these types was hocked-end. The researchers concluded that the addition of steel fibers promotes the shear behavior of SCC beams, with results showing that addition 1.0% of fiber leads to a 128% increase in shear strength capacity. In addition, the researchers also presented a new experimental formula by modifying the traditional ACI code shear equation (see Eq. 2.9). Furthermore, the researchers of this the study also presented another equation that modifies the previous equation of shear strength capacity on RC slender beams developed by the same researchers (see Eq. 2.10).

$$V = \left(0.167\sqrt{f_c'} + \alpha F \rho \frac{d}{a} + 0.9\eta_0 \tau F \right) b.d \tag{2.9}$$

$$V = \left(0.35 \left(1 + \sqrt{\frac{400}{d}} \right) f_c'^{0.18} + \left((1+F)\rho \frac{d}{a} \right)^{0.4} + 0.9\eta_0 \tau F \right) b\,d \tag{2.10}$$

Where (a) is taken as (1 N/mm2), (η_0) represents the steel fiber orientation factor, (F) represents the fiber factor, (ρ) represents the reinforcement proportion, (*d*) and (*b*) are the depth of the beam and its width, respectively. It is noticed in previous models that the fiber contribution to shear strength has taken into consideration the use of fiber factor (F).

Finally, there are some published data on the behavior of plain SCC beams in shear. Lachemi et al. (2004) examined a group of 18 prismatic beams using self-compacting concrete (SCC) and the concrete type was normal (NC), this study demonstrated that reducing the gravel size from 19 mm to 12 mm leads to

decrease in maximum shear capacity. Similarly, comparing the behavior of both normal concrete (NC) and self-compacting concrete (SCC) shown that the SCC beams reduced shear strength capacity compared to the NC beams. In both cases, behavior was related to a reduction the contribution of coarse aggregate interlock when using smaller aggregates or lesser aggregate content.

2.6.5 Shear Behavior of SCSFRC Beams

As discussed above, the addition of steel fibers to plain concrete mixtures leads to problems in workability and placement, especially when high fiber ratio is used. The usage of self-compacting concrete (SCC) has been suggested to reduce these problems and facilitate placement. SCC can flow in place or in the mold under its weight without vibration, and without the appearance of bleeding and segregation. Generally, studies have shown that the use of high-flow SCC mixture can maintain the properties of self-compacting when adding fibers at low or medium ratios, whereas reasonable workability can remain at higher fiber ratios (with little loss of self-compacting concrete properties) (Aoude, 2008).

2.7 Conclusion

In general, the use of steel fibers gives significant advantages for reinforced concrete a beam. For example, it can convert the failure mode from diagonal shear to flexural, in addition sudden failures in beams can be stopped even if the failure mode is shear because these fibers help to tie the cracks in the concrete matrix. Moreover, the addition of fiber increases the load capacity and ductility of reinforced concrete prismatic beams. The use of steel fiber in beams needs to detailed research on the fiber reinforced concrete beams.

Some researchers implemented experimental studies on SCSFRC prismatic beams. The researchers investigated several mechanical properties such as load-bearing capacity, failure mode, and ductility of SCSFRC prismatic beams as well as the possibility of replacing the minimum shear reinforcement using a certain ratio of steel fibers. They also proposed an empirical equation that modifies the conventional ACI code shear equation.

Whereas there is no study regarding the use of steel fibers in SCSFRC haunched beams with a lack of design guidance in practical codes despite its popularity.

Therefore, there must be sufficient attention to these structures in order to enhance understanding of their behaviors as well as to present design instructions with greater reliability. Significant advantages of steel fiber reinforced concrete haunched beams require detailed information and research, where there is no information about the design rule and mechanical shear behavior of SCSFRC haunched beams as well as the possibility of replacing traditional reinforcement for minimum shear reinforcement. Therefore, detailed research on steel fiber reinforced concrete haunched beam is required to discover more information. For these reasons, the experimental study in this thesis will be implemented on prismatic and haunched beams using self-compacting concrete (SCC) and steel fibers (SF) to add an initial database to the literature about the mechanical shear behavior of these elements in order to open scientific fields to discover shear design models for practical codes which are dependent on the experimental approach.

CHAPTER 3

EXPERIMENTAL WORK

3.1 Introduction

Generally, an experimental study is the best way to verify the actual behavior of structural members of reinforced concrete. Therefore, many researchers studied the shear behavior of the structural elements such as prismatic beams, columns, and other members using self-compacting concrete (SCC) and steel fibers (SF) ; in the fact, some researchers have investigated in haunched beams, but there is no research in the literature to study the mechanical behavior of haunched beams using SCC and SF. Therefore, the experimental data were not found for this type of beam using SCC and SF. Self-compacting concrete (SCC) can be used to reduce the probability of reducing the workability and to facilitate the concrete casting when adding high fiber content. This chapter will introduce an experimental study in detail. This experimental study is interested in studying the mechanical behavior of reinforced concrete haunched and prismatic beams using self-compacting concrete (SCC) with the addition of steel fiber and without shear reinforcement.

The experimental study in this thesis consists of nine SCSFRC beams divided into three groups depending on the percentage of steel fiber. Each of these groups consists of one prismatic and two haunched beams with two different angles. In general, constant parameters for all groups were beam size, shear span-to-effective depth proportion, compressive strength of concrete, and longitudinal reinforcement proportion. The first variable parameter was the steel fiber ratio, which was changed to observe the mechanical behavior of all beams whereas the second variable parameter was the inclination angle of the beam. This experimental study included preparation, casting, and testing of nine simply supported beam (prismatic and RCHBs) constructed using self-compacting concrete (SCC) and steel fiber (SF). This

chapter summarizes the details of specimens and material properties.

3.2 Objectives

The experimental study aims to:

1. Investigate the mechanical performance of reinforced concrete haunched beams compared with prismatic beams using self-compacting concrete and steel fiber (SCSFRC).

2. Investigate the shear strength crack modes and the potential enhancement of cracks control for self-compacting fiber reinforced concrete (SCSFRC) beams.

3. Investigate whether SCSFRC can be used as an alternative traditional shear reinforcement in haunched beams.

4. Determine the inclination angle of the shear failure and locate the critical section.

5. Study the influence of the hooked end steel fiber ratios on shear strength capacity, displacement capacity and failure mode.

6. Provide recommendations for the future experimental study using steel fiber in haunched beams.

3.3 Materials and Mix Design.

3.3.1 Concrete Mix Design

In this study, a number of experimental mixtures were produced for three types of concrete mixtures used in this study. These mixtures were divided into three mixtures: two mixtures were constructed with self-compacting steel fiber reinforced concrete (SCSFRC) and another mixture was constructed using self-compacting concrete (SCC). The crushed stone aggregate was used to prepare the mixture design. Gravel and sand were used from the same source to achieve the properties of SCSFRC. Therefore, the gravel gradient size was between (4-11) mm, and the sand was passed from sieve 4 mm to achieve the properties of SCSFRC. Portland cement (type 32.5R) and fly ash (type F) were used in this study. Table 3.1 clarifies the chemical composition of fly ash and cement, fly ash was 83% of cement content in all mixtures.

The mixtures were designed as a medium compressive strength of concrete, which was one value nearly 40 MPa, the real concrete strength was calculated by testing three cubes after 28 days from the date of each specimen casting. Moreover, each mixture achieved all the requirements set by the steel fiber reinforced normal strength self-compacting concrete guide (EFNARC0).

The quantities of cement, fly ash, fine aggregate, coarse aggregate, steel fibers, and water were calculated according to the compressive strength required using experimental mixtures. However, the amount of fiber required was calculated based on the specific gravity of the fiber calculated by the product.

Table 3.1 Chemical Composition of Cement (type 32.5R) and Fly Ash (type F).

Chemical analysis	SiO_2	Fe_2O_3	CaO	$A_{l2}O$	MgO	SO_3	$Na_2O + K_2O$
Cement	20.4	3.9	63.0	4.9	1.7	2.0	0.9
Fly ash	56.2	6.69	4.24	20.17	1.92	0.49	2.36

3.3.2 Steel Reinforcement

One size of deformed reinforcement bars was used in this experimental study. The longitudinal steel reinforcement consisted of 3- φ 12 bars. The purpose was to ensure that the specimen will fail in shear and not in flexure. Therefore, a medium reinforcement proportion of 1.57% was selected for longitudinal bars and without using the upper longitudinal steel bars as well as without using shear reinforcement. The properties of the main reinforcement bars were determined from three samples of the bar (φ12). The samples were taken randomly from bars package of steel reinforcement. Bars tests include yield strength (f_y) and ultimate strength (f_u); the bars were tested using the universal tension test machine as shown in Fig. 3.1. The yield strength of the bars was determined, which were 485 MPa and the ultimate strength was 595 MPa.

Figure 3.1 Reinforcement Bar Test

3.3.3 Steel Fibers

There was one type of steel fibers, type (Dramix 35/45 BG) that was used in this experimental study. Nine beams were examined in this study, which were divided into three series: the first series consists of three specimens without steel fiber as control beams (SCC), whereas the second and third series consists of six specimens with steel fibers (SCSFRC). Generally, typical fibers have a length of 35 mm with hooked ends and a diameter of 0.75 mm, so an aspect proportion (Lf / Df) is 45. The steel fibers were collated into packing by the dissolvable glue as shown in Fig. 3.2. In addition, these steel fibers were manufactured from normal strength steel wire. Mechanical properties of this type are given in Table 3.2.

Different ratios of steel fibers were used in reinforcing the beam specimens in order to investigate the influence of fiber content on the shear strength of SCSFRC beam. There were three ratios of steel fiber: without fibers 0%, 0.5%, and 1% (as volumetric). The selection of these ratios is due to a review of previous studies that showed that the usage 1.0% of steel fibers was sufficient to replace the minimum shear reinforcement with respect to the prismatic beam and able to convert the failure mode from shear to flexural. In addition, the usage of fiber ratios between 1% and 2% can increase the shear strength slightly. In other words, enhancement of shear properties of specimens that have steel fiber ratios from 0.5% to 1.0% was greater

compared with specimens with fiber ratios from 1.0 to 2.0%. As a result, 1.0% fiber ratio was taken as the acceptable ratio.

As steel fibers reduce the workability of the concrete, therefore superplasticizer type (sika viscocrete sf 18) was used to produce self-compacting concrete mix design with the addition of fiber within the range of (1.66% -1.917%) of cement weight. Amounts of ingredients are given for 1 m^3 concrete (0% SF), (0.5% SF) and (1% SF) in Tables (3.3- 3.5), respectively.

Figure 3.2 Steel Fiber Hook-end

Source http://www.tsyajs.com/en/news.php?id=94

Table 3.2 Mechanical Properties of Steel Fiber Type 3D 35/ 45BG

Fiber Type	DRAMIX 3D 45 /35 BG
Length	35mm
Diameter (D)	0.75mm
Aspect Ratio (*Lf / Df*)	45
Tensil Strength	1,225N/mm2
Minimum Dosage	30Kg/M^3
Fiber Network	7,85 Fiber/Kg
Presentation of Fiber	Glued

Table 3.3 Ingredient Amounts for the Production of 1 m^3 Concrete (f_{cu} is 40 MPa)
(0% Steel Fiber) (SCC)

Material	Gravel	Sand	Cement	Fly Ash	Steel fiber	Water	Visco-Crete
Kg/m^3	730	900	300	250	0 kg	170	5

Table 3.4 Ingredient Amounts for the Production of 1 m^3 Concrete (f_{cu} is 40 MPa)
(0.5% Steel Fiber) (SCSFRC)

Material	Gravel	Sand	Cement	Fly Ash	Steel fiber	Water	Visco-Crete
Kg/m^3	730	900	300	250	39,25	170	5,5

Table 3.5 Ingredient Amounts for the Production of 1 m3 Concrete (fcu is 40 MPa)
(1 % Steel Fiber) (SCSFRC)

Material	Gravel	Sand	Cement	Fly Ash	Steel fiber	Water	Visco-Crete
Kg/m^3	730	900	300	250	78,5	170	5,75

3.4 Geometry and Reinforcement Details of Tested Beams.

In this thesis, nine beams were prepared, poured, and examined. These beams are divided into two types: three of beams were prismatic and six beams were haunched beams which have the same mode haunched beams and have two different angles of inclination (10°and 15°), which were inclined at the upper part along the shear spans. The depth of the RCHBs was decreased at the support, as shown in (Figs. 3.4-3.5). The geometries of all the beams were selected to give more reliable. In detail, all beams have 1200mm length, 120mm width and the depth is variable along the shear span. Effective depth was varied from 180 mm to 75 mm along the member axis and the depth at the mid-span was constant of 210 mm. The geometry and steel reinforcement details for all the beams are shown in Table 3.6.

The shear span (a) of all the beams was equal to 455 mm, as shown in Table 3.7. Consequently, the proportion of shear span to effective depth was fixed at (2.527) in order to occur the shear failure for all beams.

All beams were designed without steel stirrups in order to maintain the beam stability during concrete casting, the longitudinal reinforcement bars were hooked to up by 90° behind the supports and connected by two stirrups φ 6 mm at each end in order to prevent the potential of bond failure that can occur during the testing process.

To achieve the effective concrete cover, special spacers were placed in specific positions of the formwork, and so the depth of effective concrete cover was 25 mm. All these details are shown in the Fig. 3.6.

3.4.2 Designation of Beams

The designation of a haunched beam consists of three parts, for example (B5-H10-0.5):

- The first part (B5) indicates to the beam number in the series.
- The second part (H10) consists of two part, the first part (H) indicates to the haunched beam and the second part (10) indicates to the value of the inclination angle in degree.
- The third part (0.5) indicates to the percentage value (%) of the steel fiber.

While the designation of a prismatic beam is similar to the designation of haunched beam except for the second part, which consists of a character (P) that indicates to the prismatic beam, for example (B7-P-1).
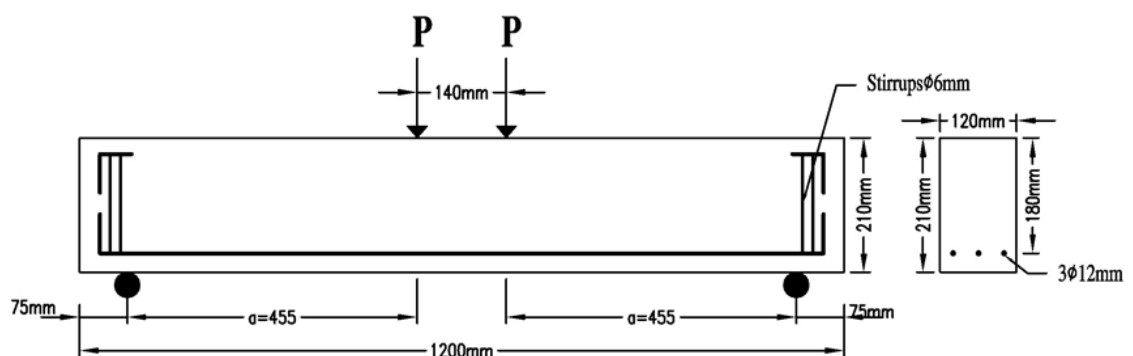
Figure 3.3 Geometry of Prismatic Beams
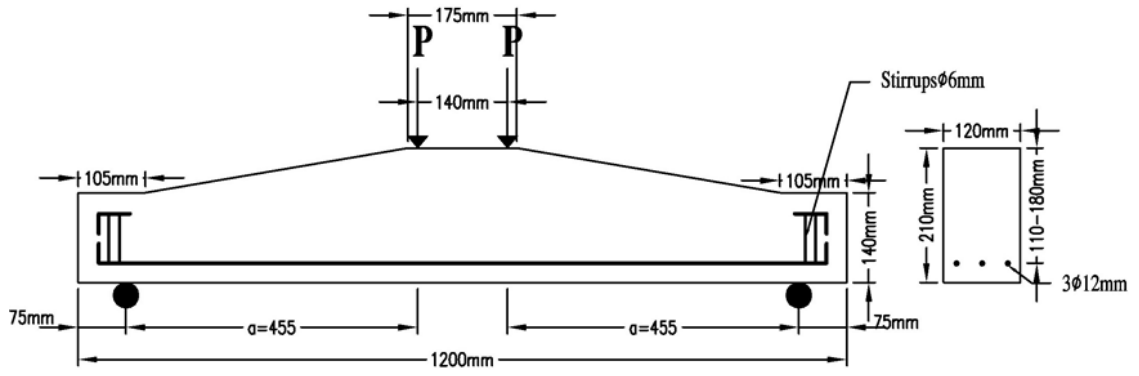
Figure 3.4 Geometry of Haunched Beams (Angle 10)
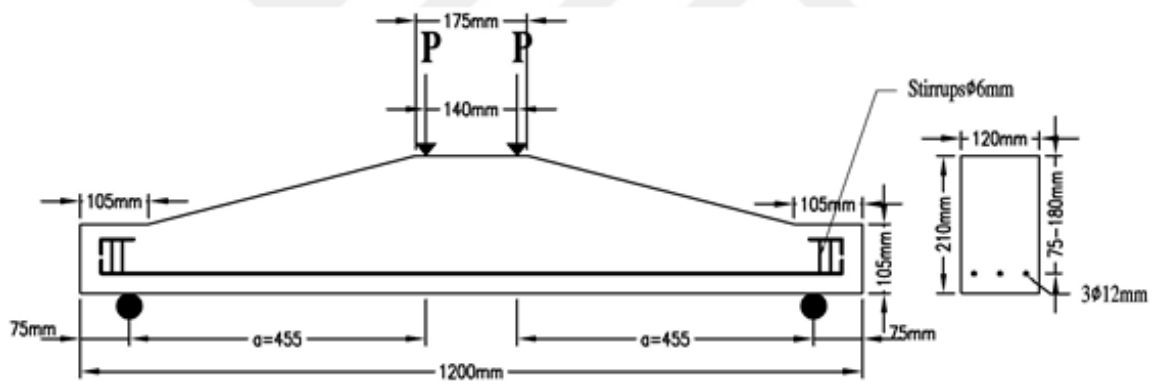
Figure 3.5 Geometry of Haunched Beams (Angle 15)

Table 3.6 Geometry and Steel Detail for Prismatic Beam and RCHBs.

Beam Code	$\alpha°$	$h_{f\,(mm)}$	$h_{S\,(mm)}$	Steel Reinforcement	Area of Steel A_s $_{(mm^2)}$	Steel Fiber Ratio (V_f) %
B1-P-0	0	210	210	3 φ 12	340	0
B2-H10-0	9.74	210	140	3 φ 12	340	0.5
B3-H15-0	14.45	210	105	3 φ 12	340	1
B4-P-0.5	0	210	210	3 φ 12	340	0
B5-H10-0.5	9.74	210	140	3 φ 12	340	0.5
B6-H15-0.5	14.45	210	105	3 φ 12	340	1
B7-P-1	0	210	210	3 φ 12	340	0
B8-H10-1	9.74	210	140	3 φ 12	340	0.5
B9-H15-1	14.45	210	105	3 φ 12	340	1

$\boldsymbol{\alpha}°$: Angle Inclination of Haunched

$\boldsymbol{h_f}$: Depth at Middle

$\boldsymbol{h_s}$: Depth at the Supports

Table 3.7 Beam Dimensions

Beam	Dimension (mm)
Width	120
Effictiv debth	180-75
a/d	2.5
Shear Span	455
Distance between Two Load	140
Total Length	1200
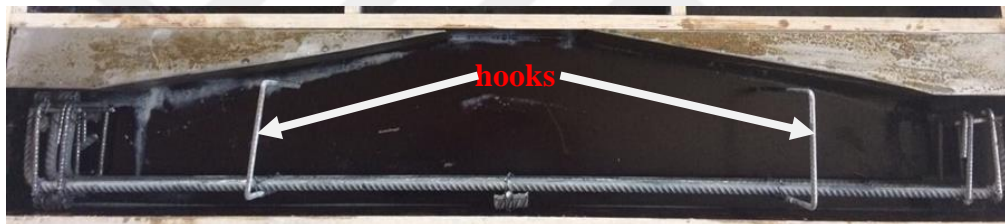
Figure 3.6 Preparing the Reinforcement

3.5 Preparation of Beams

All beams formwork made of plywood and prepared in Gaziantep University laboratories. Large attention was given to formwork for the initial install to remove them easily after each concrete casting process. Each beam reinforcement was prepared and placed in the formwork, and install two steel hooks for each beam to facilitate transportation during water curing and testing. A typical formwork and reinforcement configuration of experimented beams as shown in Fig. 3.7.

Self-compacting concrete mixtures without and with steel fiber were used to cast all beams. The concrete is poured using a mixer with capacity 0.12 m3, as shown in Fig.3.8. Dry mix procedures were implemented to prepare SCC and SCSFRC. First, the fine and coarse aggregates were mixed for 2 minutes. Similarly, the cement was

added and mixed for 2 minutes, then fly ash was gradually added to the mixture. The superplasticizer was mixed with water and added to the mixture gradually. Steel fiber was the last material added to the mix to ensure a suitable mixing and distribution of steel fibers into fresh concrete. Finally, the whole mixture was mixed for 3 minutes before emptying into the formwork. It was noted that the sequence of adding ingredients was accurate in order to achieve the required workability in all types of mixtures. The properties of SCSFRC were determined by slump follows T50 as shown in Fig. 3.9.

Figure 3.7 Formwork and Reinforcement Configuration for Experimented Beams.

a.0.12m^3 Capacity Mixer   **b**. Steel Fiber Reinforced Concrete
in Concreting Process

Figure 3.8 Concrete Mixing
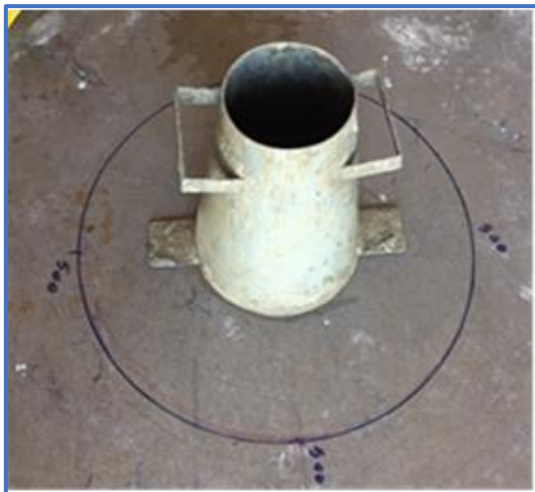
a. The Preparation of Slump Test   **b**. The Test of the Slump Flow

Figure 3.9 Fresh Properties Tests of SCSFRC

Each beam was cast from one batch of fresh concrete produced by the mixer. After complete mixing, concrete is poured directly into the formwork. At the end of the casting, the concrete face was modified in order to obtain a smooth face using trowel as shown in Fig.3.10.

In each casting process of the beam specimen, 4 cubic samples were cast that were divided into two sizes: the first consists of 3 cubes by 100*100*100 mm, whereas the second consist of 1 cubic with dimension 150*150*150 mm to determine the compressive strength of concrete. Moreover, for each batch concrete were cast 3 samples of cylindrical, with dimension 100*200 mm to calculate the splitting tensile strength of concrete. As a result, three cylinders and four cubes were taken for each beam casting. Beams and corresponding samples were treated in the same conditions. Before the concreting process, both the beams formwork and corresponding samples were painted with special grease to facilitate the opening process all formwork.
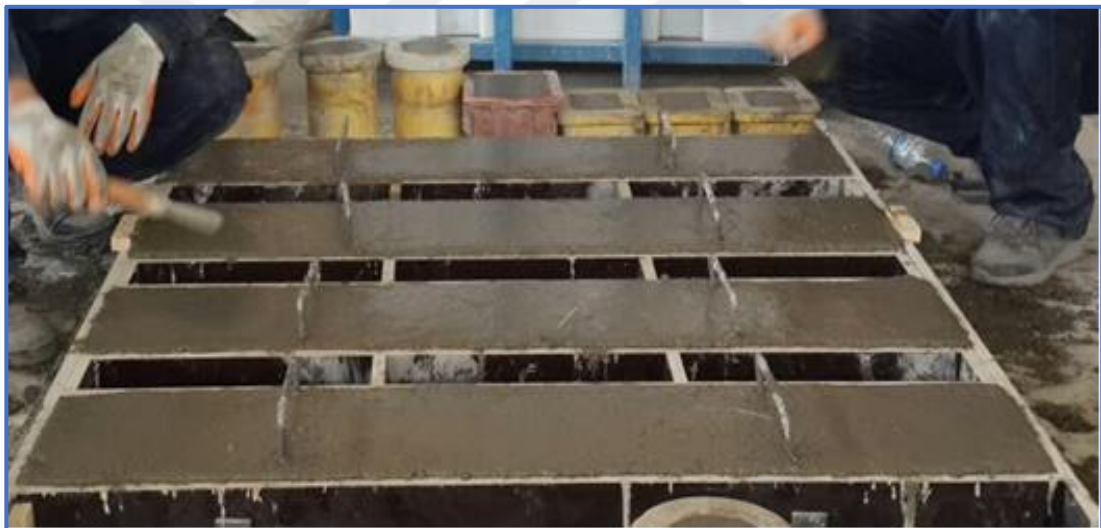
Figure 3.10 Beams and Samples of Cylinders and Cubes after Casting

During the casting process, there was no need to make the vibration for the beams that have steel fibers. All beams were removed from formwork exactly after one day of the casting process, thereafter all beams lifted to the curing tank by the coupling tool. Beams and corresponding samples were treated in the water curing tank for 14 days as shown in Fig. 3.11. Just before the test day, all beams were cleaned and painted with white cement paint. In addition, the front surface of all beams was outlined to determine the locations of the cracks that occur during the test.

Furthermore, each beam was numbered and placed in the testing machine in the correct location in order to prepare for the testing process as shown in Fig.3.12

Figure 3.11 Curing Tank

Figure 3.12 painting and Preparing Beams before Testing.

3.6 The Samples Prepare and Test

All corresponding samples for each beam were prepared to make the mentioned tests as shown in Fig. 3.13. The compressive strength of concrete was calculated according to BS 1881-116- 1983. A Compression test machine with 3000 kN loading capacity was used to examine the compressive strength with a rate of loading 4 kN/s as shown in Fig. 14. Similarly, according to ASTM C496 and EN 12390-6 that were used to calculate the indirect tensile strength (splitting test) as shown in Fig. 3.15.

Figure 3.13 Preparing the Samples
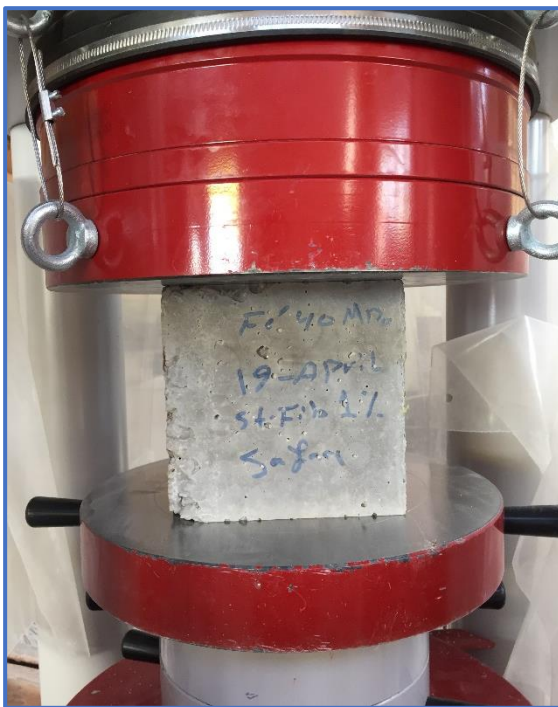
Figure 3.14 Compressive Strength Testing   **Figure 3.15** Splitting Testing

3.7 Test Procedures and Instrumentation

All beams were tested by 600KN capacity displacement controlled loading machine in the reinforced concrete lab at the University of Gaziantep. The load application was controlled by using a developed hydraulic system.

Initially, each beam was subjected to a slight load to ensure that the test setup and the machine are fully operational. The load was applied using two steel rods at mid-span. The displacement was gradually increased by an increment 0.2 mm/min using the hydraulic displacement sensor. After each displacement increase of 0.2 mm, the database was recorded such as the load, displacement, and crack propagation. The displacement was increased until the beam collapsed. Fig. 3.16 shows the loading procedure of the beam. Three displacement values for each specimen were recorded automatically by three differential transducers that were fixed along the bottom of the concrete beam and divided into three locations; the first transformer at the beam center, the second at the right portion and the last at the left portion as shown in Fig. 3.17.

The 9 beams were tested under four-point loads tangency using steel bars have 30 mm diameter. The load applied was at mid-span, the span between the load points 145 mm to ensure a stable moment region at the beam middle. The shear span was 455 mm, resulting in shear span to depth effectual proportion (*a/d*) of approximately 2.527. The span between the two supports was 1050 mm, one of the supports was fixed in order to prevent the horizontal friction. In addition, a number of instruments used to measure data by a load cell, three linear variable displacement transducers (LVDTs), a magnifying glass, and a high-resolution camera, these data consisted of applied load, displacement, and crack development.
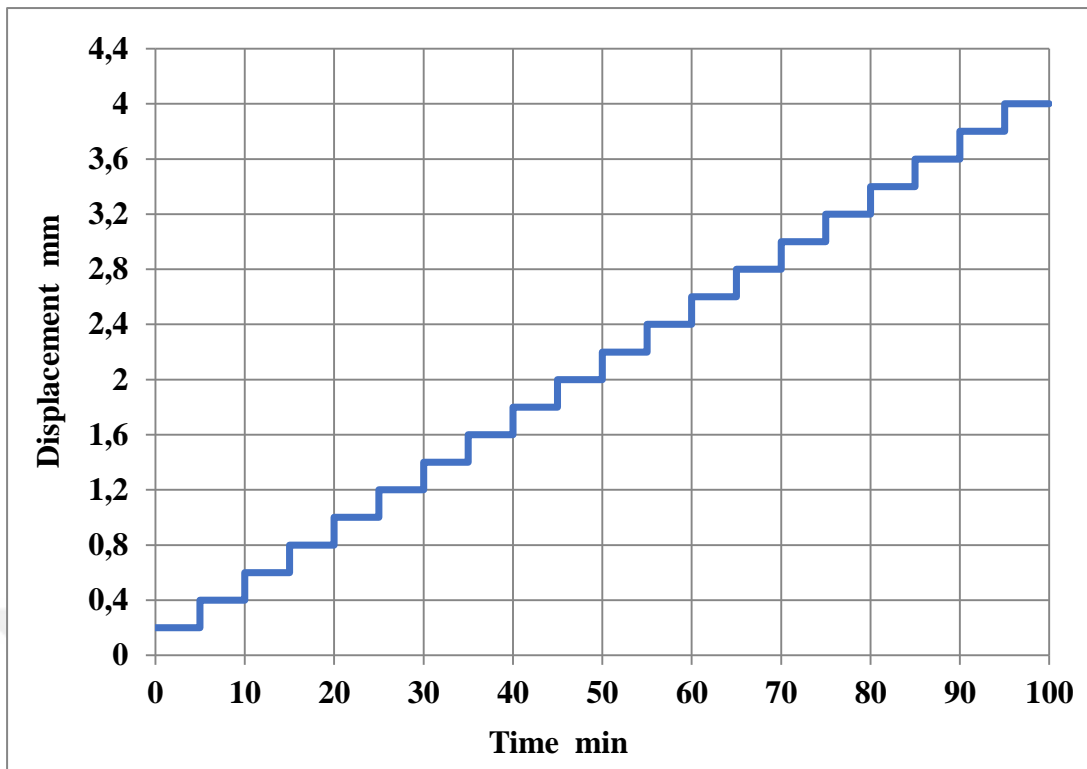
Figure 3.16 Loading Procedure
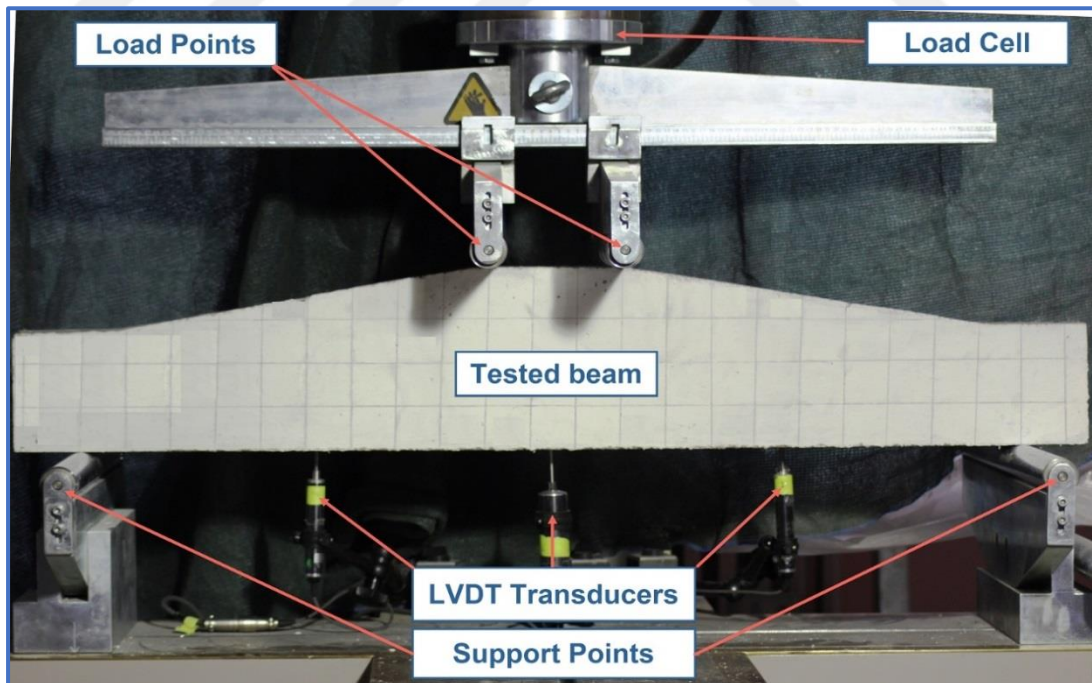
3.17 Figure Testing Installation of the Beam

CHAPTER 4

EXPERIMENTAL RESULTS AND DISCUSSION

4.1 Introduction

In this section, the behavior of three SCC and six SCSFRC beams were investigated in the experimental study. All beams were subjected to the same loading sequence, the testing process continued until the load value became less than 90% of the peak load value or until the maximum deflection reached 15 mm. All beams with corresponding samples were tested successfully. These beams are divided into three groups and each group has three different values of the inclination angle (0°,10°, and 15°) at the shear span. The first group without fibers (0%), the second group with 0.5% fibers and the third group with 1% fibers. Therefore, this study investigated the effect of two parameters on the shear behavior of reinforced concrete beams. This chapter will discuss the test results for all beams such as a failure mode, load-displacement, and crack width for all beams.

4.2 Shear Capacity, Load-Displacement Response & Failure Mode

This section compares both the maximum shear capacity, the load-displacement response, and the failure mode of the different beams that tested in this experimental study, and the explanation everything related to the effect of the different parameters such as the steel fiber ratio and the inclination angle of beams.

4.3 Testing Results

4.3.1 Material Properties

Each beam is expected to have a slightly different in the mechanical properties results of the concrete compared to the other beams due to the separate casting process of each beam. All beams were tested, and Tables (4.1-4.4) shows values the results of the testing such as compressive strengths (f_c'), tensile strengths (f_{ct}), the

load at first crack, first crack displacement, the load at the first shear diagonal crack, collapse load, a critical section of shear failure, maximum deflection at collapse load, collapse crack width, shear stress, the increase percentage in shear stress for each group and failure mode for each beam.

4.3.2 Failure Load

All beams were tested until the failure under displacement control. In (Figs. 4.1- 4.9) are shown all the crack modes results of the beams at load failure. Generally, the first group beams were designed as control beams that were without steel fibers using self-compacting concrete (SCC) and without shear reinforcement. Therefore, this group failed by shear as expected because plain concrete is brittle material. Suddenly, and without any warning, the diagonal shear crack appeared at the one portion of a beam connecting between the loading point and support location (at the shear span). It is noted that the load collapsed rapidly with the appearance of a diagonal shear crack.

The second group beams with (0.5%) fibers also failed in the shear diagonal crack, but carried loads approximately twice the load of the first group. The flexural and shear cracks gradually appeared, whereas there was some warning before the failure occurred. The three beams continued to carry an additional load despite the diagonal shear crack appeared.

Whereas the third group beams with (1%) fibers failed in flexural. These cracks were numerous, and there was no significant collapse in the load although the displacement has reached 15mm at mid-span. This group is unlike the first and second group due to the steel fiber has allowed to transfer the load across cracks. The post-cracking performance of the beam is related to the volumetric ratio of the steel fiber. It is noted that the beams of this group reached the ultimate strength, but the load did not drop as in the first and the second group. In other words, the steel fibers bridged the cracks and transferred the stress between the two faces of cracks. Therefore, beams were able to withstand against the applied load, but the load began to decline slowly when crushing of the concrete occurred in the upper face at the middle of beams, and soon appeared in the middle of the beam the flexural failure. The steel fibers provided significant ductility for the beams of this group. In other hands, soon appeared in the middle of the beam the flexural failure. The steel fibers

Provided significant ductility for the beams of this group. On the other hand, displacement was increasing and continued beams in carrying almost the same maximum load at the failure without a fall in a peak load. After this point, the load began to decrease slightly and displacement continues to increase. It can be seen from Figs.(4.4-4.9) that beams developed a greater number of cracks compared to the control specimens (first group). In addition, there were differences in the width of the cracks between the groups of beams as shown in Fig.4.10. Therefore, the result indicates that the redistribution of pressure into concrete was good. The modes of failure below will be discussed in brief. For each beam, the width of the first crack and crack at the failure was measured by the special apparatus as shown in Fig.4.11.
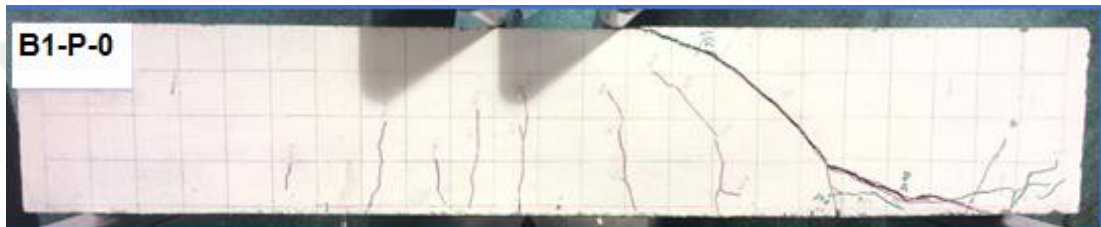
Figure 4.1 Shear Failure for Beam (B1-P-0)

Figure 4.2 Shear Failure for Beam (B2-H10-0)
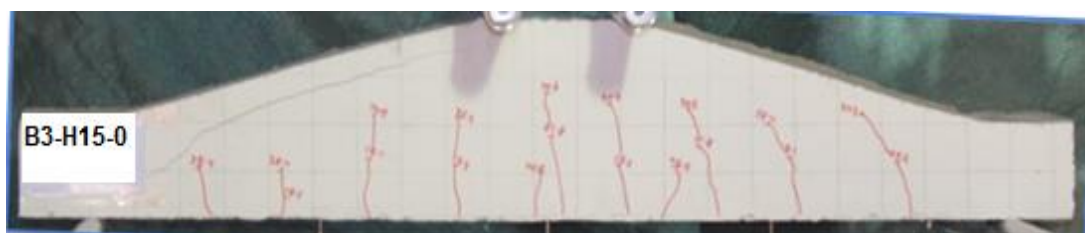
Figure 4.3 Shear Failure for Beam (B3-H15-0)

Figure 4.4 Shear Failure for Beam (B4-P-0.5)

Figure 4.5 Shear Failure for Beam (B5-H10-0.5)

Figure 4.6 Shear Failure for Beam (B6-H15-0.5)

Figure 4.7 Flexural Failure for Beam (B7-P-1)

Figure 4.8 Flexural Failure for Beam (B8-H10-1)

Figure 4.9 Flexural Failure for Beam (B9-H15-1)
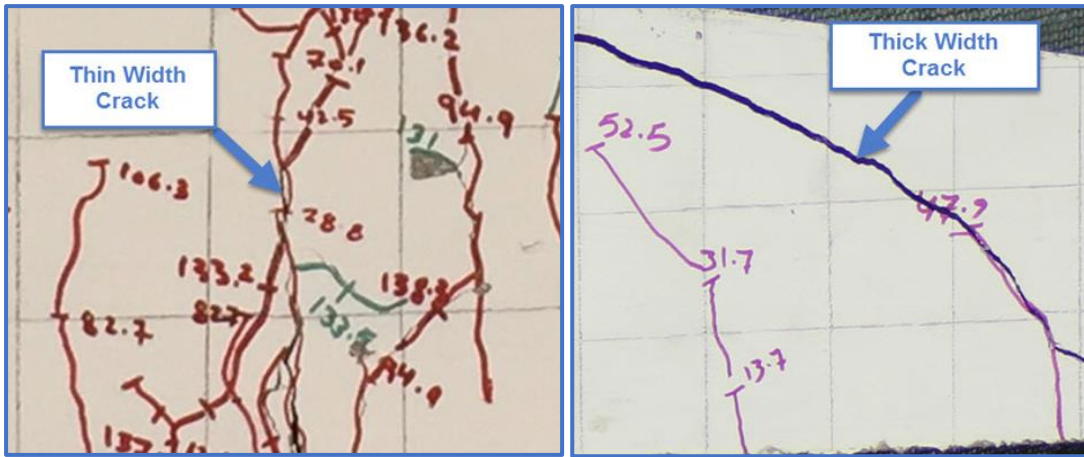
a- Thin Crack (1% Steel Fiber)   b- Thick Crack (0% Steel Fiber)

Figure 4.10 The Influence of Fibers Content on Crack Width at Failure
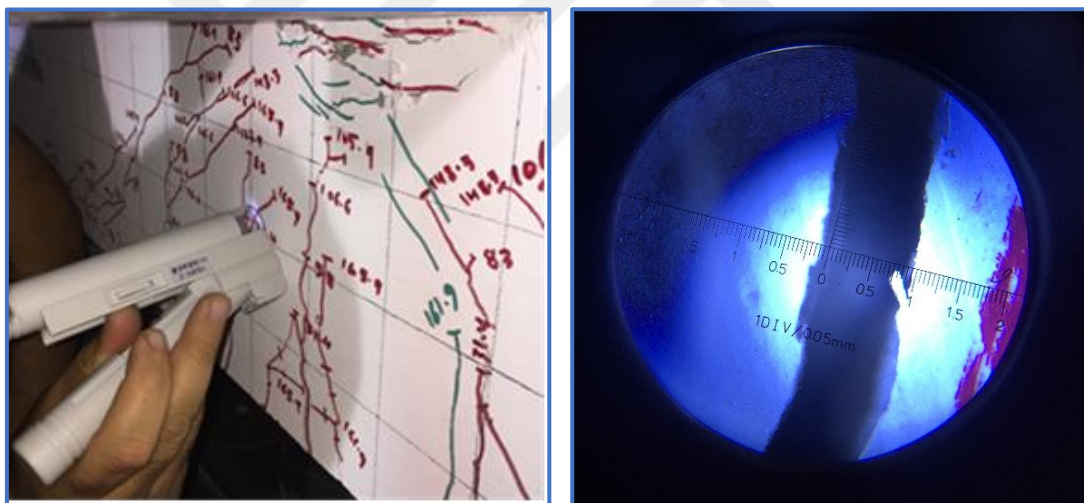
Figure 4.11 Measurement of the Crack

Table 4.1 Test Results of Beams.

Beam No.	f_c' (MPa)	f_{ct} (MPa)	First crack (kN)	First crack width (mm)	First incline crack (kN)	First shear diago. crack load (kN)	Max. Load 2P (kN)	Max. crack width (mm)	Fail. Mode
B1	47.96	3.82	12.6	0.25	41.8	54.34	54.34	1.80	S
B2	46.9	3.97	13.7	0.22	47.9	57.5	57.5	1.60	S
B3	44.50	3.77	13.3	0.22	34.3	49.56	49.56	1.30	S
B4	45.44	4.45	14.6	0.20	55.2	69.8	104.2	1.15	S
B5	39.50	4.53	32.8	0.18	64.1	73.5	109.6	1.15	S
B6	39.0	4.49	18.6	0.17	63.3	72.2	103.6	1.10	S
B7	39.60	5.05	37.3	0. 15	72.9	88.10	134.3	0.80	F
B8	40.0	5.10	18.8	0.14	67.3	82.00	140.5	0.70	F
B9	40.5	5.03	28.8	0.13	56.3	94.90	138.3	0.65	F

f_c' : compressive strength

f_{ct} : tensile strengths

S : Shear Failure Mode

F : Flexural Failure Mode

Table 4.2 Results Max. Shear Stress and Max. Displacement for Prismatic Beams

Beam Code	Shear Force at Max. Load V_c (kN)= P	Shear Stress at Max. Load V(N/mm^2) $V=V_c/b*d_{cr}$	Increase in Shear %	Critical Section (d_{cr}) (mm)	Max. Disp. at Max. Load (mm)
B1-P-0	27.17	1.258	-----	180	1.37
B4-P-0.5	52.10	2.412	92	180	4.60
B7-P-1	67.15*	3.109	147.2	180	5.98

*Beam Failed in Flexural

Table 4.3 Results Max. Shear Stress and Max. Displacement for Haunched Beams (H10).

Beam Code	Shear Force at Max. Load V_c (kN)= P	Shear Stress at Max. Load V(N/mm^2) $V=V_c/b*dcr$	Increase in Shear %	Critical Section (d_{cr}) (mm)	Max. Disp. at Max. Load (mm)
B2-H10-0	28.75	1.652	------	145	1.46
B5-H10-0.5	54.8	2.768	68	165	4.74
B8-H10-1	70.25*	3.252	97	180	8.60

*Beam Failed in Flexural

Table 4.4 Results Max. Shear Stress and Max. Displacement for Haunched Beams (H15).

Beam Code	Shear Force at Max. Load Vc (kN)= P	Shear Stress at Max. Load V (N/mm^2) V=Vc/b*d_{cr}	Increase in Shear %	Critical Section (d_{cr}) (mm)	Max. Disp. at Max. Load (mm)
B3-H15-0	24.78	1.795	-----	115	1.88
B6-H15-0.5	51.80	3.030	69	142.5	4.84
B9-H15-1	69.25*	3.206	79	180	8.98

*Beam Failed in Flexural

4.3.3 Load-Displacement Relationship

The displacement values were measured and recorded using three linear variable displacement transducers (LVDTs). Figs.(4.14-4.22) show the relationship between load and displacement at mid-span and at both portions of a beam. The shear capacity of the third group was the largest compared to the first and second groups.

In general, the addition of steel fibers helped to tie the cracks in the total concrete matrix and transport tensile pressures through two opposite faces of cracks until the fibers are completely broken or separated from the concrete. Addition steel fibers in concrete have improved the ultimate strength and have given a significant ductility to the beams in addition to having an effect on the failure mode. Below presents the detailed behavior of each beam during the testing.

4.3.3.1 Beam (B1-P-0)

This beam was the first specimen tested in the first group (control group). The first cracks were in the form of the flexural cracks at a load capacity of 12.60 kN, shear force (Vc= 6.30 kN) that occurred at the center of the specimen in the constant moment region, and the first crack width was 0.25 mm. The first flexural-shear crack occurred symmetrically on the shear spans of the specimen at a moment region, and the first crack width was 0.25 mm. The first flexural-shear crack occurred symmetrically on the shear spans of the specimen at a moment region, and the first crack width was 0.25 mm. The first flexural-shear crack occurred symmetrically on

the shear spans of the specimen at a load of 41.80 kN, shear force (Vc = 20.90 kN). At a peak load capacity of 54.34 kN, shear force (Vc = 27.17 kN) a sudden first shear diagonal crack appeared on the right portion of the specimen that was a brittle shear failure with a sudden drop in the load capacity, and this failure occurred without any warning. The test was stopped when the load capacity lost 45 % of the peak load. The maximum displacement at peak load in the mid-span was 1.37 mm. The maximum width of the diagonal shear crack at the failure was 1.8 mm.

4.3.3.2 Beam (B2-H10-0)

The first cracks were in the form of the flexural cracks at a load capacity of 13.70 kN, shear force (Vc = 6.85 kN) that occurred at the shear spans of the specimen, and the first crack width was 0.22 mm. The first flexural-shear crack occurred symmetrically in the shear spans at a load of 47.90 kN, shear force (Vc = 23.95 kN). At a peak load capacity of approximately 57.50 kN, shear force (Vc = 28.75 kN) a sudden first shear diagonal crack appeared on the right portion of the specimen that was a brittle shear failure with a sudden drop in the load capacity, and this failure occurred without any warning. The test was stopped when the load capacity lost 50 % of the peak load. The shear critical section was 145 mm. The maximum displacement at a peak load in the mid-span was 1.46 mm. The maximum width of the diagonal shear crack at the failure was 1.60 mm.

4.3.3.3 Beam (B3-H15-0)

This specimen was the last beam tested in the first group (control beams). The first cracks in the form of flexural cracks at a load capacity of 13.30 kN, shear force (Vc = 6.65 kN) that occurred in the middle of the specimen into the constant moment region and the first crack width was 0.20 mm. The first flexural-shear crack occurred in the right portion of the specimen at a load of 34.30 kN, shear force (Vc= 17.15 kN). At a peak load capacity of approximately 49.56 kN, shear force (Vc= 24.78 kN) a sudden diagonal shear crack appeared on the left portion of the specimen that was a brittle shear failure with a sudden drop in load capacity, and this failure occurred without any warning. The test was stopped when the load capacity lost 30 % of the peak load. The shear critical section was 115 mm. The maximum displacement at the maximum load in the mid-span was 1.88 mm. The maximum width of the diagonal

shear crack at the failure was 1.3 mm. As expected, the shear failure occurred before the flexural capacity because of the absence of stirrups reinforcement and steel fibers in this group.

4.3.3.4 Beam (B4-P-0.5)

This beam was the first specimen tested in the second group that contained 0.5% steel fibers. The first flexural cracks showed in the center of the specimen and in the constant moment region at a load capacity of approximately 14.60 kN, shear force (V_c = 7.30 kN), and the first crack width was 0.30 mm. The first flexural-shear cracks occurred symmetrically on the right and left shear spans at a load of 55.20 kN, shear force (V_c = 27.60 kN). At a load capacity of approximately 69.80 kN, shear force (V_c = 34.90 kN) a sudden diagonal shear cracks showed on the right and left shear spans, shear cracks began to expand along the specimen with the applicable load sequence. The flexural-shear cracks lastly large developed into the shear span which produced flexural shear crack failure on the right portion of the specimen at a load of approximately 84.20 kN, shear force (V_c = 42.10 kN). However, the specimen stayed withstand and carried the extra load until the failure that occurred at a peak load of approximately 104.20 kN, shear force (V_c = 52.10 kN), and the peak displacement in mid-span was 4.6 mm. This failure did not happen suddenly as there was a warning before the failure. The test was stopped when the load capacity lost 35 % of the peak load. The maximum width of the diagonal shear crack at the failure was 1.35 mm.

4.3.3.5 Beam (B5-H10-0.5%)

The first cracks showed into moment constant region and in the shear spans of the specimen at a load capacity of approximately 32.8 kN, shear force (V_c = 16.40 kN), and the first crack width was 0.18 mm. The first flexural-shear cracks happened symmetrically on the right and left shear spans at a load of 64.10 kN, shear force (V_c = 32.05 kN). At a load capacity of approximately 73.50 kN, shear force (V_c = 36.75 kN) a sudden diagonal shear cracks showed in the right and left shear spans, shear cracks begin to expand along the specimen with the applicable load sequence. The flexural-shear cracks lastly developed into the shear spans which produced shear crack failure on the left part of the specimen at a peak load of 109.60 kN, shear force (V_c = 54.80 kN), and the maximum displacement in mid-span was 4.74 mm.

The shear critical section was 165 mm. This failure did not happen suddenly, there was a warning before the failure. The drop of the beam was in two stages, where the first stage was inclined and the second stage was sharp. The test was stopped when the load capacity lost 33% of the peak load capacity. The ultimate width of the diagonal shear crack was 1.10 mm.

4.3.3.6 Beam (B6-H15-0.5)

The first crack happened in the center of the specimen and in the shear span region at a load capacity of 18.60 kN, shear force ($V_c = 9.30$kN), and the first crack width was 0.17mm. The first flexural-shear cracks occurred symmetrically in the right and left shear spans at a load capacity of 63.30 kN, shear force ($V_c = 31.65$ kN). At a load capacity of approximately 72.20 kN, shear force ($V_c = 36.10$ kN) a sudden diagonal shear crack happened in the left portion of the specimen, also shear cracks begin to expand on along the specimen with the applied load sequence. The flexural-shear cracks lastly developed into the right and left shear spans, the shear diagonal crack extends until the failure occurs in the left portion of the specimen at a peak load of 103.60 kN ($V_c = 56.80.33$ kN), and the maximum displacement at mid-span was 4.84 mm. The shear critical section was 142.5 mm. This failure did not happen suddenly, there was a warning before the failure. The drop of the beam was in one stage where the failure was inclined and not sharp. The test was stopped when the load capacity lost 33% of the peak load. The maximum width of the shear diagonal crack at the failure was 1.10 mm. Because of the addition of steel fibers, the ultimate load capacity of this group was increased approximately of double compared to the control group.

4.3.3.7 Beam (B7-P-1)

This beam was the first specimen tested in the third group that contained 1.0% steel fibers. The first crack happened at a load capacity of 37.30 kN, shear force ($V_c = 18.65$ kN) into the constant moment region and in the right and left shear spans, the first crack width was 0.15 mm. When the load reached 72.90 kN ($V_c = 36.45$ kN), a first flexural-shear crack began to appear on the right and left shear spans. The cracks in shear spans and in the constant moment region were developed with the load sequence. In addition, the diagonal shear cracks have appeared in the right and left

shear spans. Further loading, "expanding" cracks began to develop in the shear spans and in the mid-span. whenever the mid-span displacement increased the concrete at the compressed region started to appear marks of crushing concrete in the top of the constant moment region. The yield occurred in the longitudinal reinforcement bars. Testing continued under displacement control. Subsequently, crushing of concrete continued, the load started to drop very slightly (maximum load was 134.30 kN, Vc = 67.15 kN, and the displacement at mid-span reached 5.98 mm). The test was stopped when the load capacity was 127 kN. The capacity displacement was approaching 15 mm at a mid-span, the maximum width of flexural cracks in the center of the specimen was 0.80 mm.

4.3.3.8 Beam (B8-H10-1)

The first crack happened at a load capacity of 18.80 kN , shear force (Vc = 9.40 kN) into the constant moment region and in the shear spans, the first crack width was 0.14 mm. When the load reached 67.30 kN (Vc = 33.65 kN), a first flexural-shear crack begins to happen in the shear spans of the specimen. The cracks in the shear spans and in the constant moment region were developed with the load sequence. In addition, the diagonal shear cracks have appeared on the shear spans. Further loading, "expanding" cracks begin to develop on the shear spans and at mid-span. Whenever the mid-span displacement increased the concrete at the compression region started to appear marks of crushing concrete in the upper of the constant moment region. The yield occurred in the longitudinal reinforcement bars, testing continued under displacement control. Subsequently, crushing of concrete continued, the load started to drop very slightly (maximum load was 140.50 kN, and the displacement at mid-span reached 8.60 mm). The test was stopped when the capacity load was 133 kN. The capacity displacement was large approached 15 mm at a mid-span, the maximum width of flexural cracks in the specimen center was 0.70 mm.

4.3.3.9 Beam (B9-H15-1)

The specimen was the last beam of the third group. The first crack happened at a load capacity of 28.80 kN, shear force (Vc=14.40 kN) into constant moment region and in the shear spans, the first crack width was 0.13 mm. When the load reached 56.30 kN (Vc = 28.15 kN), a first flexural-shear crack began to appear on the shear spans of the specimen. The cracks in the shear spans and in the constant moment region were

developed with the load sequence. In addition, the diagonal shear cracks appeared on the shear spans. Further loading, "expanding" cracks began to develop on the shear spans and at mid-span. Whenever the mid-span displacement increased the concrete in the compressed region started to show marks of crushing concrete in the upper of the constant moment region. later the yield occurred in the longitudinal reinforcement bars, testing continued under displacement control. Subsequently, crushing of concrete continued, the load started to drop very slightly (maximum load was 138.30 kN, Vc = 69.15 kN, and the displacement at mid-span reached 8.98 mm). The test was stopped when the load capacity was 121 kN. Despite the capacity displacement was large approached 15 mm at a mid-span, the maximum width of flexural cracks in the center of the specimen was (0.65 mm). Despite the occurrence of the diagonal shear cracks and many cracks on the shear spans for the this group, the cracks were controlled. This can be referred to the improvement in shear capacity supplied with this amount of steel fibers. The increment shear capacity allowed the beam to reach its flexural strength. For the specimens of the third group that failed in flexural and did not fail in shear. Therefore, it is not possible to determine the shear stress exactly, but it is possible to estimate the minimum value. It is assumed that the beams of this group failed in shear at the maximum loads recorded during the test and to find this value, assume that the critical shear section (d_{cr}) will occur in the greatest depth and its value is 180 mm. The critical shear failure is defined as the location of the main diagonal shear crack which must form at an inclination angle (45), as shown in Fig. (4.12). Where the critical shear section (d_{cr}) inversely proportional to the shear stress (V = Vc/ $b*d_{cr}$). Furthermore, the shear stress values were calculated as listed in the Tables (4.2 -4.4).
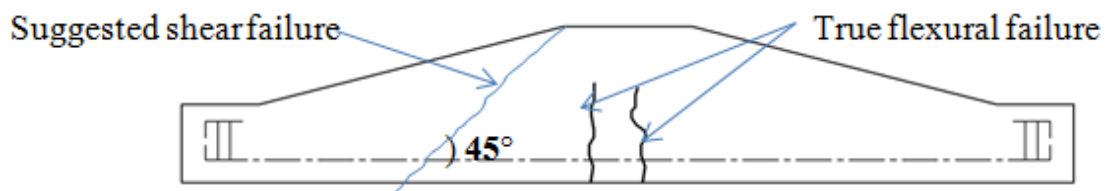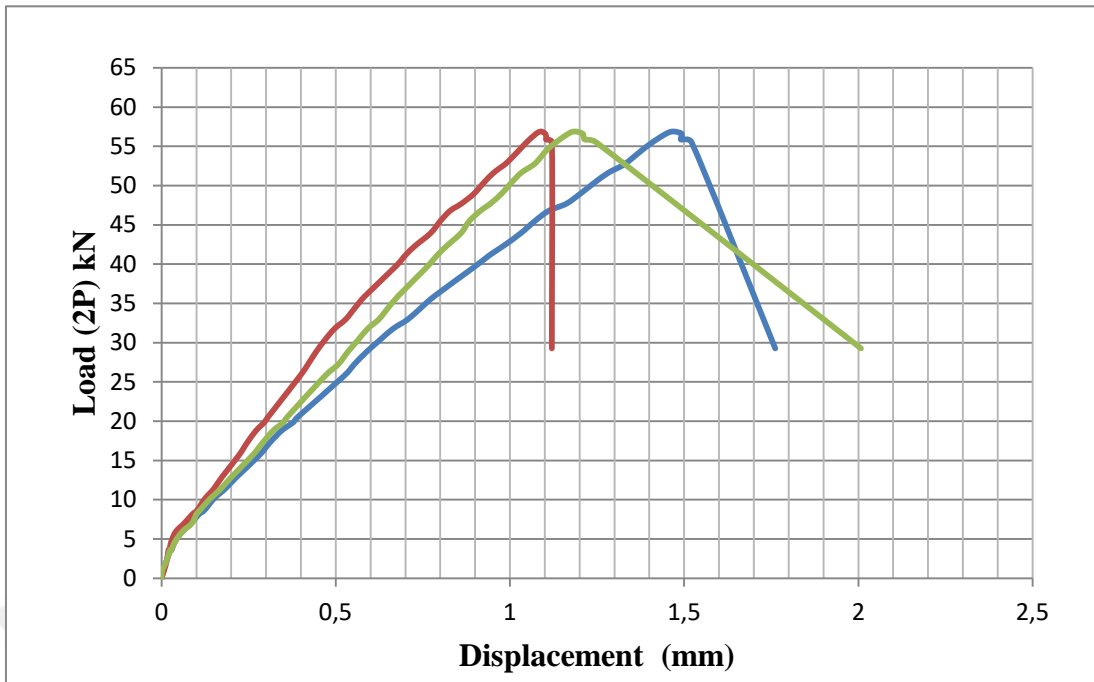

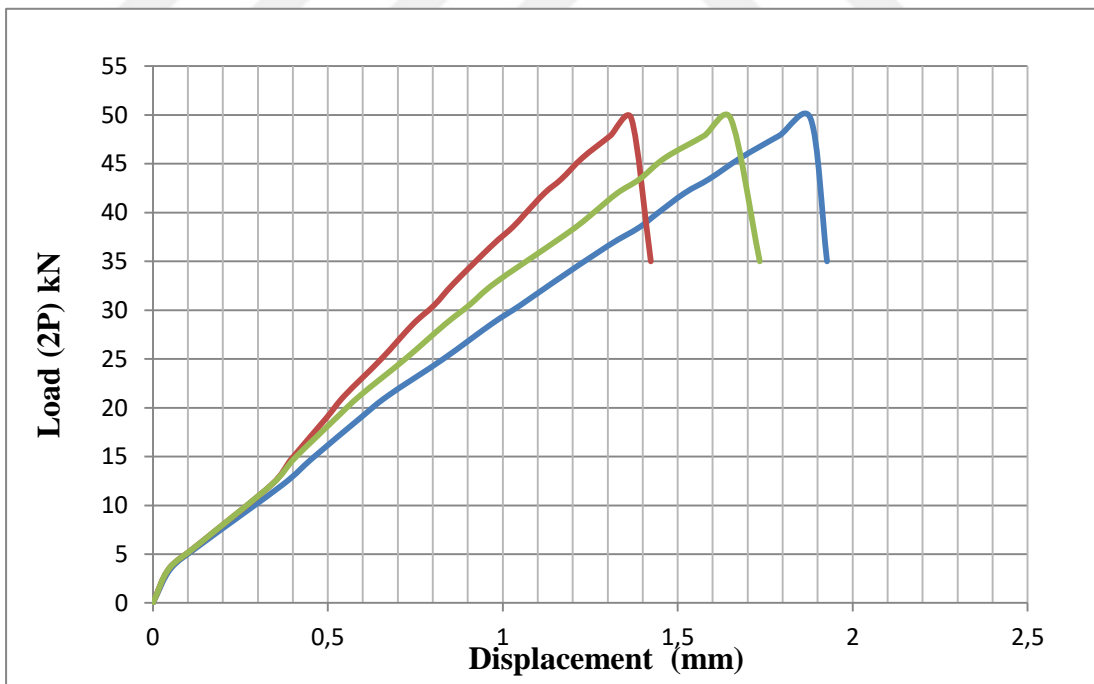**Figure 4.12** The Proposed Shear Failure Mode
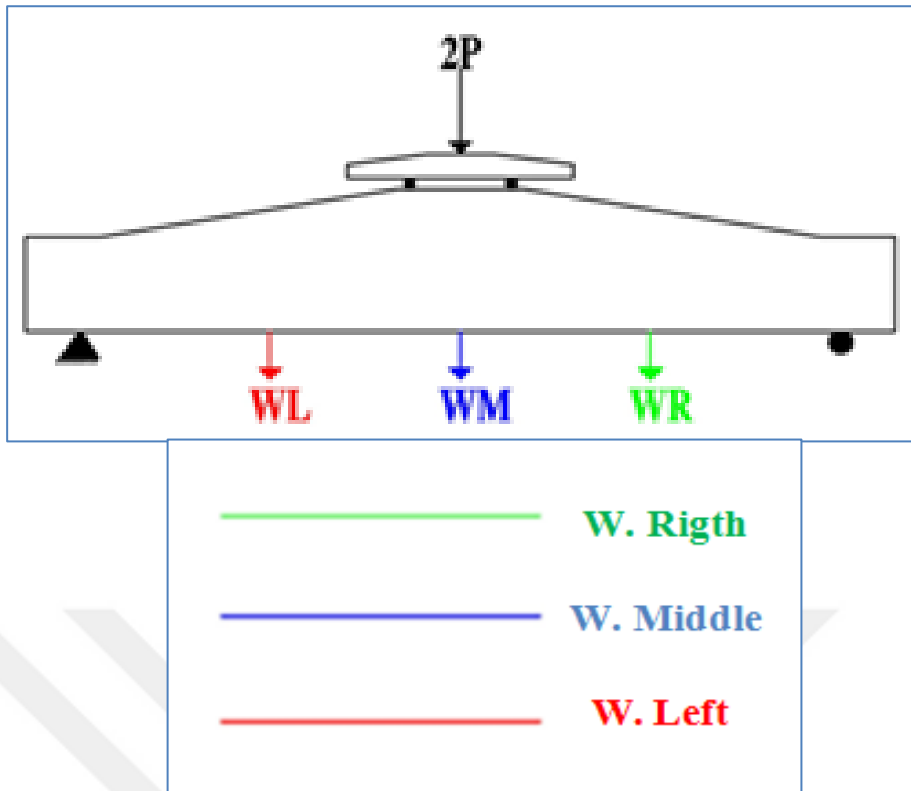
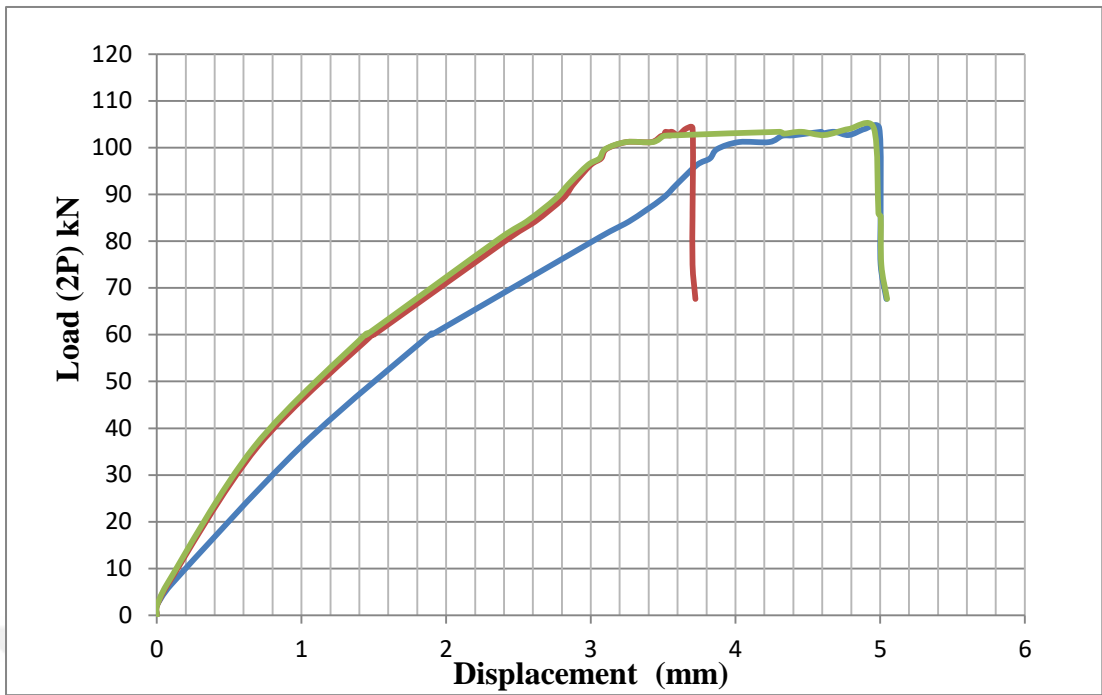**Figure 4.13** Test Result Indicators
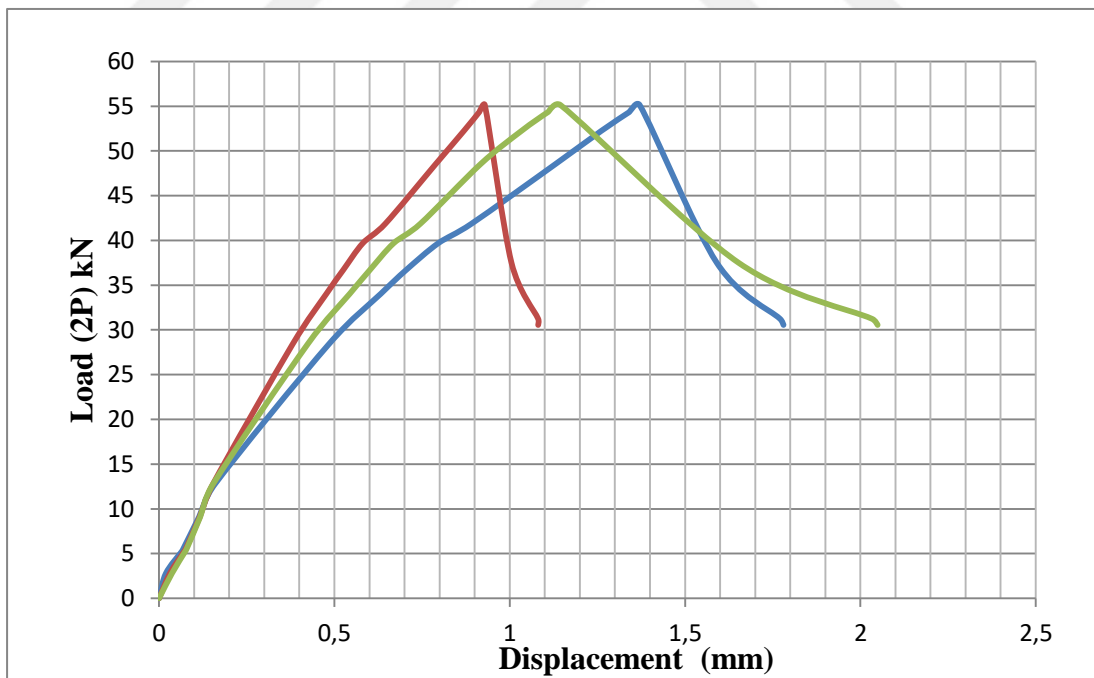
Figure 4.14 Load-Displacement Relationship for the Beam (B1-P-0)

(Prismatic Beam without Steel Fiber)

Figure 4.15 Load-Displacement Relationship for the Beam (B2-H10-0)

(Haunched Beam at10° without Steel Fiber)

Figure 4.16 Load-Displacement Relationship for the Beam (B3-H15-0)

(Haunched Beam at15° without Steel Fiber)

Figure 4.17 Load-Displacement Relationship for the Beam (B4-P-0.5)

(Prismatic Beam with steel fiber 0.5 %)

Figure 4.18 Load-Displacement Relationship for the Beam (B5-H10-0.5)

(Haunched Beam at10°with Steel Fiber 0.5%)

Figure 4.19 Load-Displacement Relationship for the Beam (B6-H15-0.5)

(Haunched Beam at15°with Steel Fiber 0.%5)

Figure 4.20 Load-Displacement Relationship for the Beam (B7-P-1)

(Prismatic Beam with Steel Fiber 1%)

61
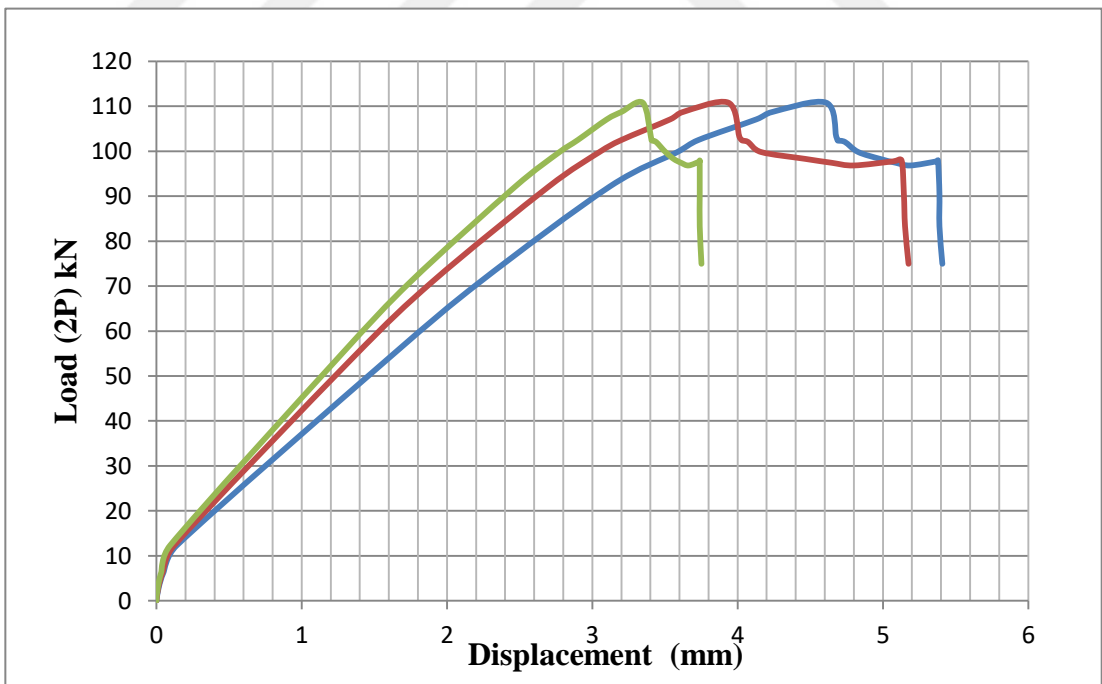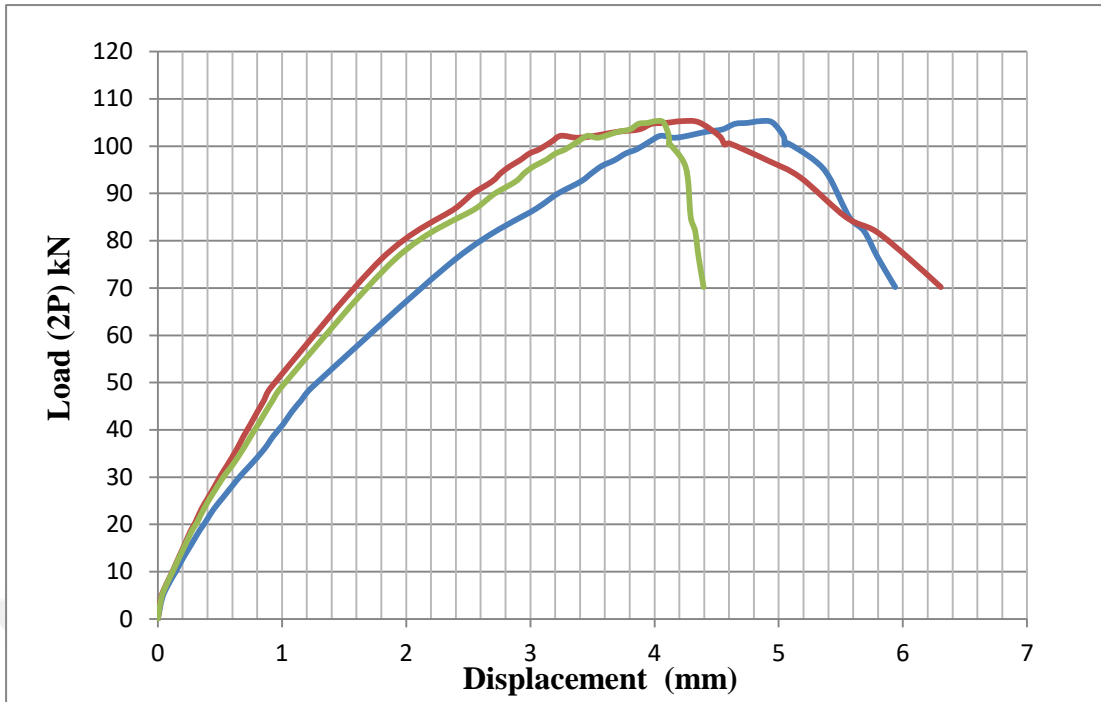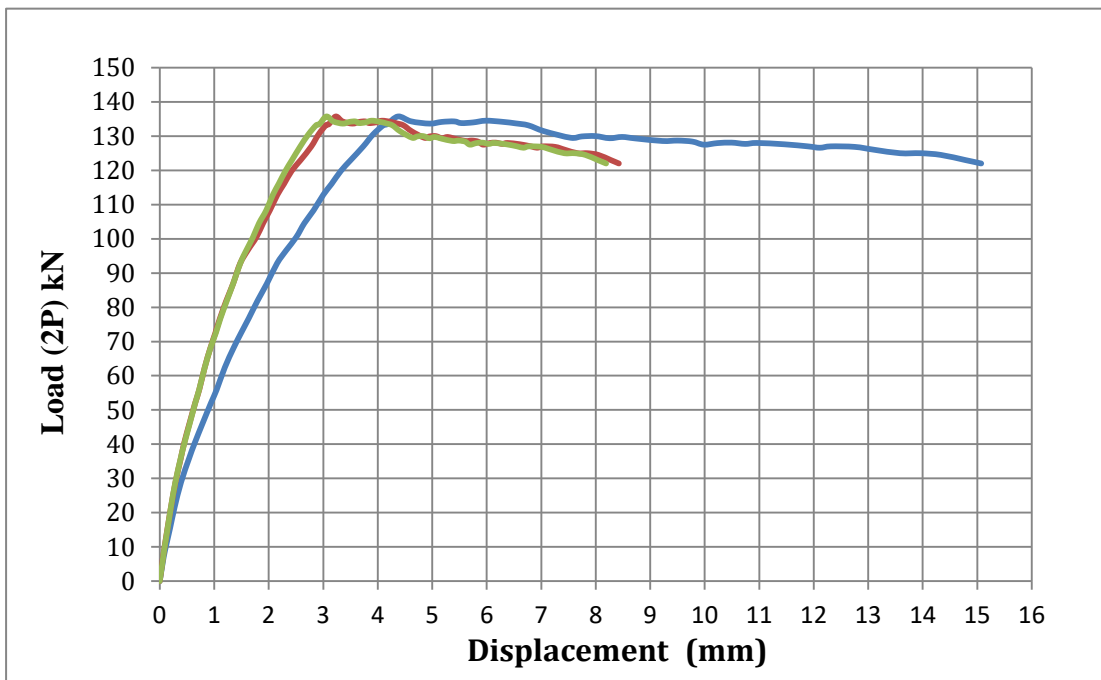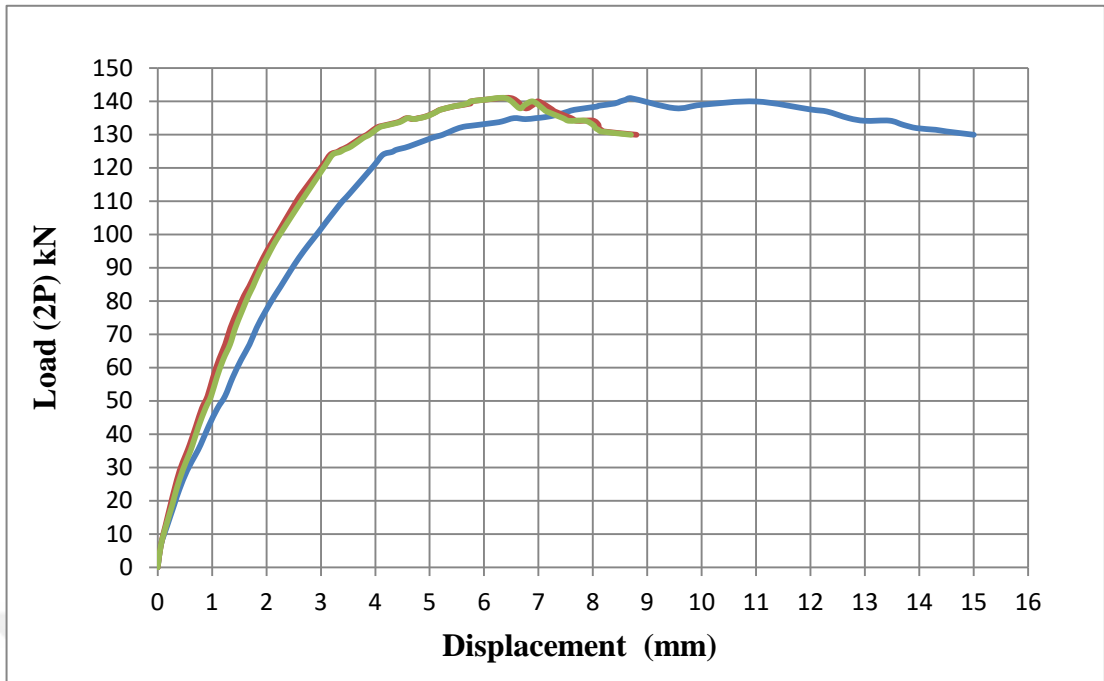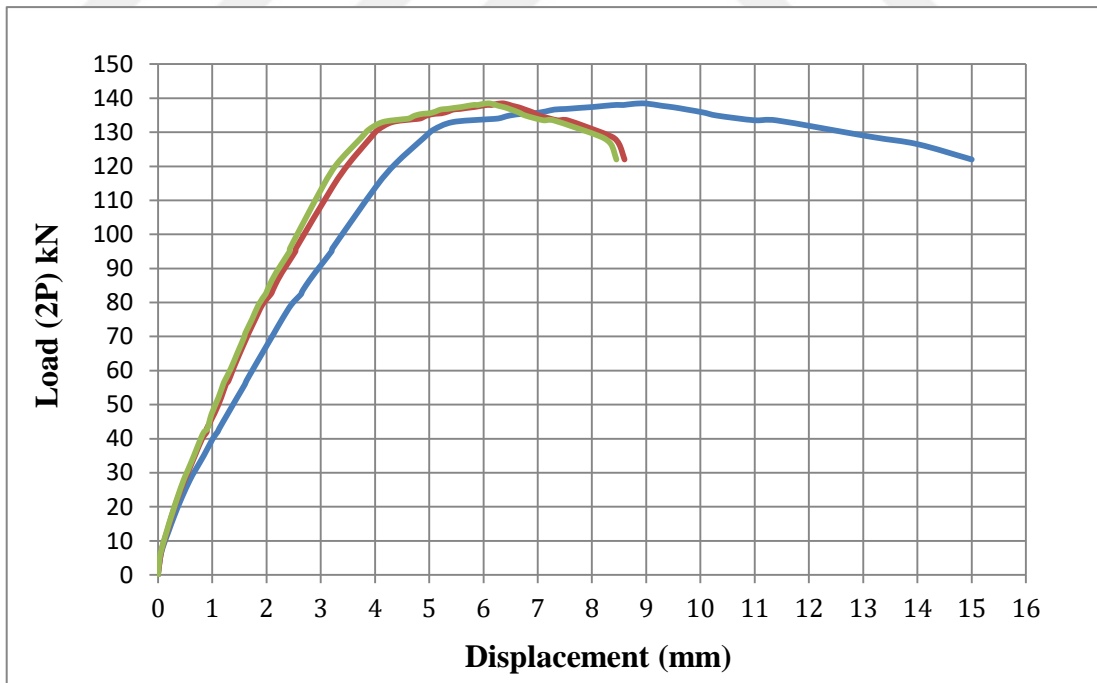
Figure 4.21 Load-Displacement Relationship for the Beam (B8-H10-1)

(Haunched Beam at 10° with Steel Fiber 1%)

Figure 4.22 Load-Displacement Relationship for the Beam (B9-H15-1)

(Haunched Beam at 15° with Steel Fiber 1%)

4.3.4 Mode of Failure

In general, the failure mode is defined by the type of cracks that caused the failure. Reinforced concrete beams in this study have a complex crack mode that depends on the inclination angle of the beam and the ratio of steel fibers. During the testing process of beams, a shear failure mode occurred for 6 beams while a flexural failure mode with concrete crushing occurred for 3 beams. Nine beams were designed to study the shear failure mechanism of RCHBs and a prismatic beam with the use of self-compacting concrete and steel fibers (SCSFRC). Therefore, all beams are designed without shear reinforcement. The propagation of the crack in the beams was different depending on the percentage of steel fiber and the value of the inclination angle. The main points observed in RCHBs and prismatic beams for three groups which failed by shear and flexural with concrete crushing were as follows:

- **first group**: As expected, the beams of this group, which without steel fibers (0%), failed in shear, and suddenly the diagonal shear cracks appeared that caused the failure. Typically, this failure was without any warning due to the brittle nature of the plain concrete. In general, the ways of initiate cracks were perpendicular to the longitudinal reinforcement, new cracks appeared in the shear span, which were vertical and slightly inclined towards the loading points. In addition, at maximum load, the diagonal tension crack appeared and inclined towards the loading point. When the failure occurred all cracks mentioned stopped growing. The angles of the shear diagonal crack were not similar in the inclination of all beams of this group where there was a difference in the values of the shear critical section. The inclination angle of the shear crack of prismatic beam was close to 45°, this angle was decreed whenever increase the inclination angle of RCHBs. All of the cracks mentioned were symmetrical in all parts of the beam until the major failure crack appeared, leading to the collapse of beams in the shear. In addition, as expected the load dropped when the failure occurred because the concrete is brittle due to the absence of steel fibers that increase the strength of concrete.

- **second group**: The beams of this group containing the steel fibers (0.5%) also failed in shear, where diagonal shear cracks showed suddenly, but the failure did not occur immediately. Typically, this failure occurred with

caution because the steel fiber added to the concrete some ductility to beams. In general, the ways of initiate cracks were perpendicular to the longitudinal reinforcement, also new cracks in the shear span appeared perpendicular and inclined toward the loading points, the diagonal tension crack appeared and inclined toward the loading point but the failure did not happen. All the mentioned cracks have increased with a load sequence, and finally the diagonal tension crack was the major failure crack but the beams continued to withstand extra loads. When the failure occurred all the cracks mentioned stopped growing. For all beams, the shear crack angles were not similar in inclination with a difference in the values of the shear critical section. The inclination angle of the shear crack of prismatic beam was close to 45°, this angle was reduced as increase the inclination angle of RCHBs. All the cracks mentioned were symmetrical in both portions of the beam until the major failure crack appeared that led to the collapse of the beam by shear. Due to the presence of steel fibers, the ultimate load capacity of this group was increased by (68% - 92%) compared to the first group (control beams). However, the amount of steel fibers used in this group was not sufficient to change the shear failure to a ductile flexural. Another important observation for the haunched beams was that the angle of shear crack failure in this group was greater compared to the first group (control beams). In addition, the load dropped slowly at failure because the steel fiber were able to add some ductility to the concrete as well as led to increased concrete strength. Fig. 4.23, shows the shear failure for six beams and also illustrates the location of the critical shear section at a (45 °).

- **third group**: Surprisingly, the beams of this group containing steel fibers (1%), failed in flexural and concrete compression crush where reinforcing bars became yield despite the absence of shear reinforcement. Typically, this failure occurred with a warning because of the added steel fiber was able to increase the ductility significantly. In general, the ways of initiate cracks were perpendicular to the longitudinal reinforcement, also new cracks in the shear span appeared perpendicular, then these cracks inclined towards the

loading points, where the diagonal tension crack appeared during the test of this group but the failure did not happen. All the mentioned cracks expanded a lot with load sequence, and finally the flexural cracks were the major failure crack at mid-span. All the cracks mentioned were symmetrical in all parts of the beam. In addition, the load did not drop at the failure due to the concrete has gained a lot of ductility due to the presence of steel fiber that increases the strength of concrete. The number of cracks increased when concrete reached the ultimate strength and continued until failure occurred. The load capacity decreased slightly under the yield load, whereas the displacement increased. The beams of this group showed good control of shear crack widths at equivalent load stages as compared to the first and second group. The main observation in this test was that the addition of 1.0% steel fibers caused an increase in shear capacity and changed the shear failure to a ductile flexural failure. In addition, this quantity of steel fibers allowed the specimens to withstand large displacement. The results show that increasing the steel fiber ratio produced additional improvements in crack control. Further, a haunched beam had a greater shear and deflection capacity compared to prismatic beams as shown in Tables (4.1-4.4). Fig. 4.24 shows the flexure failure of the beams of this group.
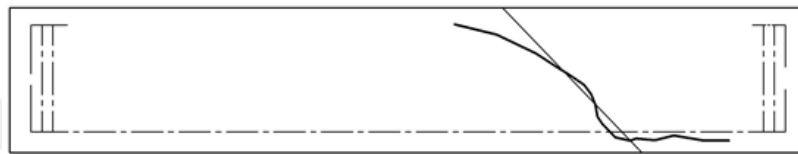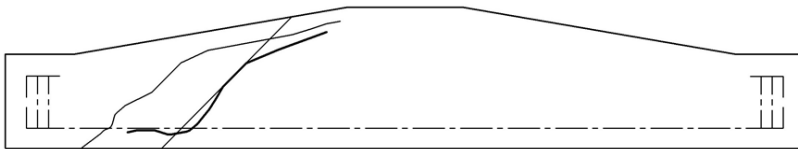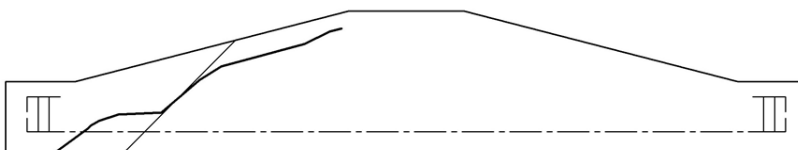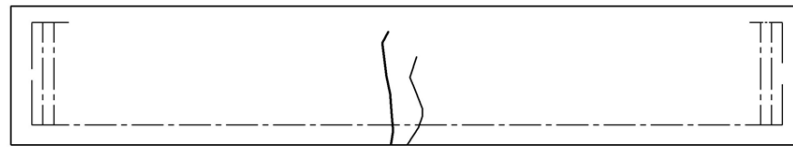
(B1-P-0)
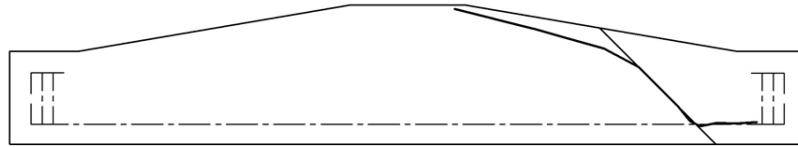
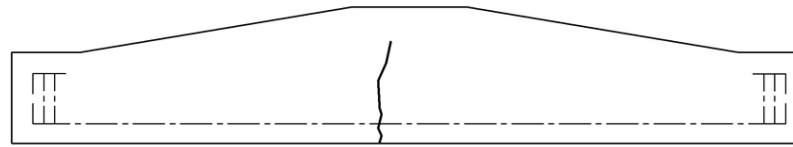**(B2-H10-0)**
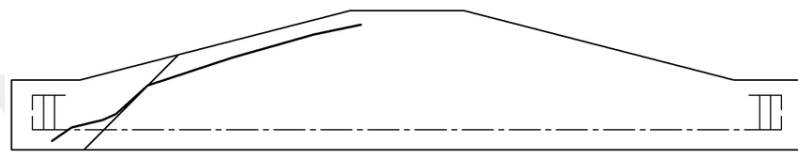
(B3-H15-0)

(B4- P-0.5)

(B5-H10-0.5)

(B6-H15-0.5)

Figure 4.23 The Diagonal Shear Cracks and Critical Shear Section

(B7-P-1)

(B8-H10-1)
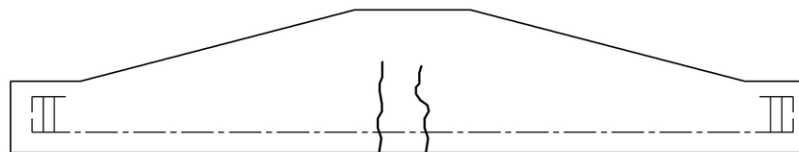
(B9-H15-1)

Figure 4.24 Flexural Failure Mode

4.3.5 The Shear Critical Section

Generally, the shear critical section is the location of the major diagonal shear crack which forms at a 45° inclining angle of the axis of the lower longitudinal bars. In this study, the critical section of the beams occurred at different locations depending on the inclining angle of the beams. For prismatic beams, the major cracks were almost in the mid of the shear span, while the critical section of haunched beam observed near the support which has a lower depth (H10°) and it was approaching the support as the angle of inclination increased. It is worth noting that the important observation that was clear during the determination of the shear critical section for the first, second and third groups was that the addition of steel fibers contributed by moving the critical section shear towards the mid-span away from the support. This can be explained by the fact that the usage of steel fibers has contributed to an increase in shear strength.

4.3.6 Effective Depth of Shear

The depth of the critical section of the beam is known as the beam depth at the location of the major diagonal shear crack at failure. The influential depth of the

prismatic beams is constant wherever the main failure occurred while the RCHBs have variable depth. Therefore, the effectual depth of the shear critical section of the haunched beams for the first and second groups is not equal. The experimental test showed different forms of failure as shown in Fig. 4.23.

4.3.7 Influence the Inclination Angle

The arch of the compression chord increases with the inclining angle as shown in Fig. 4.25, and the compression chord inhibits the crack formation in the upper region. Fig. 4.26, shows that haunched beams have shear stress greater than prismatic beams. This can be explained by the fact that the higher inclination angle of all the haunched beams has a negative influence on shear load capacity due to increase in shear stress. Figs. (4.27- 4.29) show the inclination angle influence on the load capacity for all groups.
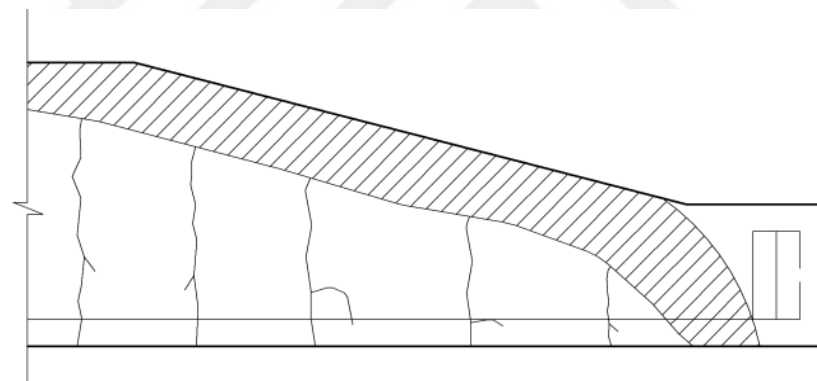
a. Haunched Beam type H15°
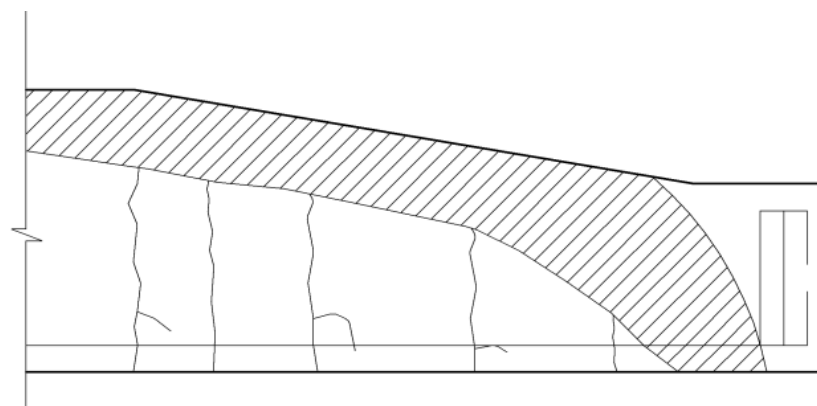
b. Haunched Beam type H10°

Figure 4.25 Unbreakable compression Chord
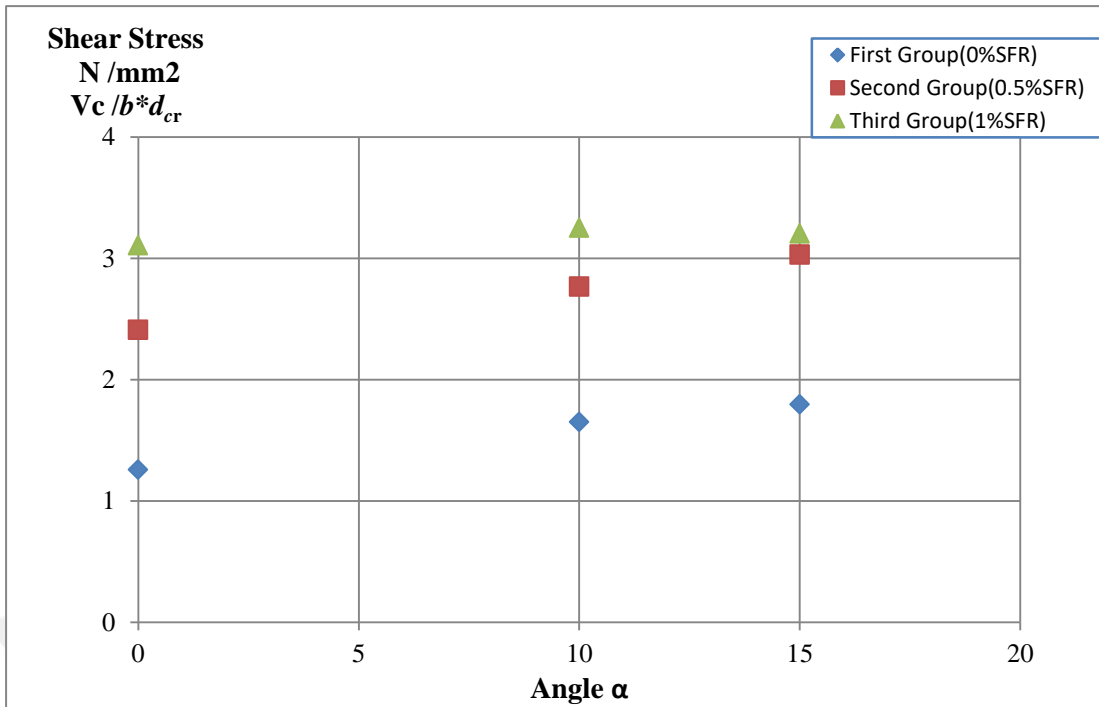
Figure 4.26 Effect of the Inclination Angle Value on the Shear Strength Capacity
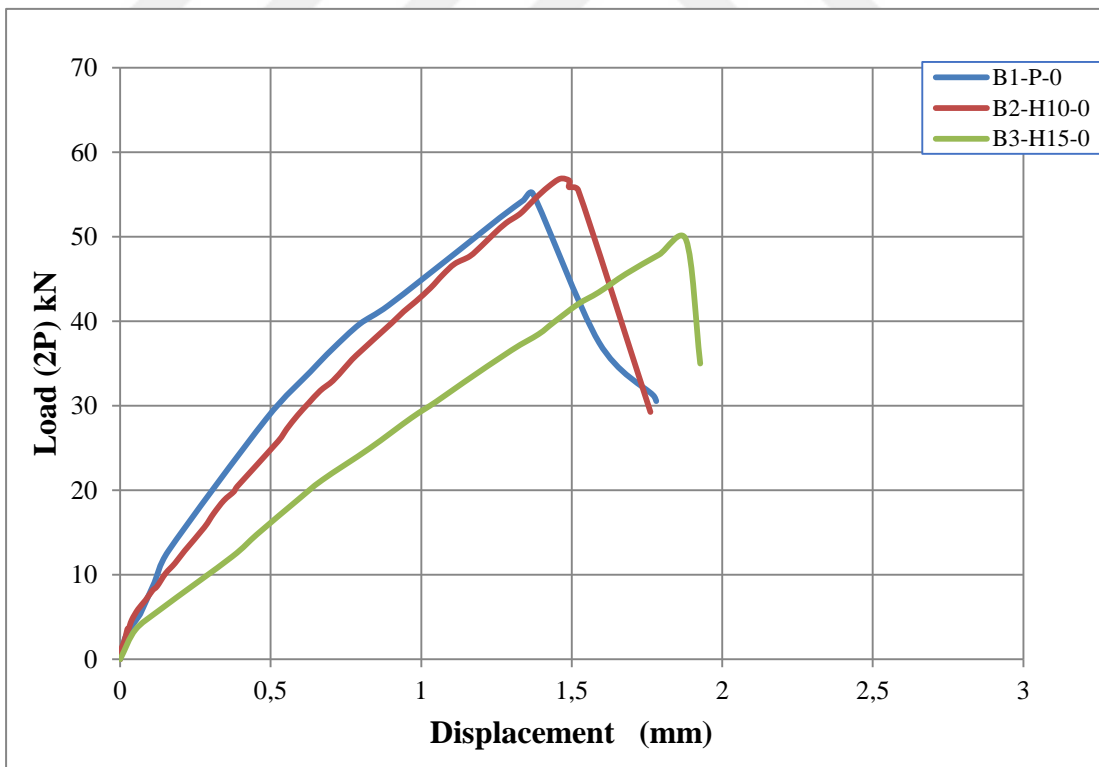
Figure 4.27 Ultimate Loads for Different Inclination Angles for the First Group
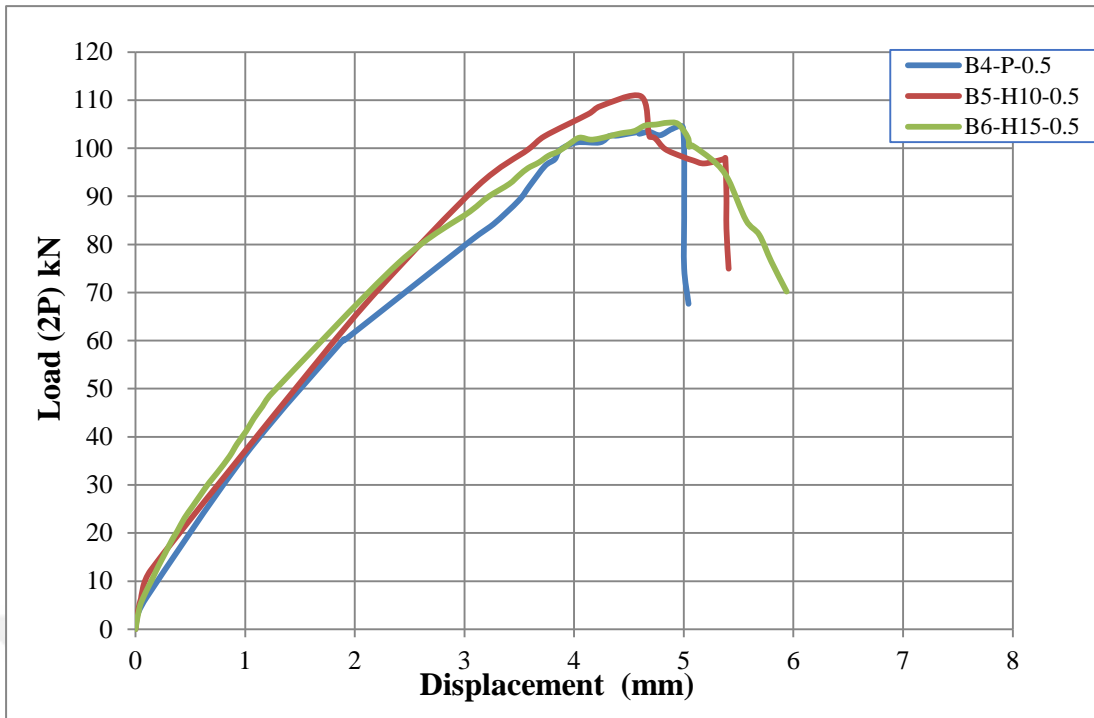
Figure 4.28 Ultimate Loads for Different Inclination Angles for the Second Group
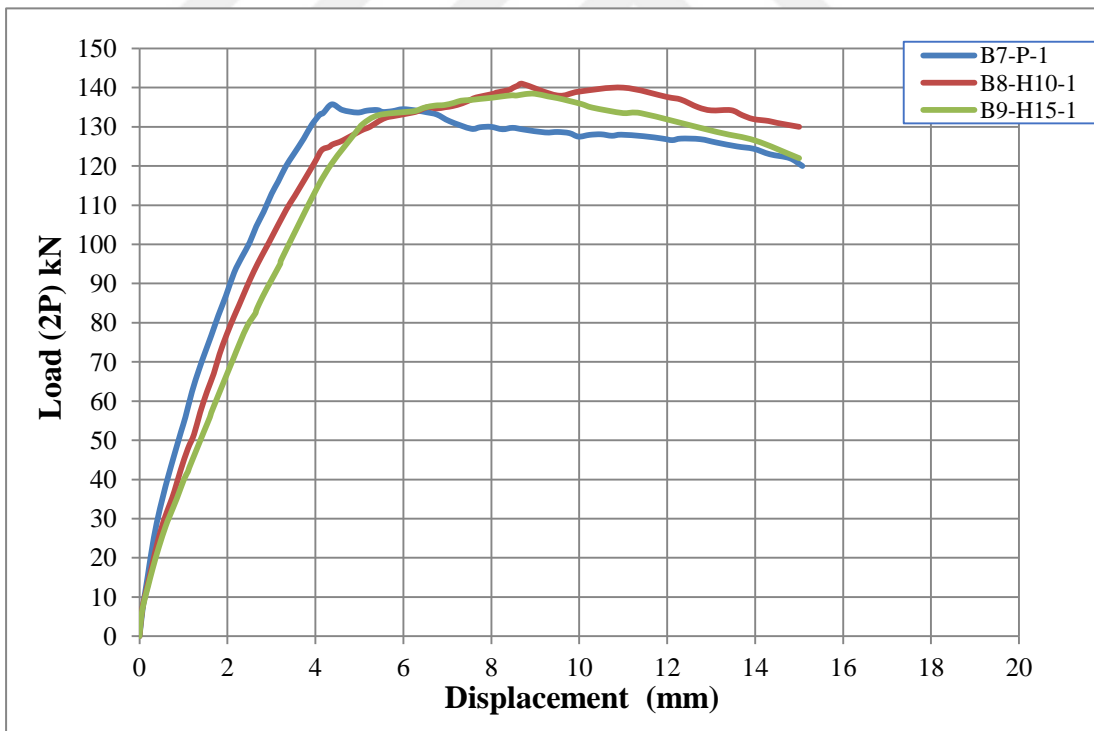
Figure 4.29 Ultimate Loads for Different Inclination Angles for the Third Group

70

4.3.8 Effect of Steel Fiber Percentage (V_f %)

The nine beams were poured using traditional SCC and SCSFRC. All beams were divided into three control beam (B1, B2, and B3) without steel fiber, and six beams (B4, B5, B6, B7, B8 & B9) with varying percentages of fiber ranging from 0.5% to 1%) using one type of steel fiber normal strength.

The influence of steel fiber percentage (V_f %) is directly linked with tensile strength of concrete. As the percentage of fiber increases, the tensile strength of concrete increases, the increment in beam load capacity can be observed simply in Figs. (4.30 -4.32). The increment in this capacity is evident for the beam without the steel fiber compared to the same beam containing the fiber. Therefore, the general conclusion that can be understood is that the beam load increases with increasing the proportion of steel fibers.

In addition, adding fibers contribute to a significant increase in the ductility of beams. It can also be simply noted from (Figs. 4.30 – 4.32) that the transformation from the reinforced concrete beam without steel fiber to the reinforced concrete beam with steel fiber, and in the same situations increases the ability of deformation without sudden loss of the load capacity. This is a good mechanical behavior for a structural element, where it acquires great ductility to provide safety, serviceability, and functionality of a structural element. The increment rate of the load capacity of SCSFRC beams becomes smaller as the steel fiber percentage increases. The addition of steel fibers into SCSFRC beams caused improvements in shear capacity.

In addition, as steel fiber percentage increases, the relative of shear strength increases. For instance, the addition of 0.5% steel fibers to the beam (B5-H10-0.5) increases the shear stress magnitude of this beam by 68 % compared to the shear stress capacity of the control beam (B2-H10-0). A further, the increase of the steel fiber percentage to 1.0% led to improved shear stress of more than 97% when compared to the same control beam. As expected, control beams that do not contain transverse steel stirrups nor steel fibers, failed in shear at a relatively low level of load and displacement (see Table 4.2).

The usage of 0.5% steel fibers did not lead to change the failure mode, therefore these beams also failed in shear. The usage of 1.0% steel fibers in beams of third

group was adequate to convert the failure mode from the fragile shear to the ductile flexural. In addition, the beams were able to withstand large displacement.
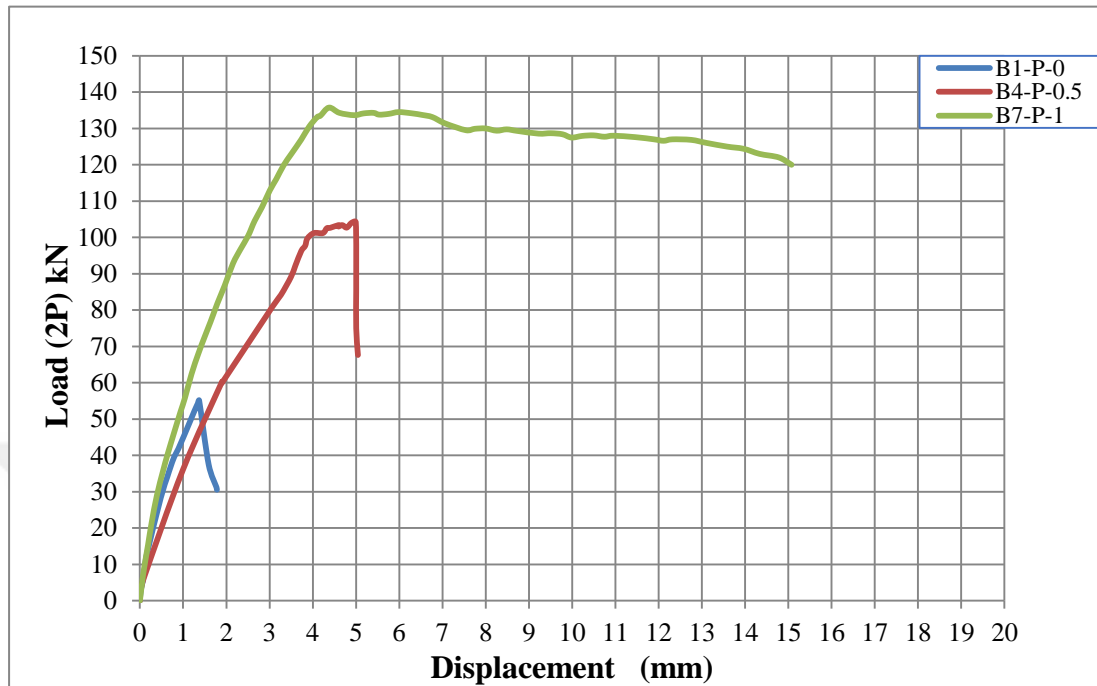
Figure 4.30 Ultimate Loads under Different Steel Fiber Content For the Prismatic Beam
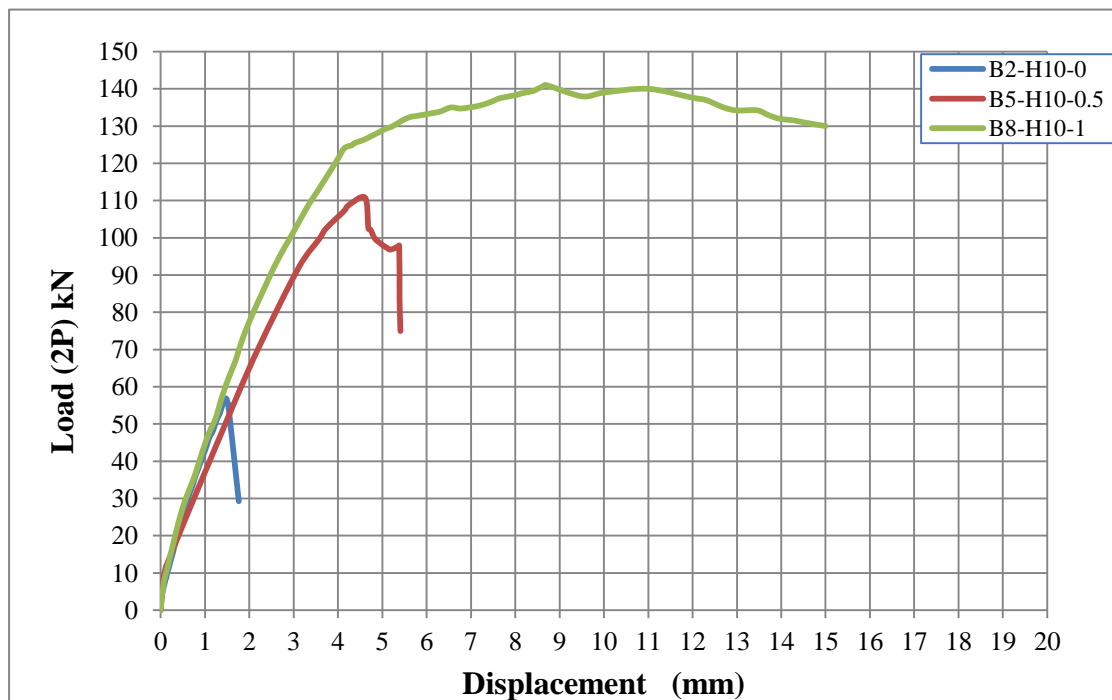
Figure 4.31 Ultimate Loads under Different Steel Fiber Content For the Haunched Beam (H10)
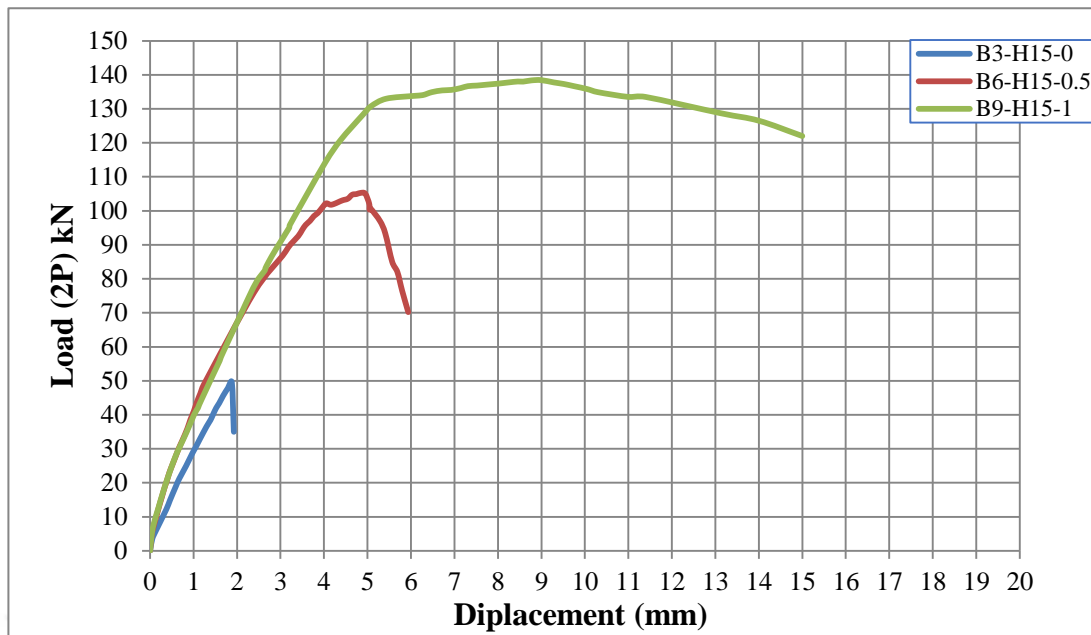
Figure 4.32 Ultimate Loads under Different Steel Fiber Content For the Haunched Beam (H15)

4.3.9 Width and Mode Crack

It has been observed from test results that all beams have grown many cracks that were different from one group to another. However, a number of cracks that were grown in the steel fiber reinforced beams were more than other beams (control beams). This special case produced a good performance in the redistribution of stress. With regard to cracks, the study results exhibited that fiber reinforced concrete beams can improve mechanical performance.

In addition to the improvements in controlling crack widths, the usage of steel fibers had a significant influence on crack patterns in the beams tested in the experimental study. For the three groups, the crack modes for the SCC control beam and the SCSFRC beams were noticeably different. Comparing the inclined cracks for the beams that failed in shear, the control beams (0% steel fiber) showed a single inclined crack followed by a fragile shear failure. On the other hand, several of the SCSFRC beams that failed in shear showed two diagonal shear cracks before failure, especially in the second group (0.5% steel fiber). Comparing between first and second group, it can be seen that the use of (0.5%) fibers has reduced the spacing between the cracks.

When comparing the control beams (0% steel fiber) with the beams that failed in flexure (1% steel fiber), it can be seen that the usage of the higher fiber content led to both reductions in crack width and spacing. In addition, the higher steel fiber ratio resulted in a more spread cracking mode with the formation of "branching" cracks with secondary cracks growing out of primary cracks. This is especially clear in the failure figures of the third group (1% steel fiber). Fig. 4.29, exhibits that the beams reinforced with fiber (1%) showed much more ductility than the first group (control specimen) and the second group (0.5% steel fiber). Figs. (4.33 to 4.41) show cracks propagation of the experimental tested specimens at different values of loading for all beams.

4.4 Discussion on Critical Fiber Content

One of the most important observations in the experimental study is the importance of selecting the most effective steel fiber quantity that is added to a particular beam, which is called "the critical fiber content". In this experimental study, the fibers in the second group were 0.5%, which was less than the critical content where the failure of this group was by shear and not by flexural, whereas the third group containing the fiber (1%), this ratio was sufficient to convert the failure mode o shear to flexural. On the other hand, through previous studies, adding fiber over critical content will not produce big improvements in capacity. Whereas, fibers play a minimum role in increasing flexural strength, although the addition of fibers more than this limit could lead to improvements in flexural ductility and crack control. Therefore, the addition of fiber in a quantity equal to the critical limit has an important effect on the ultimate capacity in beams failing in shear. Hence, it is important for the design practice to be able to choose the best suitable fiber content in order to provide a safe and inexpensive design. Moreover, in some cases, the shear demand is too large to be provided using steel fibers, due to limitations on the quantity of fiber that can be added without affecting workability. It is important to notice that this content is controlled by many parameters such as material properties for both the concrete and the steel fibers as well as beam properties.

4.5 Ability of Fiber to Replace Minimum Shear Reinforcement SCSFRC for RCHBs

Although there are many data on the use SFRC and a few data of use SCSFRC as an alternative for minimum shear reinforcement or stirrups in conventional reinforced concrete prismatic beams, there are no previous studies of structure the haunched beams with self-compacting concrete and steel fibers (SCSFRC). Therefore, it is important to search if this property is also available in a haunched beam. There are limited data in the literature review on SCSFRC prismatic beams, in Table 4.5, shows the values of shear stress at failure and characteristics of the SCSFRC beams for two studies (Greenough and Nehdi (2008) and Michael Cohen (2012). The results show that all the SCSFRC beams examined in these studies failed in shear stresses greater than $(0.17\sqrt{f'_c})$. Considering this limited group of SCSFRC prismatic beam test results, the estimated value was obtained to be $(0.32\sqrt{f'_c})$ for beams that contained $(V_f \geq 0.75\%)$. This value was obtained to be slightly more than the value of $(0.3\sqrt{f'_c})$ reported for SFRC beams (in ACI-318 code). It is also seen that the shear stress at failure for the control SCC beam in these studies was less than the initial shear stress corresponding to $(V= 0.17\sqrt{f'_c})$ in the ACI-318 code. However, the above experimental study was limited to a few beams, therefore, could be considered as an initial evidence to support the usage of steel fibers as a replacement to minimum shear reinforcement in SCSFRC haunched beams having $(V_f \geq 0.75\%)$. Therefore, it requires the need to start further research to support this property of a haunched beam. In this study, it is exciting to know that the results show that all the SCSFRC haunched beam that failed in shear stress was more than twice $(0.17\sqrt{f'_c})$ the nominal value of the shear stress corresponding to V in the ACI-318 code. Although this study is limited, the test results of SCSFRC haunched beam estimated that the minimum value of the shear stress was $(0.492\sqrt{f'_c})$ for the haunched beam that contained $(V_f =0.50\%)$. In other words, this value was obtained to be much more than the value of $(0.17\sqrt{f'_c})$ reported for SFRC prismatic beam in ACI-318 code for the prismatic beam that contained $(V_f \geq 0.50\%)$. The results also showed that the minimum value of the shear stress was $(0.562\sqrt{f'_c})$ for the haunched beam that having $(V_f =1\%)$, this value is much more than the value of $(0.30\sqrt{f'_c})$ reported for SFRC prismatic beams in ACI-318 code that contained $(V_f \geq 0.75\%)$. Is also

interesting to observe that the minimum value of the shear stress at failure for the SCC haunched beam in this study was ($0.30\sqrt{f_c'}$) that was more than the initial shear stress corresponding to (V=$0.17\sqrt{f_c'}$) in the ACI-318 code. In Table 4.6 exhibits the shear stress values at failure for all prismatic and haunched beams in this experimental study.

Table 4.5 Sampling Parameters Examined by Others Researchers on Prismatic Beam

Beam Design	b mm	d mm	(ρ) %	a/d	f_c' MPa	Df mm	Lf/Df	V_f %	Shear stress MPa
S-HE-O.5*	200	265	1.7	3.02	40	1.0	50	0.5	$0.270\sqrt{f_c'}$
S-HE-0.75*	200	265	1.7	3.02	40	1.0	50	0.75	$0.320\sqrt{f_c'}$
S-HE-1*	200	265	1.7	3.02	40	1.0	50	1.0	$0.445\sqrt{f_c'}$
M-15-0**	125	220	1.55	3.8	50	0.55	55	0.0	$0.155\sqrt{f_c'}$
M15-0.5**	125	220	1.55	3.8	50	0.55	55	0.5	$0.220\sqrt{f_c'}$
M15-1**	125	250	1.55	3.8	50	0.55	55	1.0	$0.260\sqrt{f_c'}$

*Tested by Greenough and Nehdi (2008)
**Tested by Michael (2012)

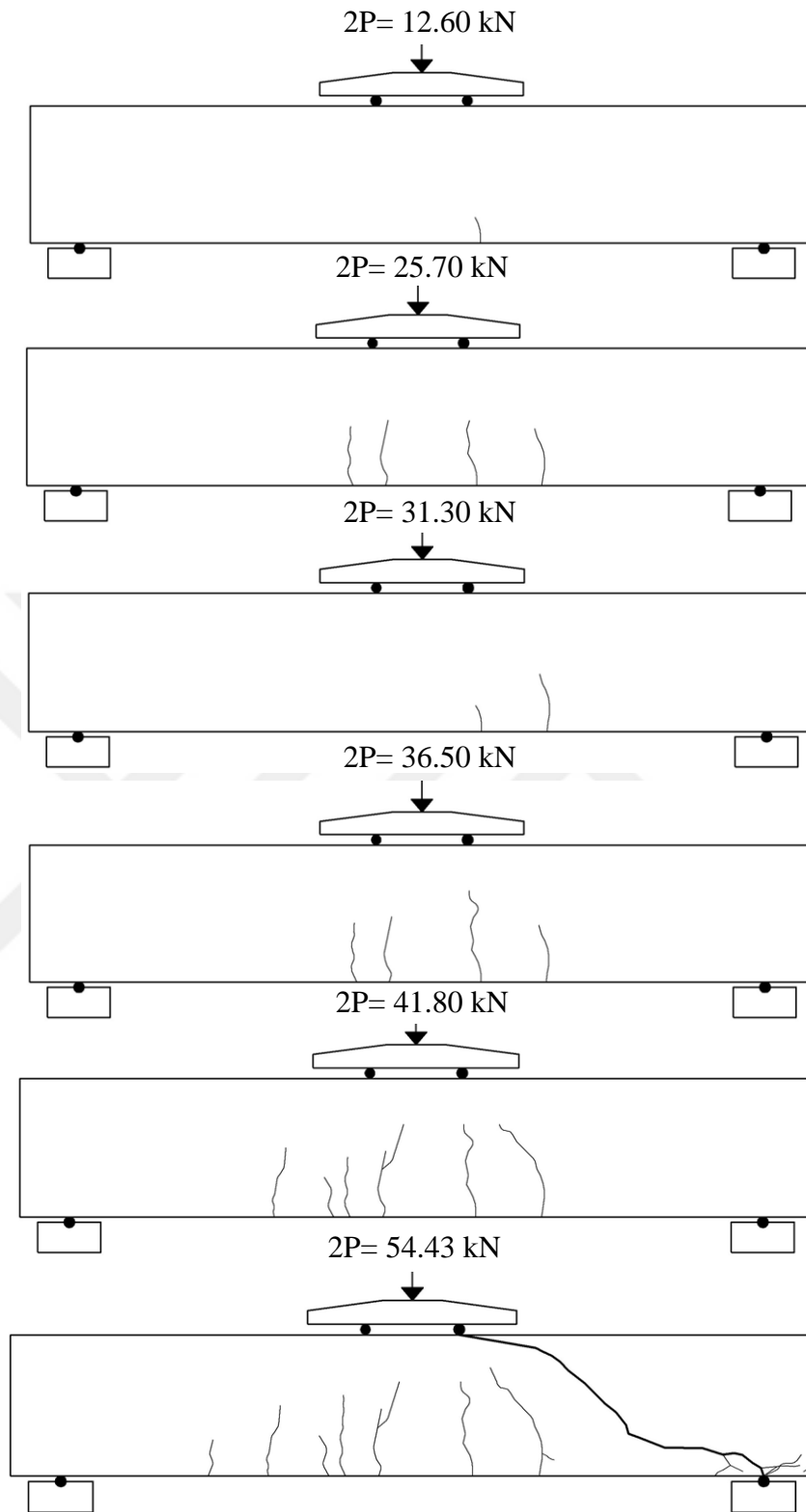b : Beam Width, d : Influential Depth, ρ : Ratio of Longtiodnal Bars, a/d: Shear Span to Influential Depth Ratio, f_c: Compressive Strength, Df: Depth of Fiber, Lf/Df: Aspect Ratio, V_f: Steel Fiber Ratio

Table 4.6 The Parameters of the Samples Tested (Prismatic and Haunched Beam) by this Study

Beam Designation	b mm	d mm	(ρ) %	a/d	Df mm	Lf/Df	V_f (%)	Shear stress MPa
B1-P-0	120	180	1.57	2.527	0.75	45	0	$0.203\sqrt{f_c'}$
B2-H10-0	120	110-180	1.57	2.527	0.75	45	0	$0.267\sqrt{f_c'}$
B3-H15-0	120	75-180	1.57	2.527	0.75	45	0	$0.300\sqrt{f_c'}$
B4-P-0.5	120	180	1.57	2.527	0.75	45	0.5	$0.400\sqrt{f_c'}$
B1-H10-0.5	120	110-180	1.57	2.527	0.75	45	0.5	$0.492\sqrt{f_c'}$
B2-H15-0.5	120	57-180	1.57	2.527	0.75	45	0.5	$0.542\sqrt{f_c'}$
B3-P-1*	120	180	1.57	2.527	0.75	45	1	$0.552\sqrt{f_c'}$
B4-H10-1*	120	110-180	1.57	2.527	0.75	45	1	$0.577\sqrt{f_c'}$
B3-H15-1*	120	75-180	1.57	2.527	0.75	45	1	$0.562\sqrt{f_c'}$

*Beams Faild in Flexural

2P= 12.60 kN

2P= 25.70 kN

2P= 31.30 kN

2P= 36.50 kN

2P= 41.80 kN

2P= 54.43 kN

Figure 4.33 Crack Propagation of the Beam (B1-P-0)
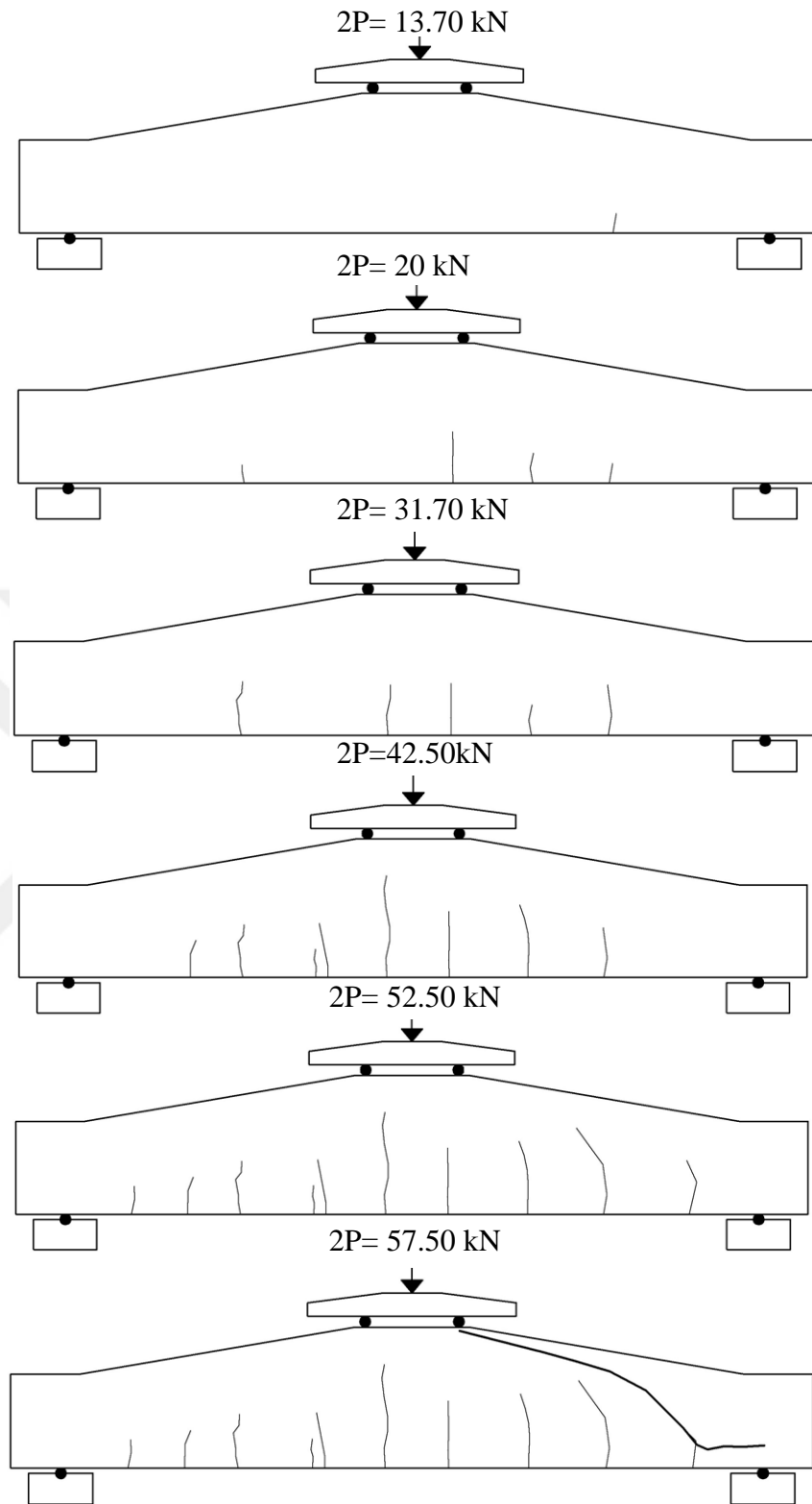
Figure 4.34 Crack Propagation of the Beam (B2-H10-0)

Figure 4.35 Crack Propagation of the Beam (B3-H15-0)
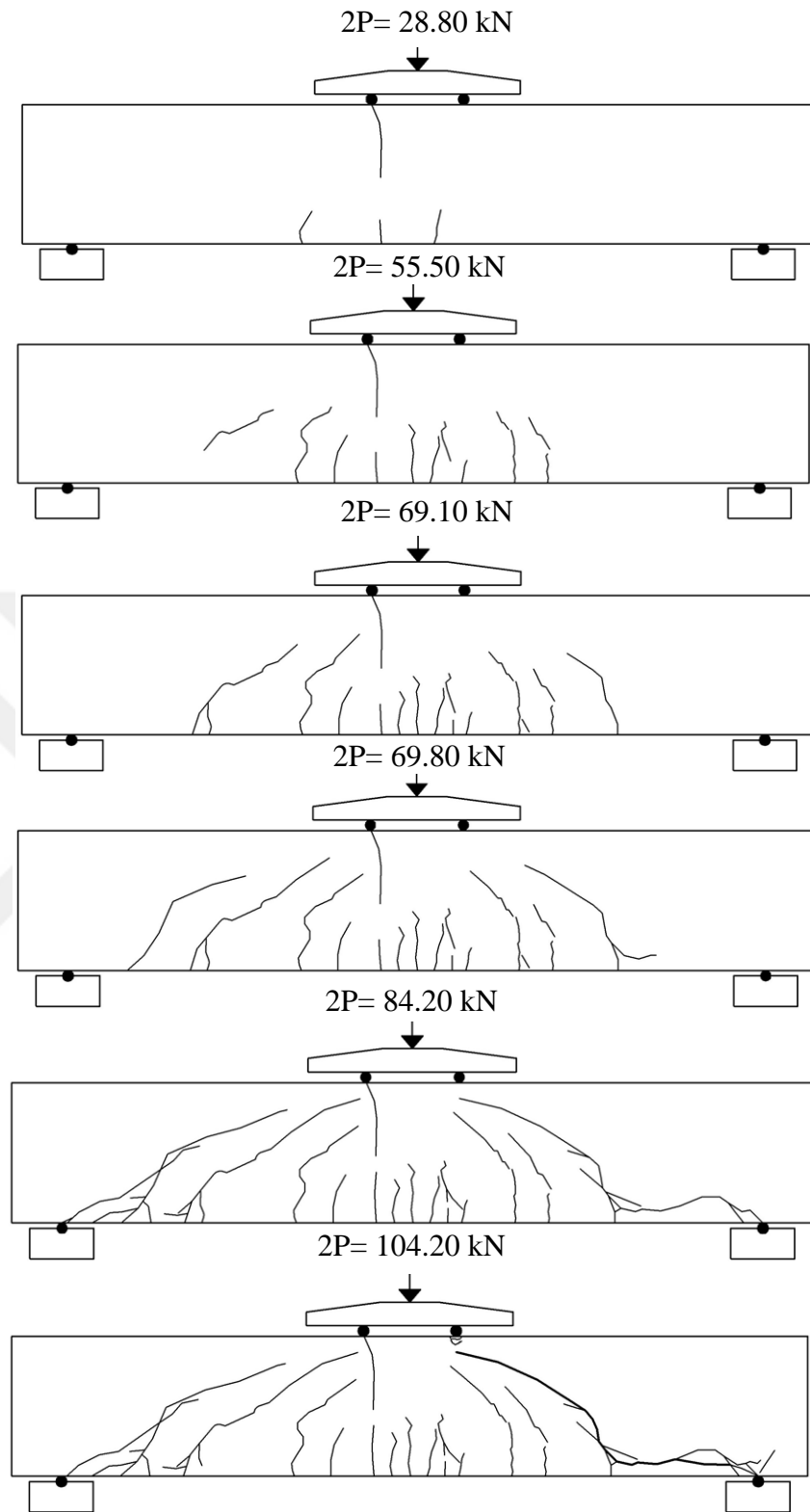
Figure 4.26 Crack Propagation of the Beam (B4-P-0.5)

2P= 32.80 kN

2P= 49.50 kN

2P= 73.50 kN

2P= 93.70kN

2P= 101.80 kN

2P= 109.60 kN
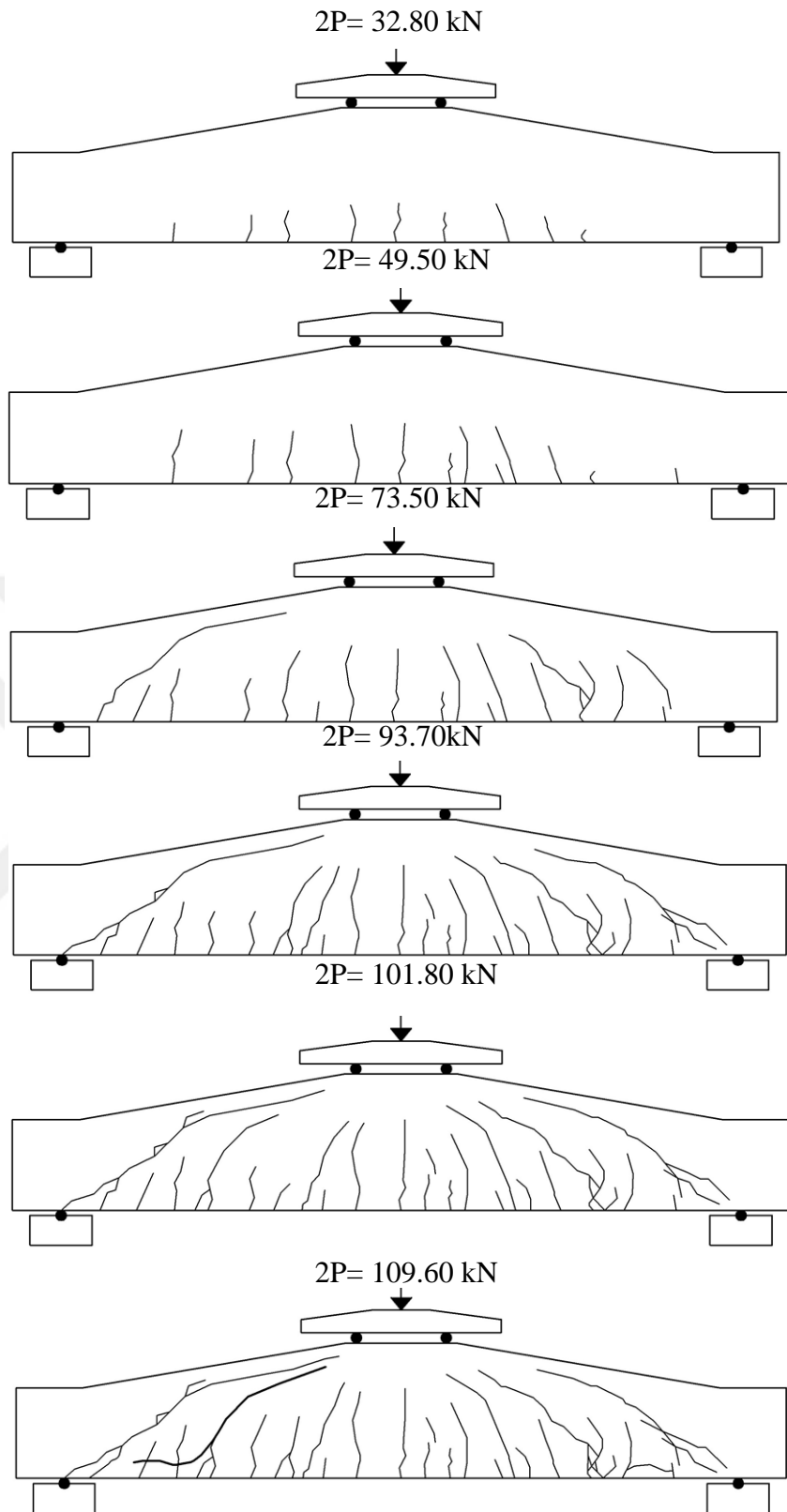
Figure 4.37 Crack Propagation of the Beam (B5-H10-0.5)

81
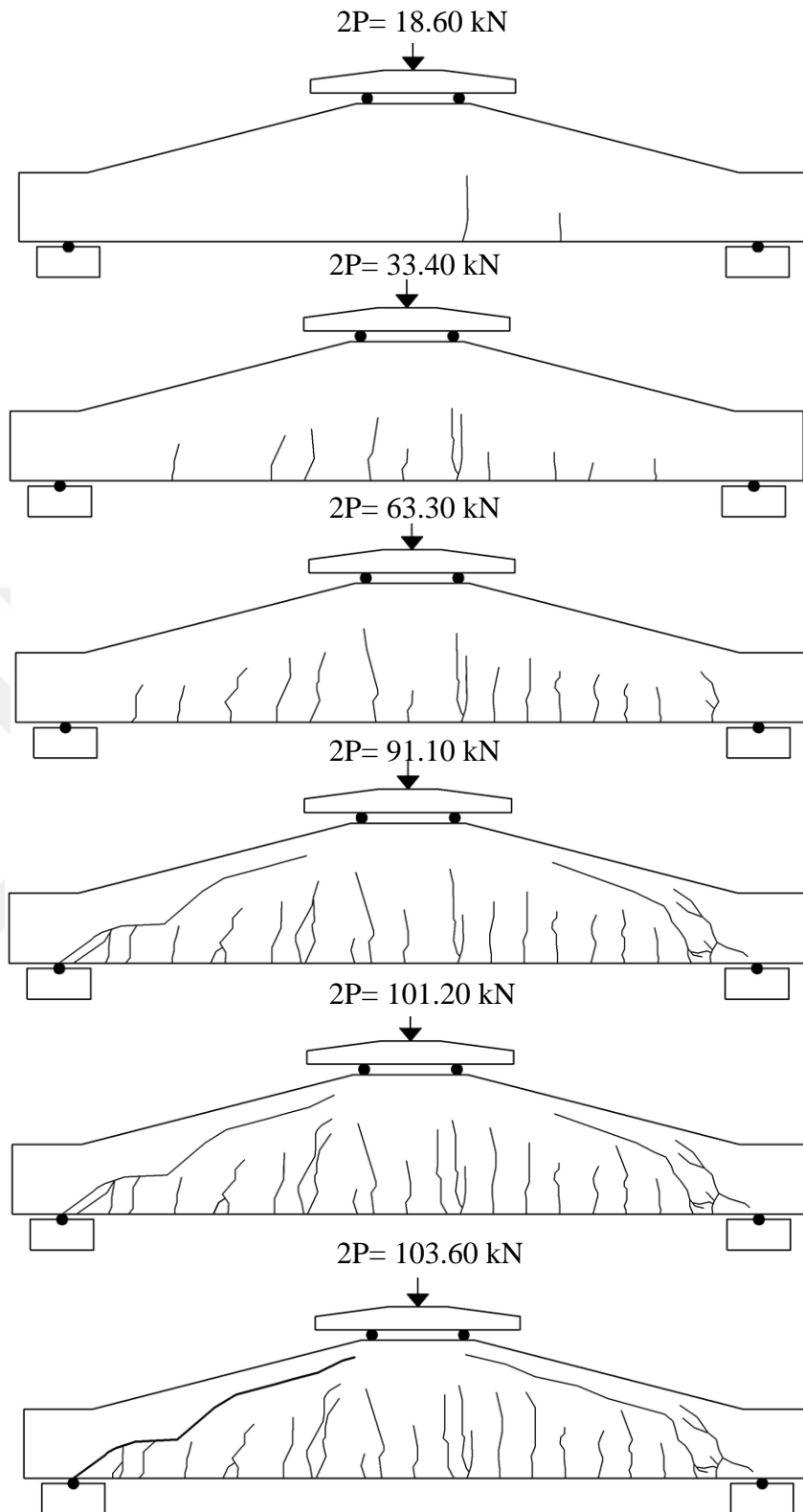
Figure 4.38 Crack Propagation of the Beam (B6-H15-0.5)

2P= 37.30 kN

2P= 72.90kN

2P= 113.70 kN

2P= 123.70 kN

2P= 133.70 kN

2P= 134.30 kN
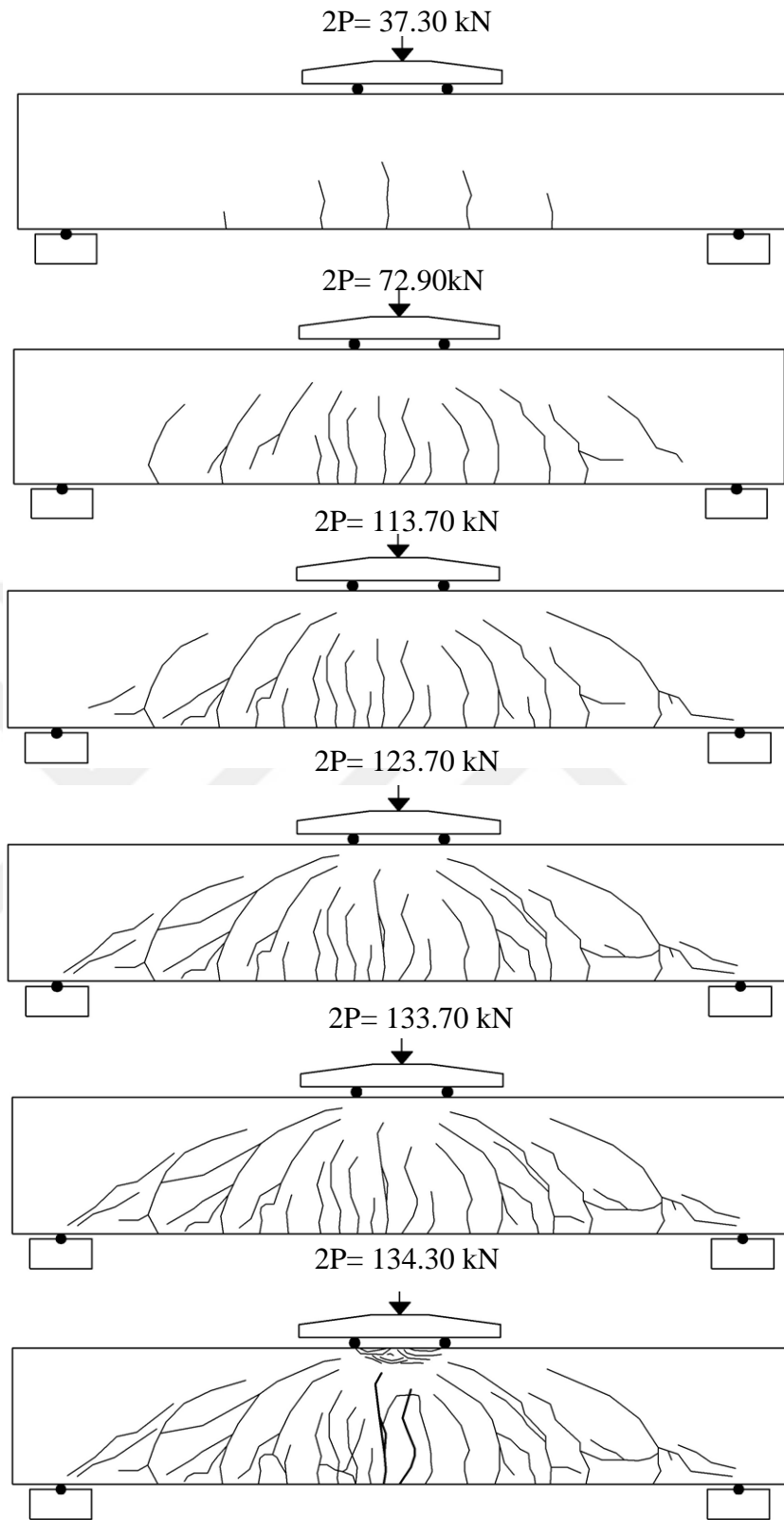
Figure 4.39 Crack Propagation of the Beam (B7-P- 1)

2P=18.80kN

2P= 35.40 kN

2P= 95.20 kN

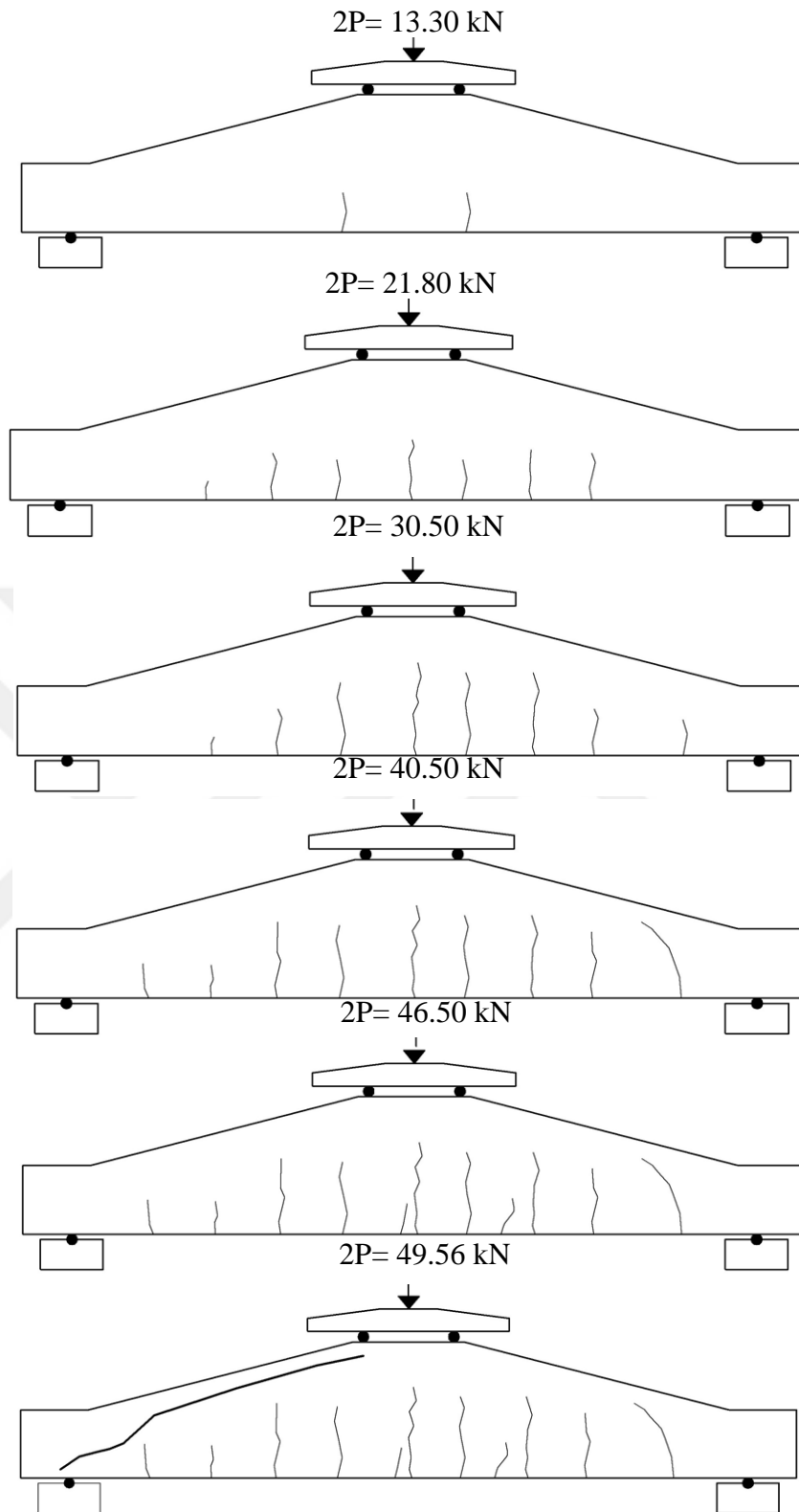2P= 125.40 kN

2P= 132.50 kN

2P= 140.50 kN
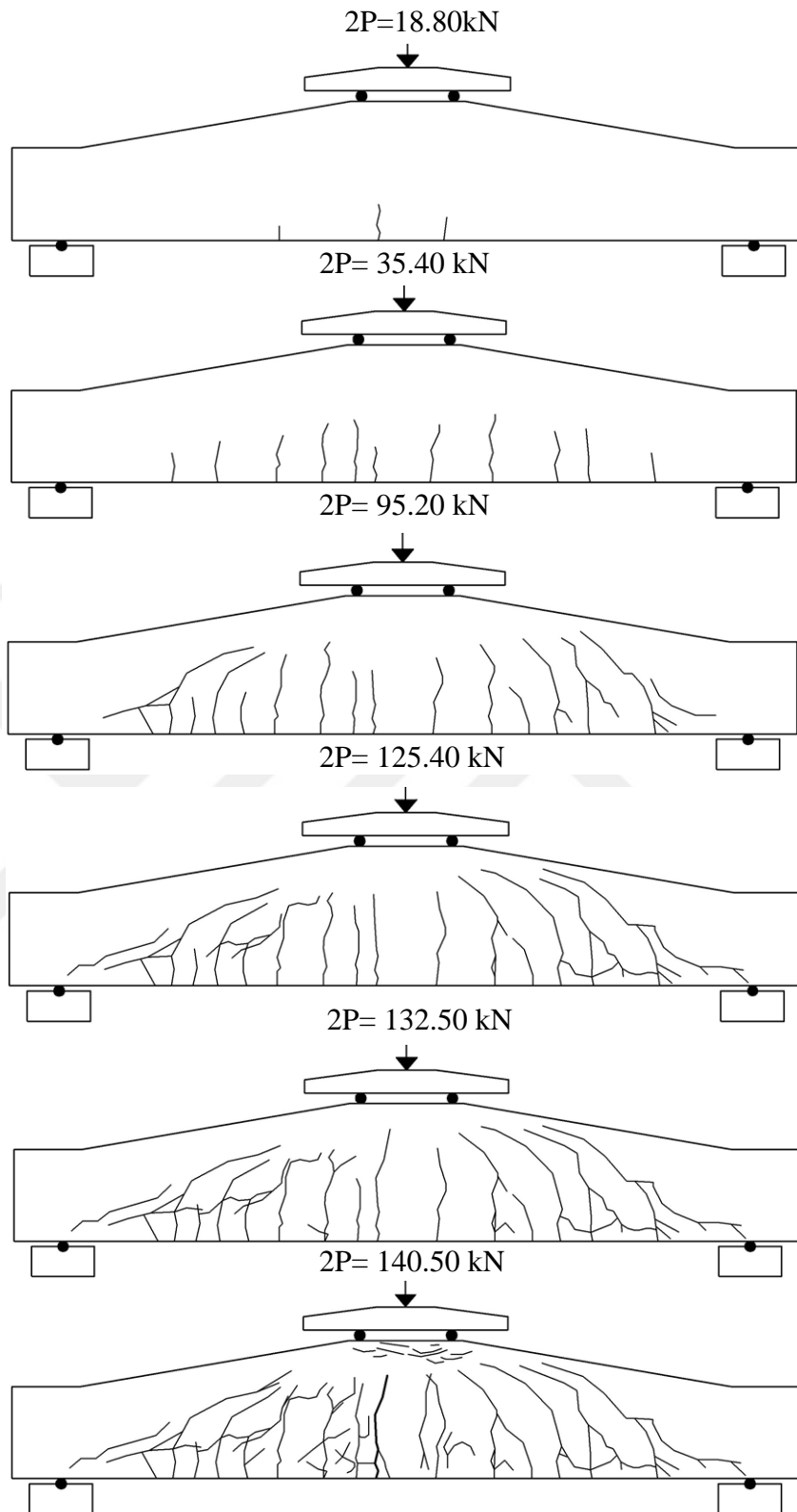
Figure 4.40 Crack Propagation of the Beam (B8-H10-1)
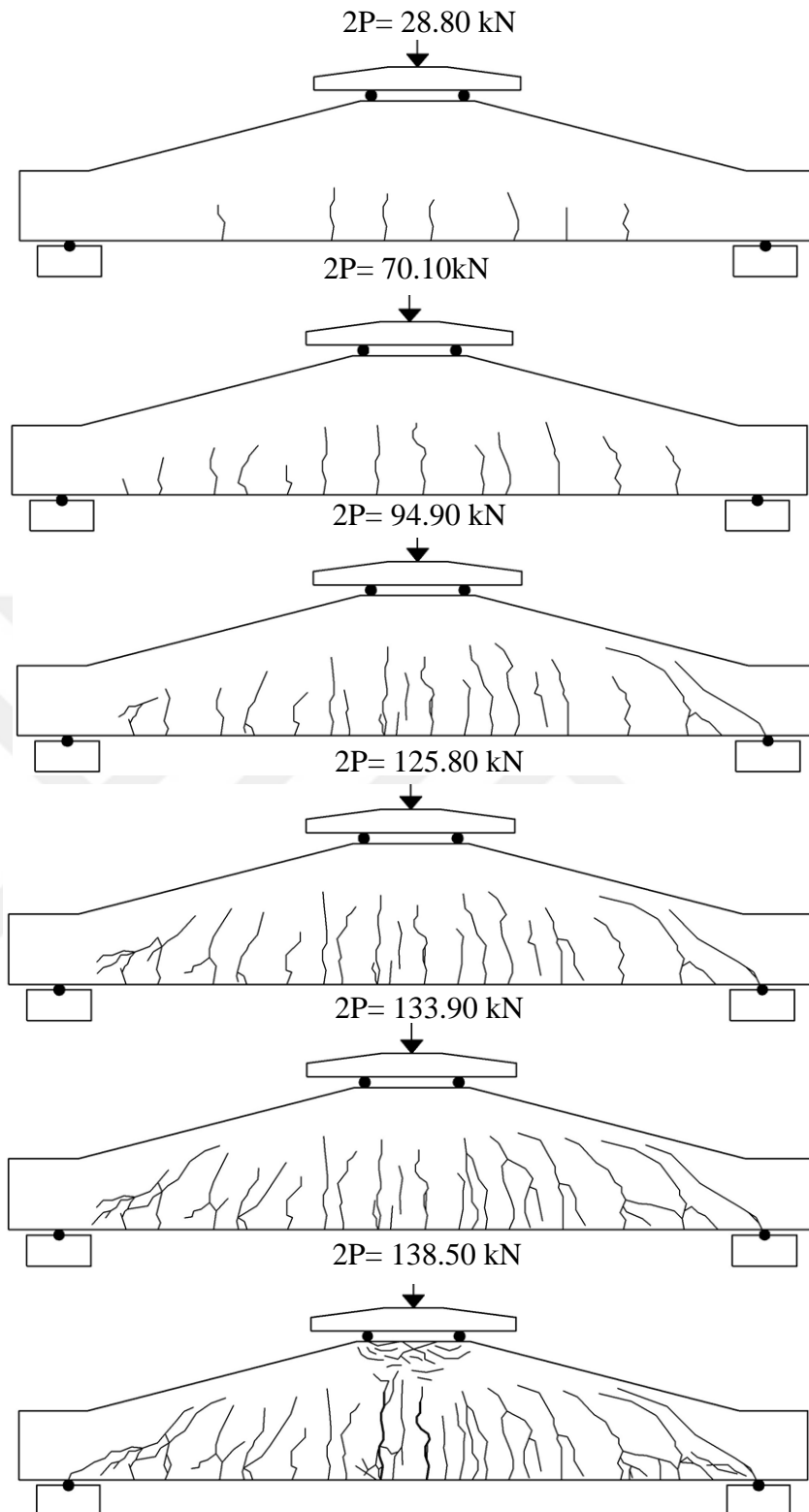
Figure 4.41 Crack Propagation of the Beam (B9-H15-1)

CHAPTER 5

CONCLUSIONS

5.1 Overview

Although the haunched beam is an important structural member and widely used in construction designs, however some research has been conducted in comparison with other structural members. In addition, the usage of steel fibers in this type of beam enhances its mechanical behavior because it is a promising material that offers many advantages that can be adopted in structural applications. This thesis presents a comprehensive and complete investigation into the possibility of using steel fibers with self-compacting concrete (SCSFRC) in the prismatic and haunched beam.

5.2 Summery

The experimental study contained 9 beams divided into 3 prismatic beams and 6 RCHBs. All beams were designed without the usage of steel stirrups to ensure that shear failure will occur, and with the usage of steel fiber. These beams were divided into three different groups according to fiber ratio. All beams were examined under a four-point load to evaluate the effect of fibers on the structural response of SCSFRC beams. The parameters examined in this work were the effect of changing in the degree of inclination in the shear region of haunched beams on the location of the critical section and the influence of changing in the fiber percentage on shear capacity and mode failure. The RCHBs were designed with two angles (10° and 15°) and 3 values of steel fiber percentage (0%), (0.5%), and 1% for the prismatic and haunched beam. Significant differences were observed in the mechanical behavior between the haunched and the prismatic beam.

Results obtained from the experimental study lead to the following conclusions:

- Tensile strength was significantly increased with the addition of steel fiber to SCC concrete. However, this height depends on the amount of added fiber.

- Experimental results carried out on SCSFRC beams show that the inclination angle and steel fibers ratio are effective parameters on the load capacities for SCSFRC beams. Where load capacity and failure mode of SCSFRC beam could be regulated by changing of these parameters.

- Whenever the quantity of the fibers increases, the load carrying capacity of SCSFRC beams increases. However, the proportion of increase decreases as the quantity of fiber increases higher and higher, for example, for the haunched beam (H15°) adding 0.5% in fiber percentage increased the ultimate shear strength of concrete by 69%, whereas adding 1% in fiber percentage increased it by 79%.

- The steel fibers are effective in increasing shear strength of concrete, especially in the haunched beam that was greater than the prismatic beam.

- Another advantage of using steel fiber in the haunched beam is the crack width. The crack width of reinforced concrete for this type of beams with fiber is much smaller compared to prismatic beam with fiber. This feature extends the service life of the haunched beam. Moreover, it facilitates a good repair process in case of a potential rehabilitation, as a result, fiber is one of the most effective and inexpensive solutions to prevent brittle failure in reinforced concrete beams.

- The use of steel fiber enhanced the post-cracking characteristics, especially for the beams of the third group (1% fiber) where the number of cracks increased, indication that the redistribution of stress was better.

- Increment the steel fiber ratio was able to change the failure mode from diagonal shear to compression failure and flexural failure that occurred in the third group.

- The results indicated that the location of critical section depends on the inclination of haunched beams, where the location of the critical section changes with the increasing inclination. It can be concluded that as an inclination of haunched beam increases, the position of critical section tends to become closer to the support point.

- As a result, steel fiber is one of the most effective and inexpensive solutions to prevent fragile failure in reinforced concrete beams.

- Although the volume of the concrete in the RCHBs is smaller than that of prismatic beams, and the shear strength capacity was close to the capacity of prismatic beams for small inclination angles. Therefore, the usage of RCHBs is more economic.

- Displacement that has been developed in SCSFRC haunched beam is more than that of SCSFRC prismatic beams. This increment is basically associated with the capacity of RCHBs to redistribute cracking along the haunched length.

- The results of SCSFRC haunched beam estimated that the minimum magnitude of the shear stress for the haunched beam that contained (V_f =0.50%) was more than the value that reported for SFRC prismatic beam in ACI-318 code for the prismatic beam that contained ($V_f \geq$ 0.50%).

- The results showed that the minimum magnitude of the shear stress for the haunched beam that having (V_f =1%) was much more than the value that reported for SFRC prismatic beams in ACI-318 code that contained ($V_f \geq 0.75\%$) which permits the usage of SFRC to replace minimum shear stirrups. Therefore, in this study, the steel fiber has shown the possibility of replacing traditional reinforcement for minimum shear reinforcement in the haunched beam.

- Minimum shear stress value at failure for the SCC haunched beam in this study was more than the initial shear stress corresponding to (V) in the ACI-318 code.

- Use of 1% of steel fibers led to a significantly improvement in the ductility of the beams. In addition, the ductility at peak load in the haunched beams was slightly higher than in the prismatic beams.

5.3 Recommendations for Further Research

The haunched members are generally used in concrete structures. Although the experimental programs presented a different behavior compared to the members of the prismatic beam, the design codes of the structural building did not contain the formula of a specific design for these types of the member for all. Therefore, it is necessary to study the following topics in the future.

- Study the mechanical behavior of SCSFRC haunched beams for different types of loading, such as uniformly load, cyclic loading, and impact loading in order to estimate the influence of steel fibers on the shear response and flexural ductility of beams.

- Fiber industry is a growing industry and many types of fibers are available like arched-hooked end steel fibers, basalt fibers, glass fibers, and Hybrid fiber, so it is recommended to use these fibers in the haunched beams to be sure the result of replacing traditional reinforcement for the minimum shear reinforcement that achieved in this study because this study was limited to one type of fiber.

- Conduct more research that focuses on the shear behavior of larger SCSFRC haunched beams to examine the influence of the increasing volume of the beam on the shear response more clearly. In addition, choose a few variables like shear span-to-effective depth proportion, the compressive strength of concrete, longitudinal steel reinforcement proportion, steel fiber percentage quantity and class of concrete.

- Check the activity of combining of steel fibers and traditional transverse reinforcement as well as check the influence of this approach on the shear response for SCSFRC haunched beams.

REFERENCES

ACI Committee 544, (1988). "Design Considerations for Steel Fiber Reinforced Concrete (ACI 544.4R-88)." American Concrete Institute, Farmington Hills, Michigan, USA, 18.

ACI. American Concrete Institute. (2002). State-of-the-Art Report on Fiber Reinforced Concrete. ACI 544.1R-96.

ACI Committee 318, (2008). Building Code Requirements for Structural Concrete (ACI 318-08) and Commentary. American Concrete Institute, Farmington Hills, Michigan, USA, 473.

Albegmprli, H. M. (2017). Experimental Investigation and Stochastic FE Modeling of Reinforced Concrete Haunched Beams. PhD thesis, Department of Civil Engineering, University of Gaziantep, Turkey.

Aoude, H. (2008). Structural Behavior of Steel Fiber Reinforced Concrete Members. PhD thesis, Department of Civil Engineering and Applied Mechanics, McGill University, Montreal, Canada.

Ashour, S. A., Hasanain, G. S., Wafa, F. F. (1992). Shear Behavior of High-Strength Fiber Reinforced Concrete Beams. *ACI Structural Journal*, **89**, 176-184.

ASTM. American Society for Testing and Materials. 2004. Standard test method for splitting tensile strength of cylindrical concrete specimens. C 496-04. West Conshohocken, PA.

Batson, G., Jenkins, E., Spatney, R. (1972). "Steel Fibers as Shear Reinforcement in Beams." *Adjournal Proceedings,* **69**, 640-644.

BS1881-116, " Method for Determination of Compressive Strength of Concrete Cubes", British Standards Institute, London, 1983.

Choi, K. K., Hong-Gun, P., Wight, J. K. (2007) "Shear Strength of Steel Fiber Reinforced Concrete Beams without Web Reinforcement." *ACI Structural Journal*, **104**, 12-21.

Cohen, M. (2012). Structural behaviour of self-consolidating steel fiber reinforced concrete beams. Master Thesis, Department of Civil Engineering, University of Ottawa (Canada).

Debaiky, S. Y., Elniema, E. I. (1982, May). Behavior and strength of reinforced concrete haunched beams in shear. *In Journal Proceedings*. **79**, 184-194.

Dinh, H. H. (2009). Shear Behavior of Steel Fiber Reinforced Concrete Beams without Stirrups Reinforcement. PhD Thesis, Department of Civil Engineering, University of Michigan, Michigan, USA.

DIN 1045-01. 2001. Tragwerke aus Beton, Stahlbeton und Spannbeton, Teil 1 Bemessung und Konstruktion. Beuth Verlag GmbH, Berlin.und Konstruktion. Beuth Verlag GmbH, Berlin.

Fanella, D. A., Naaman, A. E. (1985). Stress-strain properties of fiber reinforced mortar in compression. *ACI Journal Proceedings*. **82**, 475-483.

Greenough, T., Nehdi, M. (2008). Shear Behavior of Fiber-Reinforced Self-Consolidating Concrete Slender Beams.. *ACI Structural Journal*, **105**, 468-477.

Grunewald, S. (2004). Performance-Based Design of Self-Compacting Fiber Reinforced Concrete. Department of Structural and Building Engineering, Delft University of Technology, Delft, Germany, 20-24.

Hannant, D. J. (1978). Fiber Cement and Fiber Concrete,II John Wiley and Sons. Inc., New York., USA.
https://theconstructor.org/structural-engg/types-of-bridges/13195/.Accessed 17.02.2018.

http://www.hpcbridgeviews.com/i49/article1.asp. Accessed 08.2.2018.

https://www.slideshare.net/AMALTHANKACHAN2/frc-in-industrial-flooring. Accessed 02.1.2018.

http://zhuokainet.com/tanfuzong/cp/html/?17.html. Accessed 02.1.2018.

http://www.tsyajs.com/en/news.php?id=94. Accessed 02.1.2018.

Johnston, C. D. (1996). Proportioning, Mixing and Replacement of Fiber-Reinforced Cement and Concrete. Production Methods and Workability of Concrete, Edited by Bartos, Marrs and Cleland, E. and FN Spon, London, 155-179.

Kronenberg, J. (2006). Sliding Arch Construction Method Used on the Gotthard Base Tunnel. *Concrete Engineering International,* **10**, 19-20.

Lachemi, M., Hossain, K. M., Lambros, V. (2005). Shear resistance of self-consolidating concrete beams experimental investigations. *Canadian Journal of Civil Engineering*, **32**, 1103-1113

Liao, W. C., Chao, S. H., Park, S. Y., Naaman, A. E. (2006). Self-Consolidating High-Performance Fiber Reinforced Concrete (SCHPFRC)–Preliminary Investigation. Report No. UMCEE 06, 2.

MacLeod, I. A., Houmsi, A. (1994). Shear strength of haunched beams without shear reinforcement. *Structural Journal*, **91**, 79-89.

Mansur, M. A., Ong, K. C. G., ParamasivamA, P. (1986) Shear Strength of Fibrous Concrete Beams without Stirrups, *ASCE Journal of Structural Engineering*, **112**, 2066-2079.

Mass, G. R. (1997). SFRC Lining for an Embankment Dam. *Concrete International,* **19**, 24-27.

Minelli, F. (2005). Plain and Fiber Reinforced Concrete Beams under Shear Loading. PhD Thesis, Department of Civil Engineering, University of Brescia, Italy.

Minelli, F., Plizzari, G. A. (2006, June). Steel fibers as shear reinforcement for beams. In Proceedings of the 2nd International.

Mörsch, E. (1922). Der eisenbetonbau (reinforced concrete construction). Verlag von Konrad Wittwer, Stuttgart.

Narayanan, R. Darwish, I. Y. S. (1987) .Use of Steel Fibers as Shear Reinforcement. *ACI Structural Journal*, **84**, 216-227.

Parra-Montesinos, G. J. (2006). Shear strength of beams with deformed steel fibers. *Concrete International*, **28**, 57-66.

Sharma, A. K. (1986). Shear Strength of Steel Fiber Reinforced Concrete Beams. *Journal of the American Concrete Institute*, **83**, 624-628.

Sherwood, E. G. (2008). One-Way Shear Behavior of Large, Lightly Reinforced Concrete Beams and Slabs. PhD Thesis, Department of Civil Engineering, University of Toronto, Toronto, Canada, 333P.

Stefanou GD. (1983). Shear resistance of reinforced concrete beams with non-prismatic sections. *Engineering Fracture Mechanic*. **18**, 643-666.

Swamy, R. N., Mangat, P. S. (1974). Influence of Fiber-Aggregate Interaction on Some Properties of Steel Fiber Reinforced Concrete. *Materials and Structures Journal*, **7**, 307-314.

Tena-Colunga, A., Archundia-Aranda, H. I., González-Cuevas, Ó. M. (2008). Behavior of reinforced concrete haunched beams subjected to static shear loading. *Engineering Structures*, **30**, 478-492.

Thomas, J., Ramaswamy, A. (2007). Mechanical properties of steel fiber-reinforced concrete. *ASCE Journal of Materials in Civil Engineering*. **19**, 385-392.

Wight J. K. & MacGregor J. G. (2009). Reinforced Concrete Mechanics and Design", 5th Edition, USA, 1112 p.

Voo, J. Y., & Foster, D. S. J. (2003). Variable engagement model for fibre reinforced concrete in tension. University of New South Wales, School of Civil and Environmental Engineering.

Zanuy, C., Gallego, J. M., , Albajar, L. (2015). Fatigue Behavior of Reinforced Concrete Haunched Beams without Stirrups. *ACI Structural Journal*, **112**, 371-382.